

Friedrich Schiller University Jena
Faculty of Biology and Pharmacy

Max Planck Institute for Chemical Ecology
Department of Entomology



seit 1558

**Interaction of plant proteins with polygalacturonases
from the mustard leaf beetle *Phaedon cochleariae***

Master's thesis

to meet the requirements for the academic degree
Master of Science

submitted by
Wiebke Häger

born January 19th 1991 in Hamburg
Jena, December 17th 2015

Reviewer:

Prof. Dr. David G. Heckel

Prof. Dr. Wilhelm Boland

Index

1	List of figures	IV
2	List of tables	V
3	List of abbreviations.....	VI
4	Introduction.....	1
4.1	Herbivores' encounter with the plant cell wall.....	1
4.2	Pectinases in beetles.....	1
4.3	PGs in the mustard leaf beetle <i>P. cochleariae</i>	3
4.4	PG-PGIP interaction	4
5	Aim of Master's Thesis.....	6
6	Material and Methods	7
6.1	Material.....	7
6.1.1	Plants	7
6.1.2	Cells	7
6.1.3	Enzymes.....	7
6.1.4	Kits	7
6.1.5	Consumable Material.....	8
6.1.6	Chemicals.....	8
6.1.7	Primer.....	10
6.1.8	Plasmids.....	10
6.1.9	Devices.....	11
6.1.10	Software	11
6.1.11	Buffer and Media	11
6.2	Methods.....	15
6.2.1	Cloning of PGs into pPICZ α A	15
6.2.1.1	PCR.....	15
6.2.1.2	Purification of PCR products.....	15
6.2.1.3	Digest of PCR products and pPICZ α A vector	16
6.2.1.4	Purification of digested PCR products and pPICZ α A	16
6.2.1.5	Ligation.....	17
6.2.2	Transformation of <i>E. coli</i>	17
6.2.3	Miniprep of plasmids from <i>E. coli</i> cultures.....	17
6.2.4	Verification of pPICZ α A inserts	18
6.2.4.1	Test digest.....	18
6.2.4.2	Test PCR.....	18
6.2.4.3	Sequencing	19

6.2.5	Midiprep of plasmids from <i>E. coli</i> cultures.....	19
6.2.6	Preparing competent <i>P. pastoris</i> cells.....	20
6.2.7	Transformation of <i>P. pastoris</i>	20
6.2.7.1	Linearisation and purification of pPICZα A vectors.....	20
6.2.7.2	Electroporation	21
6.2.7.3	Determination of transformation-positive <i>P. pastoris</i> colonies	22
6.2.7.3.1	Extraction of gDNA from <i>P. pastoris</i>	22
6.2.7.3.2	PCR of gDNA from <i>P. pastoris</i>	22
6.2.8	Glycerol stocks	23
6.2.9	Small-scale expression (5 ml) of PGs in <i>P. pastoris</i>	23
6.2.10	Large-scale expression of PGs in <i>P. pastoris</i>	24
6.2.11	SDS-PAGE	24
6.2.12	Western Blot.....	24
6.2.13	Coomassie staining of gel.....	25
6.2.14	Protein quantification	25
6.2.15	Activity assays	25
6.2.15.1	Agarose diffusion assay.....	25
6.2.15.2	Quantification of PG activity by DNS assay	26
6.2.15.3	Thin layer chromatography (TLC)	27
6.2.16	Deglycosylation of PGs with Peptide-N-Glycosidase F (PNGase F)	28
6.2.17	Protein purification	28
6.2.17.1	Immobilised metal ion affinity chromatography (IMAC)	29
6.2.17.2	Lectin affinity chromatography	30
6.2.17.3	Hydrophobic interaction chromatography (HIC)	30
6.2.17.4	Cation exchange chromatography (CEC)	30
6.2.17.5	Anion exchange chromatography (AEC).....	30
6.2.17.6	Binding of PGs to insoluble pectin	31
6.2.18	Protein concentration and buffer exchange.....	31
6.2.19	AminoLink Column.....	32
6.2.20	Induction of PGIP synthesis in <i>B. rapa</i> ssp. <i>pekinensis</i>	33
6.2.21	Protein extraction from Chinese cabbage	33
6.2.21.1	Extraction of cell walls from <i>B. rapa</i> ssp. <i>pekinensis</i>	33
6.2.21.2	Protein extraction from <i>B. rapa</i> ssp. <i>pekinensis</i> cell walls	33
6.2.22	PG-PGIP interaction study.....	34
6.2.22.1	Affinity chromatography	34
6.2.22.2	Trichloroacetic acid (TCA) precipitation and sample preparation	35

6.2.22.3	Mass spectrometry (MS) analysis and data evaluation	35
6.2.22.3.1	In-gel digestion of proteins	35
6.2.22.3.2	LC-MS/MS analysis	35
6.2.22.3.3	Data processing and protein identification.....	36
6.2.22.3.4	Data Evaluation.....	37
7	Results	38
7.1	Identification of <i>B. rapa</i> ssp. <i>pekinensis</i> cell wall proteins	38
7.2	Inhibition of PGs by <i>B. rapa</i> ssp. <i>pekinensis</i> cell wall protein extracts.....	40
7.3	Co-incubation of active and inactive PGs.....	41
7.4	Expression of PGs PCO_GH28-1, PCO_GH28-3 and SSC_GH28-6.....	42
7.5	Protein characterisation	43
7.5.1	Activity assay for PCO_GH28-1, PCO_GH28-3 and SSC_GH28-6	43
7.5.2	Glycosylation of PCO_GH28-1, PCO_GH28-3 and SSC_GH28-6.....	44
7.6	Protein purification of PCO_GH28-1 and PCO_GH28-3	45
7.7	Purification and characterisation of SSC_GH28-6.....	47
7.7.1	IMAC approaches.....	47
7.7.2	Other chromatography strategies.....	49
7.7.3	Interaction of PGs with insoluble pectin	50
7.7.4	Alternative treatment for SSC_GH28-6.....	53
7.8	Affinity chromatography: PG-PGIP interaction study.....	53
8	Discussion	61
9	Future perspectives	74
10	Summary	75
11	Zusammenfassung	76
12	Literature	i
13	Supplementary Data	viii
13.1	Sequences	viii
13.2	Western Blots	x
13.3	FPLC chromatograms.....	xi
13.4	Distribution of peptides in PCO_GH28-1.....	xii
13.5	Complete tables of MS analyses containing all protein hits.....	xiii
14	Acknowledgement	xxix
15	Declaration of originality.....	xxx

1 List of figures

Figure 1: Activities of PGs PCO_GH28-1, PCO_GH28-5, PCO_GH28-9 and SSC_GH28-6 as well as <i>P. cochleariae</i> gut content with and without co-incubation with cell wall protein extracts from <i>B. rapa</i> ssp. <i>pekinensis</i>	41
Figure 2: Activities of of active PGs PCO_GH28-1 (A), -5 (B) and -9 (C) incubated with and without co-incubation with <i>B. rapa</i> ssp. <i>pekinensis</i> cell wall protein extract and inactive PCO_GH28-3, -6 and -8 respectively.....	42
Figure 3: Expression of PCO_GH28-1.....	43
Figure 4: Agarose diffusion assay for PCO_GH28-1, PCO_GH28-3 and SSC_GH28-6.....	44
Figure 5: Comparison between PCO_GH28-1, PCO_GH28-3 and SSC_GH28-6 expressed in Sf9 insect cells (I), the <i>P. pastoris</i> (Y) as well as deglycosylated proteins from yeast expression (Yd).	45
Figure 6: Coomassie-stained SDS-PAGE gel of IMAC-based purification of PGs PCO_GH28-1 and PCO_GH28-3 using IMAC.	46
Figure 7: Western Blot of PCO_GH28-1 with different temperature treatments.....	47
Figure 8: Activity of SSC_GH28-6, PCO_GH28-1 and <i>P. cochleariae</i> gut content under native and denaturing conditions.....	49
Figure 9: Binding assay of PCO_GH28-1, PCO_GH28-3 and SSC_GH28-6 to cross-linked pectin.	51
Figure 10: Thin Layer Chromatogram for SSC_GH28-6 activity towards pectin substrates.....	52
Figure 11: Coomassie-stained SDS-PAGE gel of the interaction study of SSC_GH28-6 with <i>B. rapa</i> ssp. <i>pekinensis</i> cell wall protein extracts.	54
Figure 12: Coomassie-stained SDS_PAGE gel from the interaction study of the PGs PCO_GH28-1 and PCO_GH28-3 with <i>B. rapa</i> ssp. <i>pekinensis</i> cell wall protein extracts.	56
Figure 13: Expression of PCO_GH28-3.	x
Figure 14: Expression of SSC_GH28-6.....	x
Figure 15: Western Blot of PCO_GH28-3 with different temperature treatments.....	x
Figure 16: FPLC chromatogram of PCO_GH28-1 (A) and PCO_GH-28-3 (B) IMAC purification.	xi
Figure 17: Distribution of peptides detected by MS/MS in the amino acid sequence of PCO_GH28-1.....	xii

2 List of tables

Table 1: Total number of protein hits in the MS analysis of <i>B. rapa</i> ssp. <i>pekinensis</i> cell wall protein extractions and their predicted localisation.	38
Table 2: PGIPs found in MS data for CaCl ₂ and NaCl cell wall protein extractions from <i>B. rapa</i> ssp. <i>pekinensis</i>	39
Table 3: Number of peptides, Mascot score and coverage of MS analysis hits for PCO_GH28-1 degradation products.	47
Table 4: MS results for interaction study of SSC_GH28-6 with <i>B. rapa</i> ssp. <i>pekinensis</i> cell wall protein extracts.	55
Table 5: MS results for interaction study of PCO_GH28-1 with <i>B. rapa</i> ssp. <i>pekinensis</i> cell wall protein extracts, protein band 7.....	57
Table 6: MS results for interaction study of PCO_GH28-1 with <i>B. rapa</i> ssp. <i>pekinensis</i> cell wall protein extracts.	58
Table 7: MS results for interaction study of PCO_GH28-3 with <i>B. rapa</i> ssp. <i>pekinensis</i> cell wall protein extracts.	59
Table 8: All Brassicaceae proteins found in MS data for CaCl ₂ as well as NaCl cell wall extractions from <i>B. rapa</i> ssp. <i>pekinensis</i>	xxiii
Table 9: Complete MS results of all detected Brassicaceae proteins for interaction study of SSC_GH28-6 with <i>B. rapa</i> ssp. <i>pekinensis</i> cell wall protein extracts.	xxiv
Table 10: Complete MS results of all detected Brassicaceae proteins for interaction study of PCO_GH28-1 with <i>B. rapa</i> ssp. <i>pekinensis</i> cell wall protein extracts.	xxvii
Table 11: Complete MS results of all detected Brassicaceae proteins for interaction study of PCO_GH28-3 with <i>B. rapa</i> ssp. <i>pekinensis</i> cell wall protein extracts.....	xxviii

3 List of abbreviations

AEC	anion exchange chromatography
AOX	alcohol oxidase
approx.	approximately
BMGY	buffered glycerol complex medium
BMMY	buffered methanol complex medium
BSA	bovine serum albumine
CE	carbohydrate esterase
CEC	cation exchange chromatography
ConA	concanavalin A
CV	column volume
DDA	data dependent acquisition
ddH ₂ O	bi-distilled water
DNA	deoxyribonucleic acid
DNS	3,5-dinitrosalicylic acid
e.g.	exempli gratia (for example)
EC	Enzyme Commission
ECL	enhanced chemiluminescence
eLRR	extracellular leucine-rich repeat
FPLC	fast protein liquid chromatography
g	gravity of earth
gDNA	genomic DNA
GH	glycosyl hydrolase
HIC	hydrophobic interaction chromatography
HRP	horseradish peroxidase
i.e.	id est (that is)
IMAC	immobilised metal ion affinity chromatography
LB	lysogeny broth
MES	2-(N-morpholino)ethanesulphonic acid
MS	mass spectrometry
Mut ⁺	Methanol utilization plus
OD ₆₀₀	absorbance at 600 nm
OG	oligogalacturonide
ORF	open reading frame
PCR	polymerase chain reaction
PCWDE	Plant Cell Wall Degrading Enzyme

PG	polygalacturonase
PGIP	polygalacturonase-inhibiting protein
PL	polysaccharide lyase
PME	pectin methylesterase
PNGase F	Peptide- <i>N</i> -Glycosidase F
qPCR	quantitative real-time PCR
RT	room temperature
SDS-PAGE	sodium dodecyl sulphate polyacrylamide gel electrophoresis
ssp.	subspecies
TBS	Tris buffered saline
TBST	Tris buffered saline with Tween-20
TCA	trichloroacetic acid
TLC	thin layer chromatography
Tris	tris(hydroxymethyl)aminomethane
w/v	weight/volume
w/w	weight/weight
YNB	yeast nitrogen base
YPD	yeast extract peptone dextrose
YPDS	yeast extract peptone dextrose sorbitol

4 Introduction

4.1 Herbivores' encounter with the plant cell wall

Beetles (Coleoptera) represent the largest order in the class of insects (Insecta) worldwide. Until now 360 000 species have been described, of which 35% live as herbivores and thus feed on all kinds of plant material in adult or larval stage [1].

Plant cells are encased by cell walls that provide structural integrity and protection to the cell and contribute to cell-cell adhesion and signal transduction [2], [3]. Plant cell walls are constantly modified depending on developmental stages and environmental conditions [2], [4]. During their initial growth, plant cells secrete the components of the middle lamella and primary cell wall, which are subsequently supplemented by a secondary wall in many cells [5], [4], [3]. The plant cell wall consists of polysaccharides such as cellulose, hemicellulose and pectin as well as associated proteins [2], [5], [4]. Pectin accounts for approximately 35% of primary cell walls in dicots and non-graminaceous monocots [3], [6].

Pectins are a complex mixture of galacturonic acid-rich, covalently linked polysaccharides that consist of homogalacturonan and rhamnogalacturonan II as well as substituted galacturonans such as rhamnogalacturonan I, xylogalacturonan or apiogalacturonan [6]. Approximately 65% of pectin accounts for homogalacturonan, a polymer of α -(1,4)-linked galacturonic acid. The polygalacturonic acid backbone can be modified by methylation of the C6-carboxyl group or acetylation of O-2 or O-3 of the galacturonic acid residues. These esters can be removed by pectin methylesterases or acetylesterases. Substitution of the unmodified polygalacturonic acid backbone with D-xylose or D-apiose gives rise to xylo- or apiogalacturonan. Rhamnogalacturonan II consists of a polygalacturonic acid backbone with conserved, highly complex glycosidic side chains of various sugars. Repeated units of alternating galacturonic acid and L-rhamnose residues form the backbone of rhamnogalacturonan I, which can also be substituted with carbohydrate side chains [3], [6].

4.2 Pectinases in beetles

Plant Cell Wall Degrading Enzymes (PCWDEs) such as cellulases, hemicellulases and pectinases catalyse the degradation of plant cell wall polysaccharides and predominantly possess glycosyl hydrolase activities. Pectinolytic enzymes can be classified into polysaccharide lyases (PL, EC 4.2.2.-), that cleave the galacturonic acid polymer via β -elimination [7], and glycosyl hydrolases (GH, EC 3.2.1.-) of the family GH28, which hydrolyse the glycosidic bonds of the pectin polysaccharide [8], [9].

Homogalacturonan is degraded by polygalacturonases (PGs) and is present in a highly methylesterified form in the cell wall (70 – 80%) [10]. Since most PGs showed increased activity towards lower methylated substrates [11], [12], [13], their hydrolytic activity can be supported by carbohydrate esterases (CEs), namely pectin methylesterases (PMEs, EC 3.1.1.11) of the family CE8. PMEs demethylate the homogalacturonan [14], [15] and thereby improve the activity of PGs in a synergistic manner. Endo-PGs cleave within the homogalacturonan chain giving rise to oligomers of different length as well as galacturonic acid trimers and dimers [16], [11]. In contrast, exo-PGs hydrolyse the glycosidic bonds of terminal galacturonic acid residues releasing galacturonic acid monomers. Oligomers can be degraded by oligogalacturonases [16]. The concerted action of these pectinolytic enzymes enables the complete breakdown of homogalacturonan down to monomers of galacturonic acid. A variety of PCWDEs is known from fungi and bacteria, which secrete those upon infestation of plants to access nutrients within the cell and/or to utilize cell wall carbohydrates [17]. For a long time it has been assumed that these enzymes were restricted to the domain of microorganisms. In 1998 Watanabe et al. first discovered the presence of an animal-encoded cellulase gene of the family GH9 in the termite *Reticulitermes speratus* [18] and thereby laid the foundation for the search for further PCWDEs inherent to animal genomes. In insects genes encoding for PGs are absent from the genome of model organisms such as the red flour beetle *Tribolium castaneum* [19] and the silkworm *Bombyx mori* [20], [21]. Nowadays various PGs have been discovered in herbivorous insects, e.g. in the mustard leaf beetle *Phaedon cochleariae* [22], [21], [23], in the rice weevil *Sitophilus oryzae* [24] and in stick insects (Phasmatodea) [25], but also in nematodes [26], [27]. PGs are not ubiquitously distributed among insects but are restricted to the orders of Coleoptera, Hemiptera and Phasmatodea. In beetles PG genes were found in the superfamilies Chrysomeloidea, including leaf beetles (Chrysomelidae) and longhorn beetles (Cerambycidae), and Curculionoidea with weevils (Curculionidae) and bark beetles (Scolytidae) [21], [22], [11]. Chrysomeloidea and Curculionoidea altogether are termed “Phytophaga clade” reflecting the predominant plant-feeding habit of the sister-clades’ members [28], [29]. During the evolution of Phytophaga beetles, PG genes were acquired by three independent horizontal gene transfer events. The initial horizontal gene transfer of a Pezizomycotina PG to a common ancestor of the Phytophaga occurred approximately 220 million years ago before the splitting of the sister groups Chrysomeloidea and Curculionoidea and is retained in most Chrysomelidae species [30], [11]. In the course of evolution duplication events of ancient PG genes led to a large set of sub- and likely

neo-functionalised proteins capable of the complete degradation of the pectin polymer to galacturonic acid monomers [11].

4.3 PGs in the mustard leaf beetle *P. cochleariae*

The mustard leaf beetle *P. cochleariae* belongs to the Chrysomelidae and feeds on leaves of the Brassicaceae plant family in adult and larval stage. The nearly black, metallic green or blue shining beetles live as herbivores on various cabbage (*Brassica spp.*) and radish (*Raphanus spp.*) species, shepherd's purse (*Capsella bursa pastoris*) and other host plants. The larvae are of brownish yellow colour with black heads and prefer horseradish (*Armoracia rusticana*), black mustard (*Brassica nigra*) and, in maritime regions, common scurvygrass (*Cochlearia officinalis*) [31], [32], [33]. Kirsch et al. (2012) discovered nine PG sequences in the transcriptome of *P. cochleariae*, whereof five expressed proteins were detected in the gut content (PCO_GH28-1, -3, -6, -7, and -9) [23]. Subsequently eight PGs were expressed heterologously and tested for their pectinolytic activity, revealing inactive (PCO_GH28-2, -3, -6 and -8) as well as active (PCO_GH28-1, -4, -5 and -9) PGs. The latter enzymes cleaved polygalacturonic acid in an endo-active mode. PCO_GH28-4 constitutes an exception and was not able to cleave the polymer but degraded galacturonic acid trimers to dimers and monomers [11].

PGs belong to a multi-gene family in *P. cochleariae*. Quantification of the transcripts by qPCR showed that all PGs, irrespective of their ability to degrade pectin, were expressed specifically in the gut in high abundance and proteins of active and inactive PGs were found in the gut content. In the inactive PCO_GH28-3 one of the conserved catalytic aspartate residues is replaced by an asparagine, which most likely explains the lack of activity. Purifying selection was found to act on all *P. cochleariae* PG genes, indicating maintenance of important functions of these proteins. The inability to degrade homogalacturonan suggests a neo-functionalisation of the inactive PGs [11]. The type of new functions these proteins could have acquired still needs to be elucidated.

At the Max Planck Institute for Chemical Ecology *P. cochleariae* is not kept on artificial diet but on one of its natural host plants: Chinese cabbage (*Brassica rapa ssp. pekinensis*). Interestingly, plant proteins from the beetle's diet were found still intact in the *P. cochleariae* gut content and were identified by mass spectrometry analysis [23]. After anion exchange chromatography and subsequent separation on an SDS-PAGE gel *P. cochleariae* PGs were detected in the same protein bands as host plant-derived polygalacturonase-inhibiting proteins (PGIPs). Since it is unlikely that these enzymes exhibit so similar chemico-physical properties, causing their co-occurrence in the same

fraction, an interaction between the two proteins was hypothesised by Kirsch et al. (2012) [23].

4.4 PG-PGIP interaction

PGIPs are extracellular, leucine-rich repeat glycoproteins that inhibit microbial PGs [17], [34], [35] and are ubiquitously distributed amongst the plant kingdom [36]. The number of PGIP-encoding genes ranges from two in *Arabidopsis thaliana* [37] to 16 in *Brassica napus* [38]. PGIPs are thought to play an important role in plant defence against microbial pathogens and were shown to limit fungal infections in plants [37], [39], [35]. They can be either constitutively expressed in the plant or their expression can be induced by abiotic (e.g. mechanical wounding or phytohormones) and biotic cues (e.g. pathogen infection or feeding of herbivores) [34], [40], [38]. Inhibition of PGs by PGIPs favors the accumulation of oligogalacturonides (OGs), elicitors of plant defence, and the expression of PGIPs induced by OGs, as for example known for PvPGIP2 and -3 [34] and AtPGIP1 [37], directly links the pectin degradation by PGs to the plant defence reaction [41]. Two models exist for the inhibition of PGs by PGIPs, which can occur in both a competitive [42] or non-competitive [43] inhibition mode. First, during face-to-face orientation of PGIP and PG the substrate binding site of the PG is covered, whereas this site is still accessible to the substrate in the second binding model [44]. PGIPs are not specific inhibitors for individual enzymes, but may bind a variety of different PGs. Recognition, however, is maintained by only a few amino acids, supported by the observation that a single point mutation can be sufficient to alter the PG-PGIP interaction towards loss or gain of recognition. PGIP-1 from *Phaseolus vulgaris* for example is not able to interact with a PG from *Fusarium moniliforme* but after one amino acid exchange this mutated PGIP was capable of binding and inhibiting the PG completely [45]. A functional redundancy and subfunctionalisation of PGIPs evolved probably to adapt plant defences against the variety of PGs of pathogenic microorganisms and phytophagous insects, leading to diverse PGIPs with different induction stimuli and PG recognition properties [34], [38]. Literature provides evidence for the inhibition of not only fungal but also insect PGs by PGIPs [46], [34]. PvPGIP3 and PvPGIP4 from bean (*P. vulgaris*), for example, were able to inhibit salivary PG activity of the two mirid plant bugs *Lygus rugulipennis* and *Adelphocoris lineolatus*. If PGs from *P. cochleariae* are also inhibited by plant-derived PGIPs, namely from its host plant *B. rapa* ssp. *pekinensis*, needs to be investigated. Active and inactive PGs have been shown to be expressed in a comparable abundance in *P. cochleariae* [11], but the function of the inactive proteins is still unknown. The large set of inactive, but yet expressed, PGs may contribute to plant

inhibitor circumvention. Kirsch et al. (2014) stated that “catalytically inactive proteins may act as “decoy” targets for PGIPs, thus protecting the active PGs from inhibition” [11]. The questions if first, plant PGIPs inhibit beetle PGs like their microbial counterparts and second, inactive PG proteins exhibit a different affinity towards PGIPs compared to active PGs are further addressed in this Master’s thesis.

5 Aim of Master's Thesis

The scope of my Master's thesis is to test for the inhibitory activity of plant extracts against *P. cochleariae* PGs and to identify plant-derived proteinaceous interaction partners potentially inhibiting the beetle's pectinases.

Therefor a yeast expression system for beetle PGs should be established in *Pichia pastoris*. Two PGs from *P. cochleariae*, the active PCO_GH28-1 and the inactive PCO_GH28-3, should be heterologously expressed and purified. Amongst the inactive proteins PCO_GH28-3 was selected due to the amino acid exchange from a conserved, catalytically important aspartate to an asparagine to make a potential later discovery of activity towards another substrate unlikely. The purified PGs should be immobilised on stationary phases and used for interaction studies with crude protein extracts from *B. rapa* ssp. *pekinensis* cell walls. The protocol for plant cell wall protein extraction of Feiz et al. [47] should be adapted and established for the use with *B. rapa* ssp. *pekinensis*. During the interaction studies SSC_GH28-6 should function as a positive control, a fungal PG which is known to interact with a PGIP from *B. napus*, which is closely related to *B. rapa* ssp. *pekinensis*. Potential plant interaction partners of the PGs should be identified with mass spectrometry to detect putative differential interactions of active and inactive PGs with plant proteins. Finally, this should help to test the hypothesis of Kirsch et al. (2014) that "catalytically inactive proteins may act as "decoy" targets for PGIPs, thus protecting the active PGs from inhibition" [11].

6 Material and Methods

6.1 Material

6.1.1 Plants

B. rapa ssp. *pekinensis*

Reared at Max Planck Institute for Chemical Ecology

6.1.2 Cells

Escherichia coli

One Shot® TOP10 Competent Cells

Thermo Fischer Scientific GmbH, Bonn

P. pastoris

SMD1168H *Pichia pastoris* Yeast Strain

Thermo Fischer Scientific GmbH, Bonn

6.1.3 Enzymes

KpnI

New England Biolabs GmbH, Frankfurt am Main

P. cochleariae gut content

Provided by Dr. Roy Kirsch

PCO_GH28-1, expressed in Sf9 insect cells

Provided by Dr. Roy Kirsch

PCO_GH28-3, expressed in Sf9 insect cells

Provided by Dr. Roy Kirsch

PCO_GH28-5, expressed in Sf9 insect cells

Provided by Dr. Roy Kirsch

PCO_GH28-6, expressed in Sf9 insect cells

Provided by Dr. Roy Kirsch

PCO_GH28-8, expressed in Sf9 insect cells

Provided by Dr. Roy Kirsch

PCO_GH28-9, expressed in Sf9 insect cells

Provided by Dr. Roy Kirsch

Phusion® High-Fidelity DNA Polymerase

New England Biolabs GmbH, Frankfurt am Main

PmeI

New England Biolabs GmbH, Frankfurt am Main

PmlI

New England Biolabs GmbH, Frankfurt am Main

PNGase F

New England Biolabs GmbH, Frankfurt am Main

SacI

New England Biolabs GmbH, Frankfurt am Main

SSC_GH28-6, expressed in Sf9 insect cells

Provided by Dr. Roy Kirsch

6.1.4 Kits

AminoLink® Plus Immobilization Kit

Thermo Fischer Scientific GmbH, Bonn

DNA Clean & Concentrator-5 Kit

Zymo Research Corporation, Irvine, CA, USA

EasySelect™ *Pichia* Expression Kit

Thermo Fischer Scientific GmbH, Bonn

GeneJET Plasmid Miniprep Kit

Thermo Fischer Scientific GmbH, Bonn

LigaFast™ Rapid DNA Ligation System Kit

Promega GmbH, Mannheim

PureLink® HiPure Plasmid Filter Midiprep Kit

Thermo Fischer Scientific GmbH, Bonn

SuperSignal™ West Dura Extended Duration Substrate Kit

Thermo Fischer Scientific GmbH, Bonn

Taq PCR Master Mix Kit

Qiagen GmbH, Hilden

ZR Fungal/Bacterial DNA MiniPrep™ Kit

Zymo Research Corporation, Irvine, CA, USA

Zymoclean™ Gel DNA Recovery Kit

Zymo Research Corporation, Irvine, CA, USA

6.1.5 Consumable Material

Amersham Hyperfilm DCL	GE Healthcare Life Sciences, München
CELLSTAR® CELLreactor™ Filter Tubes 15 ml and 50 ml	Greiner Bio-One GmbH, Frickenhausen
Criterion™ XT Bis-Tris Precast Gels	Bio-Rad Laboratories GmbH, München
Extra Thick Blot Filter Paper, Precut, 7.5x10 cm	Bio-Rad Laboratories GmbH, München
Gene Pulser®/Micropulser™ electroporation cuvettes, 0.2 cm	Bio-Rad Laboratories GmbH, München
HiTrap TALON® crude, 1 ml	GE Healthcare Life Sciences, München
HiTrap™ Phenyl FF (high sub), 1 ml	GE Healthcare Life Sciences, München
HiTrap™ ConA 4B, 1 ml	GE Healthcare Life Sciences, München
Immun Blot PVDF Membrane	Bio-Rad Laboratories GmbH, München
Microplate Nunc™ 0.2 ml flat bottom 96-well	Thermo Fischer Scientific GmbH, Bonn
Miracloth	Merck Chemicals GmbH, Darmstadt
Nalgene™ Single-Use PETG Erlenmeyer Flasks with Baffled Bottom, Sterile, 0.25 l, 0.5 l, 1 l and 2 l	Thermo Fischer Scientific GmbH, Bonn
Pierce™ Protein Concentrators, 9K MWCO, 20mL	Thermo Fischer Scientific GmbH, Bonn
Polypropylene Columns 1 ml	Qiagen GmbH, Hilden
RESOURCE S, 6 ml	GE Healthcare Life Sciences, München
RESOURCE Q, 6 ml	GE Healthcare Life Sciences, München
Slide-A-Lyzer™ Dialysis Cassettes, 10K MWCO, 12 mL	Thermo Fischer Scientific GmbH, Bonn
SnakeSkin™ Dialysis Tubing 35 mm I.D., 10K MWCO	Thermo Fisher Scientific Inc., Waltham, MA USA
TALON® Superflow, 10 ml	GE Healthcare Life Sciences, München
TLC Silica Gel 60	Merck KGaA, Darmstadt
Zeba™ Spin Desalting Column	Thermo Fischer Scientific GmbH, Bonn

6.1.6 Chemicals

2-(N-morpholino)ethanesulphonic acid (MES)	Carl Roth GmbH + Co. KG, Karlsruhe
3,5-Dinitrosalicylic acid	Sigma-Aldrich Chemie GmbH, Hamburg
Acetic acid	Carl Roth GmbH + Co. KG, Karlsruhe
Acetone	Carl Roth GmbH + Co. KG, Karlsruhe
Agar	Sigma-Aldrich Chemie GmbH, Hamburg
Ammonium acetate	Carl Roth GmbH + Co. KG, Karlsruhe
Ammonium sulphate	Carl Roth GmbH + Co. KG, Karlsruhe
Anti-His(C-term)-HRP Antibody	Thermo Fischer Scientific GmbH, Bonn
Anti-V5-HRP Antibody	Thermo Fischer Scientific GmbH, Bonn
Biotin	Sigma-Aldrich Chemie GmbH, Hamburg
BSA	Bio-Rad Laboratories GmbH, München
Calcium chloride	Carl Roth GmbH + Co. KG, Karlsruhe
Citric acid	Carl Roth GmbH + Co. KG, Karlsruhe
Coumaric acid	Sigma-Aldrich Chemie GmbH, Hamburg
Cross-linked pectin	Provided by Dr. Roy Kirsch
Cross-linked pectin, methylated	Provided by Dr. Roy Kirsch
Digalacturonic acid	Santa Cruz Biotechnology, Inc., Dallas, TX, USA
Di-potassium hydrogen phosphate	Carl Roth GmbH + Co. KG, Karlsruhe

Di-sodium hydrogen phosphate	Carl Roth GmbH + Co. KG, Karlsruhe
DL-Dithiothreitol	Sigma-Aldrich Chemie GmbH, Hamburg
dNTPs	Carl Roth GmbH + Co. KG, Karlsruhe
Ethanol	VWR International GmbH, Darmstadt
Ethidium bromide solution 1%	Carl Roth GmbH + Co. KG, Karlsruhe
Ethyl acetate	Merck KGaA, Darmstadt
Formic acid	Carl Roth GmbH + Co. KG, Karlsruhe
GBX Developer and Replenisher	Kodak GmbH, Stuttgart
GBX Fixer and Replenisher	Kodak GmbH, Stuttgart
Glucose	Carl Roth GmbH + Co. KG, Karlsruhe
Glycerol	Carl Roth GmbH + Co. KG, Karlsruhe
Hydrochloric acid	Thermo Fischer Scientific GmbH, Bonn
Hydrogen peroxide	Honeywell Specialty Chemicals Seelze GmbH, Seelze
Imidazole	Carl Roth GmbH + Co. KG, Karlsruhe
Isopropanol	Carl Roth GmbH + Co. KG, Karlsruhe
LiChrosolv® Water	Merck KGaA, Darmstadt
Lithium acetate	Sigma-Aldrich Chemie GmbH, Hamburg
Luminol	Fluka Biochemika, Buchs, CH
Manganese chloride	Sigma-Aldrich Chemie GmbH, Hamburg
Methanol	Carl Roth GmbH + Co. KG, Karlsruhe
Methyl- α -D-glucoside	Sigma-Aldrich Chemie GmbH, Hamburg
Monogalacturonic acid	Santa Cruz Biotechnology, Inc., Dallas, TX, USA
O'Gene Ruler 1 kb DNA Ladder Plus	Thermo Fischer Scientific GmbH, Bonn
Orange DNA Loading Dye 6x	Thermo Fischer Scientific GmbH, Bonn
Orcinol	Sigma-Aldrich Chemie GmbH, Hamburg
PageBlue Protein Staining Solution	Thermo Fischer Scientific GmbH, Bonn
PageRuler Plus Prestained Protein Ladder	Thermo Fischer Scientific GmbH, Bonn
Pectin from apple	Sigma-Aldrich Chemie GmbH, Hamburg
Pectin, esterified from citrus fruit	Sigma-Aldrich Chemie GmbH, Hamburg
Pectin, from citrus peel	Sigma-Aldrich Chemie GmbH, Hamburg
Phenol	Acros Organics N.V., Geel, BE
Polygalacturonic acid demethylated, prepared from citrus pectin	Megazyme International Ireland, Bray, IRL
Potassium di-hydrogen phosphate	Carl Roth GmbH + Co. KG, Karlsruhe
Potassium sodium tartrate	Sigma-Aldrich Chemie GmbH, Hamburg
Protease Inhibitor Cocktail (for plant cell and tissue extracts)	Sigma-Aldrich Chemie GmbH, Hamburg
Protein Assay Dye Reagent Concentrate	Bio-Rad Laboratories GmbH, München
Roti®-Phenol/Chloroform/Isoamylalcohol	Carl Roth GmbH + Co. KG, Karlsruhe
Ruthenium Red	Sigma-Aldrich Chemie GmbH, Hamburg
SeaKem® LE Agarose	Lonza Verviers, S.p.r.l., Verviers, B
Sodium acetate	Carl Roth GmbH + Co. KG, Karlsruhe
Sodium azide	Fluka Biochemika, Buchs, CH
Sodium chloride	Carl Roth GmbH + Co. KG, Karlsruhe
Sodium deoxycholate	Fluka Biochemika, Buchs, CH

Sodium di-hydrogen phosphate	Carl Roth GmbH + Co. KG, Karlsruhe
Sodium dodecyl sulphate	Carl Roth GmbH + Co. KG, Karlsruhe
Sodium hydroxide	Carl Roth GmbH + Co. KG, Karlsruhe
Sodium sulphite	Sigma-Aldrich Chemie GmbH, Hamburg
Sorbitol	Carl Roth GmbH + Co. KG, Karlsruhe
Sucrose	Carl Roth GmbH + Co. KG, Karlsruhe
Sulphuric acid	Carl Roth GmbH + Co. KG, Karlsruhe
SYBR [®] Safe DNA Gel Stain	Thermo Fischer Scientific GmbH, Bonn
Trichloroacetic acid (TCA)	Sigma-Aldrich Chemie GmbH, Hamburg
Trigalacturonic acid	Santa Cruz Biotechnology, Inc., Dallas, TX, USA
Tris(hydroxymethyl)aminomethane (Tris)	Carl Roth GmbH + Co. KG, Karlsruhe
Tryptone	Duchefa Biochemie B.V, Haarlem, NL
Tween-20	Sigma-Aldrich Chemie GmbH, Hamburg
XT Reducing Agent (20x)	Bio-Rad Laboratories GmbH, München
Yeast extract	Duchefa Biochemie B.V, Haarlem, NL
Yeast Nitrogen Base (YNB)	Thermo Fischer Scientific GmbH, Bonn
Zeocin [™] (100 mg/ml)	Thermo Fischer Scientific GmbH, Bonn

6.1.7 Primer

URP-pIBV5H6-Kpn-STOP	attaggtagcTCAATGGTGATGGTGATGATGACC
5' AOX1 <i>Pichia</i> Primer	GACTGGTTCCAATTGACAAGC
3' AOX1 <i>Pichia</i> Primer	GCAAATGGCATTCTGACATCC
PCO28-1pPICZaA-F	taatcacgtggACCCCGGTTGCTGATTCCG
PCO28-3pPICZaA-F	taatcacgtggAAATCTGCCCTTGAGACAACCTGC
SSC28-6pPICZaA-F	taatcacgtggCAAACAGCATGCACTGCTTCAG

6.1.8 Plasmids

<u>pIB/V5-His TOPO[®] Vector</u>	Thermo Fischer Scientific GmbH, Bonn Provided by Dr. Roy Kirsch
pIB/V5-His- <i>PCO_GH28-1</i> (codes for PG PCO_GH28-1 ORF from <i>P. cochleariae</i>)	
pIB/V5-His- <i>PCO_GH28-3</i> (codes for PG PCO_GH28-3 ORF from <i>P. cochleariae</i>)	
pIB/V5-His-SSC_ <i>GH28-6</i> (codes for PG SSC_GH28-6 ORF from <i>Sclerotinia sclerotiorum</i>)	
<u>pPICZα A vector</u>	Thermo Fischer Scientific GmbH, Bonn
pPICZα A- <i>PCO_GH28-1</i> (codes for PG PCO_GH28-1 ORF from <i>P. cochleariae</i>)	
pPICZα A- <i>PCO_GH28-3</i> (codes for PG PCO_GH28-3 ORF from <i>P. cochleariae</i>)	
pPICZα A-SSC_ <i>GH28-6</i> (codes for PG SSC_GH28-6 ORF from <i>S. sclerotiorum</i>)	

6.1.9 Devices

ÄKTA FPLC System	GE Healthcare Life Sciences, München
Dark Reader DR195M Transilluminator	Clare Chemical Research, Inc., Dolores, CO, USA
GenePulser Xcell™ Electroporation System	Bio-Rad Laboratories GmbH, München
Infinite® M200	Tecan Group Ltd. Männedorf, CH
Mastercycler EP Gradient	Eppendorf AG, Hamburg
NanoDrop ND-1000 Spectrophotometer	Peqlab Biotechnologie GmbH, Erlangen
Tissue Lyser LT	Qiagen GmbH, Hilden
Trans-Blot® transfer cell	Bio-Rad Laboratories GmbH, München

6.1.10 Software

BLAST Alignment (bl2seq)	http://blast.ncbi.nlm.nih.gov , National Center for Biotechnology Information (NCBI), Bethesda, MD, USA
Edit Seq	DNAStar, Inc., Madison, WI, USA
EnsemblPlants <i>B. rapa</i> BLAST search	http://plants.ensembl.org , The European Bioinformatics Institute, Hinxton, UK
i-control™ Microplate Reader Software	Tecan Group Ltd. Männedorf, CH
Microsoft Excel® 2010	Microsoft Corporation, Redmond, WA, USA
NetNGlyc 1.0	http://www.cbs.dtu.dk/services/NetNGlyc/ , Technical University of Denmark, DK
PCR Primer Design Tool Eurofins Genomics	http://www.mwg-biotech.com/ , MWG-Biotech AG, Ebersberg
PSORT Prediction	http://psort.hgc.jp/form.html , Kenta Nakai, University of Tokyo, J
SeqMan Pro	DNAStar, Inc., Madison, WI, USA
SignalP 4.1	http://www.cbs.dtu.dk/services/SignalP/ , Technical University of Denmark, DK

6.1.11 Buffer and Media

XT MES Running Buffer	Bio-Rad Laboratories GmbH, München
TBS 10x	Bio-Rad Laboratories GmbH, München
Rotiphorese® 50x TAE Buffer	Carl Roth GmbH + Co. KG, Karlsruhe
S.O.C. medium	Thermo Fischer Scientific GmbH, Bonn
NEBuffer 1.1	New England Biolabs GmbH, Frankfurt am Main
10x Tris/Glycin Buffer	Bio-Rad Laboratories GmbH, München
XT Sample Buffer (4x)	Bio-Rad Laboratories GmbH, München
Phusion® HF Buffer (5x)	New England Biolabs GmbH, Frankfurt am Main

AEC Binding Buffer	20 mM	Tris-HCl, pH 8.0
AEC Elution Buffer	20 mM	Tris-HCl, pH 8.0
	1 M	Sodium chloride
AminoLink® Binding/Wash Buffer	50 mM	Citrate phosphate buffer, pH 5.0
	0.15 M	NaCl
AminoLink® Elution Buffer	0.1 M	Glycine HCl pH 2.0

AminoLink [®] Neutralisation Buffer	1 M	Tris
BMGY Medium	1%	Yeast extract
	2%	Tryptone
	0.1 M	Potassium phosphate buffer, pH 6.0
	1.34%	YNB
	4·10 ⁻⁵ %	Biotin
	1%	Glycerol
BMMY Medium	1%	Yeast extract
	2%	Tryptone
	0.1 M	Potassium phosphate buffer, pH 6.0
	1.34%	YNB
	4·10 ⁻⁵ %	Biotin
	1%	Methanol
CEC Binding Buffer	20 mM	MES, pH 6.0
CEC Elution Buffer	20 mM	MES, pH 6.0
	1 M	NaCl
Cell Wall Extraction Buffer I	5 mM	Sodium acetate, pH 4.6
	0.4 M	Sucrose
Cell Wall Extraction Buffer II	5 mM	Sodium acetate, pH 4.6
	0.6 M	Sucrose
Cell Wall Extraction Buffer III	5 mM	Sodium acetate, pH 4.6
	1 M	Sucrose
Citrate phosphate buffer, pH 5.0, 0.2 M	0.1 M	Citric acid
	0.2 M	Di-sodium hydrogen phosphate
ConA Binding Buffer	20 mM	Tris-HCl pH7.4
	0.5 M	Sodium chloride
	1 mM	Manganese chloride
	1 mM	Calcium Chloride

ConA Elution Buffer	20 mM	Tris-HCl pH7.4
	0.5 M	Sodium chloride
	0.5 M	Methyl- α -D-glucoside
DNS assay solution1	1%	3,5-Dinitrosalicylic acid
	0,2%	Phenol
	1%	Sodium hydroxide
DNS assay solution 2	5%	Sodium sulphite
DNS assay solution 3	40%	Potassium sodium tartrate
HIC Binding Buffer	50 mM	Sodium phosphate buffer, pH 7.0
	1.5 M	Ammonium sulphate
HIC Elution Buffer	50 mM	Sodium phosphate buffer, pH 7.0
IMAC Binding Buffer	50 mM	Sodium phosphate buffer, pH 7.4 / pH 8.0
	0.5 M	NaCl
IMAC Wash Buffer	50 mM	Sodium phosphate buffer, pH 7.4 pH 8.0
	0.3 M	NaCl
	10 mM	Imidazole
IMAC Elution Buffer	50 mM	Sodium phosphate buffer, pH 7.4
	0.3 M	Imidazole
Lithium acetate buffer [48]	0.1 mM	Lithium acetate
	10 mM	Dithiothreitol
	0.6 M	Sorbitol
	10 mM	Tris-HCl, pH 7.5
Low Salt LB Agar	1%	Tryptone
	5%	Sodium chloride
	5%	Yeast extract
	2%	Agar
Low Salt LB Medium	1%	Tryptone
	5%	Sodium chloride
	5%	Yeast extract

PBS pH 7.2	0.1 M	Sodium phosphate buffer pH 7.2	
	0.15 M	Sodium chloride	
Plant protein extraction 0.2 M CaCl ₂ solution	5 mM	Sodium acetate, pH 4.6	
	0.2 M	Calcium chloride	
	10 µl	Protease Inhibitor Cocktail (per 0.65 g dry cell wall)	
Plant protein extraction 1 M NaCl solution	5 mM	Sodium acetate, pH 4.6	
	1 M	NaCl	
	10 µl	Protease Inhibitor Cocktail (per 0.65 g dry cell wall)	
TBST	20 mM	Tris-HCl, pH 7.4	10x TBS
	0.5 M	NaCl	
	0,1%	Tween-20	
Western Blot Transfer Buffer	25 mM	Tris-HCl, pH 8.3	10x Tris/Glycin Buffer
	0.19 M	Glycine	
	10 %	Methanol	
YPD Medium	1%	Yeast extract	
	2%	Tryptone	
	2%	Glucose	
YPDS Agar	1%	Yeast extract	
	2%	Tryptone	
	2%	Glucose	
	1 M	Sorbitol	
	2%	Agar	

Sodium and potassium phosphate buffers were prepared by mixing the corresponding salt solutions (Na₂HPO₄/NaH₂PO₄ or K₂HPO₄/KH₂PO₄) until the desired pH was reached.

All buffers and media were prepared using ddH₂O or ultrapure H₂O. For all other reactions LiChrosolv[®] Water was used.

6.2 Methods

6.2.1 Cloning of PGs into pPICZα A

6.2.1.1 PCR

The open reading frames (ORFs) for the PGs PCO_GH28-1, PCO_GH28-3 and SSC_GH28-6 were cloned into a pIB/V5-His-TOPO[®] vector [49], [50] and provided by Dr. Roy Kirsch (sequences see Supplementary Data 13.1). To amplify the sequences, a PCR was performed using the respective forward primers PCO28-1pPICZαA-F, PCO28-3pPICZαA-F and SSC28-6pPICZαA-F as well as the reverse primer URP-pIBV5H6-Kpn-STOP (for primer sequences see 6.1.7). The primers were designed in a way that they introduced recognition sequences for the restriction enzyme Pml upstream of the PG ORF. Downstream of the ORF a recognition site for KpnI as well as a translation termination signal was introduced, including the V5 and the His₆ epitope from the pIB/V5-His-TOPO[®] vector into the amplified sequence. The PCR Primer Design tool on the Eurofins Genomics website was used to determine the respective melting temperatures.

The PCR reaction was performed using a *Taq* PCR Master Mix Kit [51] and a Mastercycler EP Gradient.

A		Volume [μl]		B		35x
2x <i>Taq</i> PCR Master Mix	25			94°C	2 min	
Primer fwd (10 mM)	1			94°C	20 s	
Primer rev (10 mM)	1			58°C	20 s	
Template DNA (10 ng/μl)	1			72°C	2 min	
H ₂ O	22			4°C	∞	
Total volume	50					

Volumes used for a 50 μl PCR (A) and PCR program with *Taq* PCR Master Mix Kit and gene specific primers (B).

6.2.1.2 Purification of PCR products

The PCR products were purified with the DNA Clean & Concentrator[™]-5 Kit according to the manufacturer's instructions [52]. All centrifugation steps were carried out at 16 000 x g. Two volumes of Binding Buffer were added to each volume of PCR solution and the mixture was loaded onto a Zymo-Spin[™] Column, which was placed in a 2 ml Collection Tube. After centrifugation (30 s) the flow-through was discarded. 200 μl of

Wash Buffer were added, spun down (30 s) and the washing step was repeated. Afterwards the column was placed in a new 1.5 ml reaction tube and eluted with 8 µl DNA Elution Buffer by centrifugation (1 min).

The concentration and quality of the purified PCR products were measured with a NanoDrop ND-1000 Spectrophotometer and monitored on a 1.2% agarose gel (0.07% ethidium bromide, 120 V, 30 min).

6.2.1.3 Digest of PCR products and pPICZα A vector

To clone the PCR products into the plasmid pPICZα A both, the PCR product as well as the plasmid, needed to be digested with the restriction enzymes KpnI and PmlI. A double digest was performed with the two enzymes for 2 h at 37°C. The reaction solution of the plasmid pPICZα A was separated on a 1.2% agarose gel (0.07% ethidium bromide, 120 V, 30 min) to monitor the digestion efficiency.

	Volume [µl]
PCR product / pPICα A	1 µg
KpnI	1
PmlI	1
10x NEBuffer 1.1	3
H ₂ O	ad 30

Volumes used for a 30 µl double digest with KpnI and PmlI.

6.2.1.4 Purification of digested PCR products and pPICZα A

Analogous to 6.2.1.2 the cut PCR products were purified with the DNA Clean & Concentrator™-5 Kit. Purification of the cut vector pPICZα A was performed with the Zymoclean™ Gel DNA Recovery Kit according to the manufacturer's instructions [53]. After separation on a 1.2% agarose gel (5% SYBR® Safe DNA Gel Stain, 120 V, 30 min) the band of the digested vector was cut out on a Dark Reader DR195M Transilluminator and 3 volumes of ABD were added to each volume excised from the gel. As soon as the agarose gel was completely dissolved at 50°C it was transferred to a Zymo-Spin™ Column in a Collection Tube and centrifuged (1 min). All centrifugation steps were carried out at 16 000 x g. The flow-through was discarded and the column was washed two times. For this 200 µl DNA Wash Buffer were added and centrifuged (30 s). Then the column was placed in a new 1.5 ml reaction tube and the DNA was eluted by the addition of 8 µl DNA Elution Buffer and subsequent 30 s centrifugation.

The DNA concentration and quality were measured with a NanoDrop ND-1000 Spectrophotometer. The purified PCR products and vector were stored at -20°C until further use.

6.2.1.5 Ligation

For the ligation of the PCR products with the plasmid pPICZα A the plasmid and the PCR product were mixed in an approximate 2:1 ratio. The use of the LigaFast™ DNA Ligation System allows a ligation at room temperature in 15 min [54]. After the ligation reaction the ligase was heat inactivated by incubating the mixture at 70°C for 10 min.

	Volume
pPICZα A	90 ng
PCR product (cut with KpnI, PmlI)	44 – 66 ng
T4 DNA Ligase	1 µl
2x Rapid Ligation Buffer	5 µl
H ₂ O	ad 10 µl

Volumes used for a 10 µl ligation reaction.

6.2.2 Transformation of *E. coli*

E. coli were transformed with the plasmid pPICZα A as well as the plasmid containing the sequences for the PGs (pPICZα A-PCO_GH28-1, pPICZα A PCO_GH28-3 and pPICZα A-SSC_GH28-6). 0.5 µg plasmid pPICZα A were mixed with 50 µl *E. coli* One Shot® TOP10 Competent Cells as well as 3 µl ligation solution (6.2.1.5) with 25 µl *E. coli* respectively and kept on ice for 15 min. After 30 s of heat shock at 42°C 250 µl S.O.C medium was added. The cells were incubated for 1 h at 37°C and 250 rpm.

E. coli transformed with pPICZα A without insert were inoculated in 5 ml LB Medium (25 µg/ml Zeocin™) and cultured in 15 ml filter tubes overnight (37°C, 250 rpm). Alternatively, they were plated on Low Salt LB Agar (25 µg/ml Zeocin™) and grown over night at 37°C. The latter was done for *E. coli* that were transformed with the ligation solution. Colonies growing on the plates were inoculated in 5 ml LB Medium (25 µg/ml Zeocin™) and cultured overnight (37°C, 250 rpm). Due to the light instability of Zeocin™ all overnight cultures were grown in the dark.

6.2.3 Miniprep of plasmids from *E. coli* cultures

A plasmid isolation from *E. coli* cultures was performed with the GeneJET Plasmid Miniprep Kit according to the manufacturer's instructions [55]. All centrifugations were carried out at 16 000 x g, if not stated otherwise. 4 ml of *E. coli* overnight culture were

harvested by centrifugation (6800 x g, 2 min). The supernatant was decanted and the pellet was resuspended in 250 µl Resuspension Solution by vortexing.

After adding 250 µl Lysis Solution and inverting the reaction tube 350 µl of Neutralisation Solution were added and mixed carefully. Centrifugation for 10 min pelleted cell debris and chromosomal DNA. The supernatant was transferred to a GeneJET Spin Column and centrifuged (1 min). The flow-through was discarded, the column was washed with 500 µl Wash Solution and the flow-through was discarded again. The plasmid DNA was eluted with 30 µl of Elution Buffer by 2 min of centrifugation. Concentration and quality of the isolated DNA were measured with a NanoDrop ND-1000 Spectrophotometer. The solution was stored at -20°C until further use.

6.2.4 Verification of pPICZα A inserts

6.2.4.1 Test digest

The isolated plasmids were cut with the restriction enzymes KpnI and PmlI to see if a PCR product had successfully integrated into the vector. The mixture was incubated at 37°C for 1 h and afterwards separated on a 1.2% agarose gel (0.07% ethidium bromide, 120 V, 30 min).

	Volume [µl]
Plasmid DNA	1
KpnI	1
PmlI	1
10x NEBuffer 1.1	1,5
H ₂ O	11,5
Total volume	15

Volumes used for a 15 µl test digest of isolated plasmids.

6.2.4.2 Test PCR

Additionally, a PCR using 3' AOX1 *Pichia* Primer and 5' AOX1 *Pichia* Primer was performed to amplify a potential insert from the plasmid. AOX1 priming sites are located upstream and downstream of the multiple cloning site in which the insert should integrate. Subsequently the solution was separated on a 1.2% agarose gel (0.07% ethidium bromide, 120 V, 30 min).

A	Volume [μ l]	B	
2x <i>Taq</i> PCR Master Mix	10	94°C	2 min
Primer fwd (10 mM)	0.5	94°C	20 s
Primer rev (10 mM)	0.5	56°C	20 s
Template DNA (10 ng/ μ l)	0.5	72°C	2 min
H ₂ O	8.5	4°C	∞
Total volume	20		

35x

Volumes used for a 20 μ l PCR (A) and PCR program with *Taq* PCR Master Mix Kit and AOX1 *Pichia* Primers (B).

6.2.4.3 Sequencing

Plasmids tested positively for an insert were used for sequencing to verify the sequence identity of the inserts in the pPICZ α A plasmids. Sequencing was performed by the in-house sequencing service using 3' AOX1 *Pichia* Primer and 5' AOX1 *Pichia* Primer for a forward and reverse sequence of the insert respectively.

	Volume [μ l]
Primer fwd or rev (10 mM)	0.5
Template DNA	0.5
H ₂ O	ad 6 μ l

Volumes used for a sequencing PCR. The residual solutions are added by the sequencing service.

6.2.5 Midiprep of plasmids from *E. coli* cultures

For *E. coli* colonies whose plasmids have been confirmed to carry a correct insert 200 μ l of a 5 ml overnight pre-culture were inoculated into 50 ml LB Medium (25 μ g/ml ZeocinTM) and cultured at 37°C and 250 rpm overnight in the dark. To isolate the plasmids the PureLink[®] HiPure Plasmid Filter Midiprep Kit was used according to the manufacturer's instructions for Midiprep Procedure [56]. The cells of the total culture were harvested by 10 min centrifugation at 4000 x g and the medium was removed. Then 10 ml Resuspension Buffer were used to resuspend the cells until it became a homogenous suspension. Cell lysis was achieved by adding 10 ml of Lysis Buffer and inverting the tube to mix the lysate to homogeneity. After 5 min incubation at room temperature 10 ml of Precipitation Buffer were added and mixed immediately. The mixture was transferred into a HiPure Filter Midi Column that was equilibrated with

15 ml Equilibration Buffer beforehand. When the lysate had drained through the column by gravity flow, the flow-through was discarded and the inner Filtration Cartridge was removed. The Midi Column was washed with 20 ml Wash Buffer and the flow-through was discarded after gravity-driven dripping of the solution through the column. Elution of the DNA was achieved by adding 5 ml Elution Buffer and letting the eluate drain by gravity flow. For the precipitation of DNA 3.5 ml isopropanol were added to the eluate and incubated for 1 h at 4°C. The DNA was pelleted by centrifugation (30 min, 16 000 x g, 4°C). To wash the pellet it was resuspended in 500 µl 70% ethanol and centrifuged again (5 min, 16 000 x g, 4°C). After removal of the supernatant and air-drying the pellet was resuspended in 20 µl TE Buffer. Concentration and quality of the isolated plasmid DNA were measured with a NanoDrop ND-1000 Spectrophotometer. The solutions were stored at -20°C until further use.

6.2.6 Preparing competent *P. pastoris* cells

For the transformation of *P. pastoris* competent cells are needed. For this a combination of the protocol from the EasySelect™ *Pichia* Expression Kit manual [57] and chemical pretreatment described by Wu et al. [48] was used.

First *P. pastoris* SMD1168H cells were inoculated into 5 ml YPD Medium in 50 ml filter tubes and grown overnight (30°C, 250 rpm). Then they were inoculated in 100 ml YPD medium in a way that they grew to a cell density of $OD_{600} = 1 - 1.5$ overnight. 1 OD_{600} , the absorbance at 600 nm, is equivalent to $5 \cdot 10^7$ cells/ml [57].

The cells of the 100 ml overnight cultures were pelleted by centrifugation (5 min, 3000 x g, 4°C). The pellet was resuspended in ice-cold sterilised water and pelleted again, first using 100 ml, then 50 ml. $8 \cdot 10^8$ cells were suspended in 8 ml lithium acetate buffer and incubated at room temperature for 30 min. Then the cells were again pelleted and resuspended in 10 ml ice-cold 1 M sorbitol. After another centrifugation step the cell pellet was washed two times with 1.5 ml sorbitol. At last the pellet was resolved in 1 ml sorbitol and 100 µl aliquots were stored at -80°C.

6.2.7 Transformation of *P. pastoris*

6.2.7.1 Linearisation and purification of pPICZα A vectors

Linearised pPICZα A integrates into the AOX1 region of *P. pastoris* by gene insertion [57]. Therefor pPICZα A, pPICZα A-PCO_GH28-1, pPICZα A PCO_GH28-3 and pPICZα A-SSC_GH28-6 were linearised with the restriction enzyme PmeI. The mixture was incubated at 37°C for 1 h.

	Volume [μ l]
Plasmid	10 ng
PmeI	10
10x NEBuffer CutSmart	10
H ₂ O	ad 100

Volumes used for a 100 μ l linearisation of pICZ α A plasmid with and without insert.

After adding 100 μ l H₂O to the reaction mixture the purification of the DNA was performed using an equal volume of phenol/chloroform/isoamyl alcohol (25:24:1) and vortexing for 10 s. Centrifugation (5 min, 16 000 x g) results in the formation of different phases. The DNA is contained in the upper aqueous phase and was transferred to a new reaction tube. 1/10 volume of ammonium acetate (pH 5.2) was added and after subsequent mixing 2 volumes of ice-cold 100% ethanol were added. The mixture was placed on ice for 5 min and then centrifuged (5 min, 16 000 x g) to pellet the DNA. The samples were washed with 1 ml of 70% ethanol (room temperature) by inverting it several times and pelleting it by centrifugation once more. The pellet was air-dried after the removal of the supernatant and resolved in 10 μ l H₂O. The concentration and quality of the isolated DNA were measured with a NanoDrop ND-1000 Spectrophotometer and the solution was stored at -20°C until further use. The success of the linearisation was determined via agarose gel electrophoresis (1.2% agarose gel, 0.07% ethidium bromide, 120 V, 30 min) by comparison of digested and non-digested plasmid.

6.2.7.2 Electroporation

To transform the competent *P. pastoris* cells (6.2.6) with the linearised plasmids electroporation was used. 5 μ g of linearised and subsequently purified plasmid DNA in a total volume of 10 μ l were mixed with 90 μ l of competent *P. pastoris* SMD1168H cells on ice by gently adding the cells to the plasmid solution without pipetting up and down. The mixture was transferred to a pre-cooled 0.2 cm Gene Pulser[®]/Micropulser[™] electroporation cuvette and pulsed in a GenePulser Xcell[™] Electroporation System (1500 V, 25 μ F, 200 Ω and 0.2 cm cuvette). Immediately 1 ml of ice-cold 1 M sorbitol was added. The mixture was transferred to a 15 ml filter tube and incubated at 30°C for 1 h without shaking. Afterwards 100 and 400 μ l of the transformation solution were plated each on YPDS agar plates containing 100 and 250 μ g/ml Zeocin[™] respectively. They were kept at 30°C in the dark until colonies were visible.

6.2.7.3 Determination of transformation-positive *P. pastoris* colonies

Furthermore it should be determined which of the colonies of the transformation had successfully integrated the linearised plasmid into the genome. Therefor single colonies were inoculated in YPD Medium, grown over night at 30°C and 250 rpm in 50 ml filter tubes and pelleted by centrifugation (2 min, 2500 x g). The gDNA was extracted and subsequently a PCR was performed using AOX1 and gene specific primers respectively.

6.2.7.3.1 Extraction of gDNA from *P. pastoris*

For the gDNA extraction from *P. pastoris* the ZR Fungal/Bacterial DNA MiniPrep™ Kit was used according to the manufacturer's instructions [58]. 100 mg of *P. pastoris* cells (wet weight) were resuspended in 200 µl H₂O, transferred to a ZR BashingBead™ Lysis Tube and mixed with 750 µl Lysis Solution. Cell lysis was accomplished by mechanical forces in a Tissue Lyser LT (5 min, 50 oscillations/s). In addition to the protocol the samples were incubated at 55°C for 30 min with vortexing in between. Afterwards centrifugation was performed at 10 000 x g for 1 min, the supernatant was transferred to a Zymo-Spin™ IV Spin Filter in a Collection Tube and centrifuged again (1 min, 7000 x g). 1.2 ml of Fungal/Bacterial DNA Binding Buffer were added to the flow-through, 800 µl of the mixture was transferred to a Zymo-Spin™ IIC Column in a Collection Tube and centrifuged. This and all following centrifugation steps were carried out at 10 000 x g for 1 min. After discard of the flow-through another 800 µl were added to the column and spun down. The column was washed with 200 µl of DNA Pre-Wash Buffer and 500 µl Fungal/Bacterial DNA Wash Buffer under subsequent centrifugation respectively. Then it was placed in a 1.5 ml reaction tube and the DNA was eluted by addition of 100 µl H₂O and subsequent centrifugation. The concentration and quality of the isolated DNA were measured with a NanoDrop ND-1000 Spectrophotometer.

6.2.7.3.2 PCR of gDNA from *P. pastoris*

For the determination of insert-positive clones a PCR was performed using the respective 3' and 5' AOX1 *Pichia* primer or gene-specific primer (PCO28-1pPICZaA-F, PCO28-3pPICZaA-F or SSC28-6pPICZaA-F and URP-pIBV5H6-Kpn-STOP). The AOX1 *Pichia* primer amplify the insert as well as the *P. pastoris* AOX1 gene (approx. 2.2 kb [57]), while the gene-specific primers result in only one product, if the clone is positive for the insert.

A		Volume [μl]	B		
5x Phusion HF Buffer	4		98°C	1 min	
dNTPs (10 mM)	0,4		98°C	20 s	35x
Primer fwd (10 mM)	0.5		56°C	20 s	
Primer rev (10 mM)	0.5		72°C	2 min	
Template DNA	100 ng		4°C	∞	
Phusion® DNA Polymerase	0.2				
H ₂ O	ad 20				
Volumes used for a 20 μl PCR of gDNA from <i>P. pastoris</i> (A) and PCR programs. (B) PCR program using the Phusion® DNA Polymerase and AOX1 primer, (C) and PCR program for Phusion® DNA polymerase and gene-specific primer.			C		
			98°C	2 min	
			98°C	20 s	35x
			58°C	20 s	
			72°C	2 min	
			4°C	∞	

6.2.8 Glycerol stocks

Glycerol stocks were made to preserve *P. pastoris* as well as *E. coli* cells that were tested positive for a specific insert or plasmid for later experiments. Therefore 1 ml of YPD (*P. pastoris*) or LB (*E. coli*) overnight culture was mixed with 20% glycerol, frozen in liquid nitrogen and stored at -80°C.

6.2.9 Small-scale expression (5 ml) of PGs in *P. pastoris*

The *P. pastoris* clones that were tested positive for the integration of the PG ORF-containing insert into the genome were tested for the expression of the recombinant proteins. A small-scale expression using 5 ml medium in 50 ml filter tubes and subsequent Western Blot or Coomassie staining of a polyacrylamide gel was used to detect the potential expression of recombinant proteins. The expression was performed as a combination of the EasySelect™ *Pichia* Expression Kit manual [57] and the small-scale expression protocol described by Li et al. (2010) [59].

First 50 μl *P. pastoris* glycerol stock were inoculated in 5 ml YPD Medium in 50 ml filter tubes and grown to stationary phase overnight (30°C, 250 rpm). Then the cells were inoculated in 5 ml BMGY Medium in a way that the cultures reached an optical density of OD₆₀₀ = 2 – 6 the next day, so that the cells will be in log phase growth. The doubling time for Mut⁺ *P. pastoris* strains, such as SMD1168H, is approximately 2 h [57]. After determining the optical density 5 · 10⁸ cells, which are equivalent to 10 OD₆₀₀ units, were pelleted by centrifugation (2 min, 2500 x g) and washed once with 1 ml BMMY Medium. The cell pellet was resuspended in 1 ml BMMY Medium and combined with

BMMY Medium to a total volume of 5 ml. While growing at 30°C and 250 rpm the expression was induced with a 1% methanol pulse every 12 h or in alternating intervals of 8 and 16 h respectively, keeping one of the treatments constant during one expression. 100 µl samples were taken at each point of induction, centrifuged (5 min, 3000 x g) and the supernatant was stored at -20°C for further analysis. At the same time samples were taken for the measurement of the optical density and the volumes were refilled to 5 ml with BMMY medium.

6.2.10 Large-scale expression of PGs in *P. pastoris*

Prior to the expression *P. pastoris* from a glycerol stock were streaked out on YPDS agar plates containing 100 µg/ml ZeocinTM and grown at 30°C in the dark for 4 days. Single clones were inoculated in 5 ml YPD or BMGY Medium in 50 ml filter tubes and grown to stationary phase for two days (30°C, 250 rpm). To have cells in log phase growth the cells were inoculated in 25 ml BMGY medium in 250 ml baffled flasks in a way that the cultures reached an optical density of OD₆₀₀ = 2 – 6 the next day. The doubling time accounts for approximately 2 h for SMD1168H, a Mut⁺ *P. pastoris* strain [57]. After the determination of the optical density the cells were pelleted by centrifugation (2 min, 3000 x g) and washed once with 25 ml BMMY Medium. The cell pellet was resuspended in BMMY Medium to an OD₆₀₀ of 2 and grown in baffled flasks at 30°C and 250 rpm filling 1/10 of the flask volume at maximum. Expression of protein was maintained by induction with 1% methanol every 12 h or in alternating intervals of 8 and 16 h respectively, keeping one treatment constant for one expression.

6.2.11 SDS-PAGE

For sodium dodecyl sulphate polyacrylamide gel electrophoresis (SDS-PAGE) protein samples were mixed with 4x XT Sample Buffer and 20x XT Reducing Agent, boiled for 5 min at 99°C and then applied to the polyacrylamide gel. CriterionTM XT Bis-Tris Precast Gels were used with XT MES Running Buffer. Proteins were separated by SDS-PAGE at 125 V for 1.5 h. The PageRuler Plus Prestained Protein Ladder was used as a size standard.

6.2.12 Western Blot

Prior to the blotting of the proteins from an SDS-PAGE gel, the Immun Blot PVDF Membrane was activated in methanol. The gel, Extra Thick Blot Filter Paper and the membrane were incubated in Western Blot Transfer Buffer for 15 min. The transfer of the proteins was carried out at 100 V for 30 min in Western Blot Transfer Buffer in a Trans-Blot[®] transfer cell. Afterwards the membrane was blocked with 25 ml 5% skimmed milk powder in TBST for 1 h at room temperature whilst swivelling.

Incubation with Anti-V5-HRP Antibody (1:10 000 in 5% skimmed milk powder in TBST) was carried out for 2 h (room temperature, 25 rpm) or overnight (4°C, 25 rpm). Alternatively to the standard procedure, an Anti-His(C-term)-HRP Antibody (1:5000 in 5% skimmed milk powder in TBST) was used.

The HRP-coupled antibody binds to the respective recombinant epitope on the proteins and was detected using the SuperSignal™ West Dura Extended Duration Substrate Kit. Respectively, 1 ml of each solution (Super Signal™ West Stable Peroxide Buffer and Super Signal™ West Dura Luminol/Enhancer Solution) were mixed and applied to the membrane for 5 min. Alternatively the ECL method was used for Western Blot development. Solution A (5 ml 100 mM Tris-HCl pH 8.5, 22 µl coumaric acid (90 mM in DMSO), 50 µl luminol (250 mM in DMSO)) and Solution B (5 ml 100 mM Tris-HCl pH 8.5, 4 µl H₂O₂ (30% w/w)) were mixed and applied onto the membrane for 1 min.

The resulting luminescence signal was documented with Amersham Hyperfilm DCL chemiluminescence films, which were developed using GBX Developer and Replenisher and GBX Fixer and Replenisher.

6.2.13 Coomassie staining of gel

For the Coomassie staining the gel was first equilibrated in H₂O for 5 min. To fix and focus the bands the gel was incubated in 100 ml acetic acid/ethanol/H₂O (10:40:50) for 1 h. Afterwards the gel was rehydrated and washed three times in H₂O for 10 min. The gel was stained with PageBlue Protein Staining Solution overnight. Destaining was achieved by washing repeatedly with H₂O.

6.2.14 Protein quantification

Protein concentrations were determined using the Protein Assay Dye Reagent Concentrate with the Standard Procedure for Microtiter Plates. 2, 5, 10 and 20 µl protein solution of unknown concentration were applied onto a Nunc™ 96-well microtiter plate. A standard curve of BSA (0 – 11 µg in duplicates) was used for protein quantification. H₂O was added to a total volume of 20 µl per sample. 200 µl of 1:5 diluted dye reagent concentrate was added to the 20 µl of protein solution, mixed by pipetting up and down and incubated for 10 – 15 min. The absorbance was measured at 595 nm.

6.2.15 Activity assays

6.2.15.1 Agarose diffusion assay

To examine the activity of the PGs an agarose diffusion assay was performed. Pectin substrates (demethylated polygalacturonic acid or pectin from citrus) were combined

with citrate phosphate buffer, H₂O and melted agarose (55°C) and poured into a balanced petri dish.

	Volume [ml]
Pectin solution (1% w/v in H ₂ O)	2
0.2 M Citrate phosphate buffer	5
H ₂ O	5
Agarose (1% w/v) in H ₂ O	8
Total volume	20

Volumes used for an agar plate for an agarose diffusion assay.

After cooling the petri dish was closed and left at room temperature overnight. Small holes were pricked out with a cut pipet tip and a total sample volume of 10 µl was applied per hole in 5 µl steps. The plates were incubated at 40°C for 2 h or overnight. The applied sample diffuses into the agarose gel and potential PGs, that show an activity towards the respective subject, digest the pectin substrates within the gel. The inorganic dye Ruthenium Red stains polygalacturonic acid but not its endo-PG breakdown products. A solution of 0.1% Ruthenium Red (25 ml per plate) was applied on the agarose gel and incubated for 1 h at room temperature and 25 rpm. Repeated washing with H₂O destains those areas in which the pectin polymer is absent, i.e. spots where cleavage by endo-PGs has occurred. Complete destaining of the spots can be achieved by incubation of the gel with H₂O overnight at room temperature.

6.2.15.2 Quantification of PG activity by DNS assay

Quantification of PG activity is feasible using the 3,5-dinitrosalicylic acid (DNS) assay. Cleavage of the pectin polymer results in an increase of reducing sugar acids. In the presence of these free carbonyl groups 3,5-dinitrosalicylic acid is reduced to 3-amino-5-nitrosalicylic acid, which can be observed in a colour change from yellow to red and quantified by measuring the absorption at 575 nm [60].

Protein solutions, that have been dialysed and desalted beforehand, were incubated with the pectin substrate and optionally with plant cell wall protein extract (6.2.21) overnight at 40°C. To avoid possible effects of the plant's potential PME already demethylated polygalacturonic acid (PGA) was used.

	Volume [μ l]
0.2 M Citrate phosphate buffer	6
PGA demethylated (1% w/v in H ₂ O)	12
Protein solution	x
Plant protein extract	x
H ₂ O	x
Total volume	60

Volumes used for DNS assay. Detailed volumes concerning protein and plant cell wall protein extracts are given at the respective passage.

After 19 h of incubation 1 volume of pre-mixed DNS assay solution 1+2 (ratio 99:1) was added to 1 volume of sample and boiled at 99°C for 5 min. A change in colour is visible after heating if reducing sugars have been released during the reaction. Then DNS assay solution 3 was added to the sample/DNS assay solution 1+2 mixture in a ratio of 1:3:3 (e.g. 20 μ l solution 3 to 60 μ l solution 1+2 and 60 μ l of sample). The absorbance was measured at 575 nm.

6.2.15.3 Thin layer chromatography (TLC)

TLC – in contrast to other methods such as agarose diffusion assay or DNS assay – enables to monitor not only the PG activity itself, but also reveals details about the breakdown products.

Protein samples were incubated overnight in 0.2 M citrate phosphate buffer at 40°C with different pectin substrates: Galacturonic acid polymers with various degrees of methylation (decreasing order: esterified pectin from citrus, pectin from apple, pectin from citrus, demethylated polygalacturonic acid) and di- or trigalacturonic acid were used.

The samples were applied onto a TLC Silica Gel in 4 μ l steps. Additionally a size standard mixture of mono-, di- and trigalacturonic acid of 1 μ g/ μ l respectively was plotted onto the TLC plate. A mixture of ethyl acetate:formic acid:methanol:H₂O (9:3:1:4) was used as mobile phase. After the run the TLC was sprayed with 0.2% orcinol in methanol:sulphuric acid (9:1) and blown dry with hot air until bands appeared visible on the plate.

	Volume [μl]	
Protein solution	14	14
Pectin solution (1% w/v in H ₂ O)	4	
Galacturonic acid trimer/dimer (10 μg/μl)		1
0.2 M Citrate phosphate buffer	2	2
H ₂ O		3
Total volume	20	20

Volumes used for TLC.

6.2.16 Deglycosylation of PGs with Peptide-*N*-Glycosidase F (PNGase F)

The PGs PCO_GH28-1, PCO_GH28-3 and SSC_GH28-6 expressed in Sf9 insect cells as well as *P. pastoris* were deglycosylated using PNGase F according to the manufacturer's protocol for Denaturing Reaction Conditions [61]. Since the exact concentrations of heterologously expressed proteins in the culture medium were unknown, volumes were used that resulted in approximately the same intensity in the Western Blot (B). Denaturation was achieved by adding 1 μl 10x Glycoprotein Denaturing Buffer and ad 10 μl H₂O and heating at 100°C for 10 min. After addition of 10x G7 Reaction Buffer, 10% NP40 and PNGase F, the mixture was incubated for deglycosylation at 37°C for 1 h. The deglycosylation of proteins was monitored by Western Blot.

A	Volume [μl]	B	Volume PG culture medium [μl]	
PG culture medium	x		Sf9 insect cells	<i>P. pastoris</i>
10x Glycoprotein Denaturing Buffer	1	PCO_GH28-1	1	0.05
H ₂ O	ad 10	PCO_GH28-3	5	0.125
10x G7 Reaction Buffer	2	SSC_GH28-6	5	2.5
10% NP40	2	Volumes used for PNGase F deglycosylation.		
PNGase F	1			
Total volume	20			

Volumes used for PNGase F deglycosylation.

6.2.17 Protein purification

Secreted proteins, such as the heterologously expressed PGs, are present in the culture medium. After 48 – 108 h the cells from the expression culture were pelleted by centrifugation at 3000 x g for 3 min. The supernatant was transferred into pre-soaked

SnakeSkin™ Dialysis Tubing (35 mm I.D., 10K MWCO) and dialysed overnight against a 10fold volume the respective Binding Buffer while gently stirring. Dialysis baths were changed 3 times. To remove potential precipitate the dialysed sample was centrifuged at 10 000 x g for 5 min and the supernatant was used for protein purification. Samples were taken from the culture medium before and after dialysis, from the pellet (if occurring), from the flow-through, the washing fraction and the elutions E0 to E4 for further analysis to monitor the success and efficiency of the protein purification.

6.2.17.1 Immobilised metal ion affinity chromatography (IMAC)

The recombinant PGs contain a His₆ tag that forms chelate complexes with bivalent ions such as cobalt or nickel. HiTrap™ TALON agarose resin containing either cobalt (PCO_GH28-1, PCO_GH28-3 and SSC_GH28-6) or nickel ions (SSC_GH28-6) was used for PG purification either in a batch or fast protein liquid chromatography (FPLC). For batch purification 1 ml of HiTrap™ TALON Superflow agarose beads (= 1 column volume (CV)) were added to the dialysed protein sample and incubated rotating at 4°C for 1 h. Afterwards the sample was poured onto a gravity flow column that holds back beads and thereto bound proteins and is permeable for the residual liquid. As soon as the beads settled down in the column it was washed with 10 CV of IMAC Wash Buffer. Small amounts of imidazole reduce unspecific binding to the column during washing. Elution was achieved in a multi-step process. 1 CV of IMAC Elution Buffer was applied onto the column. The displaced liquid is still part of the wash fraction, but was collected separately (E0). After the bottom of the column was closed with a cap an additional 1 CV of IMAC Elution Buffer was added. The column was incubated for 5 min to allow the imidazole to compete with bound proteins. Removal of the cap lets the liquid drain from the column and the flow-through was collected as elution E1. This was repeated for another 3 times.

FPLC purification was carried out with an ÄKTA FPLC Protein Purification System and pre-packed HiTrap™ TALON crude 1 ml columns. After sample loading the column was washed with 10 CV IMAC Wash Buffer. Elution was performed in a stepwise manner as described for batch purification by pausing and resuming the FPLC ÄKTA System manually for every 1 CV of IMAC Elution Buffer.

Additionally to these standard protocols different varieties of IMAC purification were performed to optimize the procedure. Binding of His₆-tagged proteins is pH-dependent. His₆ residues are protonated at low pH and show decreased binding to the IMAC resin. Alternatively to the standard buffer IMAC Binding Buffer at pH 8.0 was used. Also 10% glycerol was added to the IMAC Binding Buffer to reduce protein precipitation during dialysis and thereby increase the amount of intact protein exposed to the column.

To expose the potentially masked His₆ tag to the IMAC resin SSC_GH28-6 was denatured using 6 M guanidine hydrochloride and purified with the FPLC method. 6 M guanidine hydrochloride was included into the IMAC Binding and the Elution Buffer. The same was done for the batch method using 3 M urea.

6.2.17.2 Lectin affinity chromatography

PGs are extracellular, highly glycosylated proteins. Lectins, such as Concanavalin A (ConA), bind molecules with sugar moieties (α -D-Mannopyranosyl, α -D-Glucopyranosyl and sterically related residues) via C-3, C-4 and C-5 hydroxyl groups [62]. Columns with immobilised ConA can be used for purification of glycoproteins.

Purification of PGs was performed using the FPLC ÄKTA System and HiTrap™ ConA 4B 1 ml columns. Dialysed protein samples were loaded onto the column, which was afterwards washed with 10 CV ConA Binding Buffer. Elution was performed as described for IMAC purification (6.2.17.1) with 5 min incubation time of ConA Elution Buffer on the column.

6.2.17.3 Hydrophobic interaction chromatography (HIC)

During HIC proteins adsorb to a hydrophobic matrix in the presence of anti-chaotropic salts such as ammonium sulphate [63]. A HiTrap™ Phenyl FF (high sub) 1 ml column was used with the FPLC ÄKTA System. After loading of the samples onto the column it was washed with 10 CV of HIC Binding Buffer and eluted with a gradient of increasing concentration of HIC Elution Buffer.

6.2.17.4 Cation exchange chromatography (CEC)

Depending on their charge and the pH of the buffer proteins bind to ion exchange columns. The FPLC ÄKTA System and a RESOURCE S column were used for CEC. Positively charged proteins adsorb to the negatively charged matrix depending on their charge and the pH of the CEC Binding Buffer. Loading of protein samples onto the column was followed by washing with 10 CV CEC Binding Buffer. The proteins were eluted from the column by an increasing amount of CEC Elution Buffer.

6.2.17.5 Anion exchange chromatography (AEC)

AEC was performed with the FPLC ÄKTA System and a RESOURCE Q 1 ml column. Negatively charged proteins adsorb to the positively charged matrix when loaded onto the column. Washing was performed with 10 CV of AEC Binding Buffer. An increasing gradient of AEC Elution Buffer desorbs the proteins from the column.

6.2.17.6 Binding of PGs to insoluble pectin

Active endo-PGs bind to pectin in order to cleave it. Cross-linking pectin [64], [65] produces an insoluble pectic substrate (provided by Dr. Roy Kirsch) that can be targeted, but not hydrolysed, which results in a permanent binding of endo-PGs to such substrate. The cross-linked pectin and potentially bound PGs can thus be centrifuged to be separated from the supernatant.

20 µl of PG-containing culture medium were incubated with 50 µl of cross-linked pectin (50% slurry) and 30 µl of H₂O at 4°C for 1 h while inverting at 10 rpm. The supernatant with non-bound PGs was separated from the insoluble pectin by centrifugation (2 min, 16 000 x g, 4°C). The pellet was washed with 500 µl 50 mM Citrate phosphate buffer and the supernatant was kept as wash fraction. Washing was repeated two times with 1 ml 50 mM Citrate phosphate buffer, but the liquid was discarded. The pellet was resuspended in 100 µl H₂O. A Western Blot was performed with culture medium, supernatant, wash and pellet fraction to monitor the localisation of the PGs. Volumes of supernatant, wash and pellet fraction were adjusted in a way that they were equivalent to the initially used amount of culture medium. Thus the protein present in supernatant, wash and pellet fraction sums up to the displayed protein amount in the culture medium.

Volume [µl]			
		PCO_GH28-1, PCO-GH28-3	SSC_GH28-6
Culture medium	20	1 (1:50)	1 (1:10)
Supernatant	approx. 100	5 (1:50)	5 (1:10)
Wash	approx. 500	0.5	2.5
Pellet (in H ₂ O)	approx. 100	1 (1:10)	0.5

Volumes used for Western Blot of binding assay with cross-linked pectin.

The protein solutions (ad 6 µl with H₂O) were boiled for 5 min at 99°C with 4x Sample Buffer, 20x Reducing Agent and 1% SDS and used for Western Blot (246.2.12).

6.2.18 Protein concentration and buffer exchange

The purified protein solutions needed to be concentrated for the further use with AminoLink[®] columns. Samples containing more than 10 µg protein were pooled and concentrated using Pierce[™] Protein Concentrators, 9K MWCO, 20 mL according to the manufacturer's instructions [66]. The Protein Concentrator was pre-rinsed by adding 12 ml water to the upper sample chamber and centrifuging at 3000 x g until more than 5 ml filtrate was produced. Then the water was removed, the protein solutions were

applied onto the column and centrifuged until they were concentrated to approximately 2 ml. The protein solution was recovered from the upper chamber by gentle pipetting and added to a Zeba™ Spin Desalting Column.

The buffer exchange was carried out according to the manufacturer's instructions [67]. Prior to the addition of protein sample the storage buffer was removed by centrifugation and the column was equilibrated with Coupling Buffer BupH™ Phosphate Buffered Saline pH 7.2 by adding 4 times 2.5 ml buffer and centrifuging (2 min, 1000 x g) respectively. The sample was recollected by centrifugation.

For SSC_GH28-6 and non-transfected SMD1168H *P. pastoris* 50 ml of crude culture medium were concentrated to 4 ml and dialysed in Slide-A-Lyzer™ Dialysis Cassettes (10 K MWCO, 12 mL) overnight against PBS pH 7.2. Dialysis baths were changed 3 times.

6.2.19 AminoLink Column

The purified proteins were bound to a column using the AminoLink® Plus Immobilisation Kit according to the manufacturer's instructions for Coupling Protein Using the pH 7.2 Coupling Buffer [68].

After resuspension of the resin and opening of the column the storage buffer was removed by centrifugation. All centrifugation steps were carried out at 1000 x g for 1 min. The column was washed three times with 2 ml of Coupling Buffer BupH™ Phosphate Buffered Saline pH 7.2 and the bottom cap was replaced. 2 – 3 ml of concentrated protein solution in Coupling Buffer were applied onto the column. The Schiff Bases that are formed between the AminoLink™ Resin and the protein's primary amines are converted into stable secondary amine bonds by the addition of 40 µl Sodium Cyanoborohydride Solution. The column with replaced caps was incubated with end-over-end rocking overnight at 4°C. Non-bound proteins were collected by centrifugation the next day. Each flow-through of the column preparation was saved to monitor protein coupling efficiency and potential loss of protein from the column in the following steps.

To block remaining active sites the Coupling Buffer was removed from the column and it was washed two times with 2 ml Quenching Buffer. Then 2 ml of Quenching Buffer that have been supplemented with 40 µl Sodium Cyanoborohydride Solution were added to the column, which was subsequently gently mixed by end-over-end-rocking for 30 min.

Following the removal of the Quenching Buffer the column was washed five times with 2 ml Wash Solution. Afterwards the column was equilibrated with 2 ml of Storage Buffer (Coupling Buffer BupH Phosphate Buffered Saline pH 7.2, 0.05% sodium azide)

3 times. After the last centrifugation the bottom cap was replaced and 2 ml of Storage Buffer were added to the column. The AminoLink[®] affinity column was stored upright at 4°C until further use.

6.2.20 Induction of PGIP synthesis in *B. rapa* ssp. *pekinensis*

Some PGIPs are constantly expressed in plants, while others are produced upon certain environmental cues [37], [69]. To trigger potential PGIP synthesis in *B. rapa* ssp. *pekinensis* single plants were placed in culture boxes and infested with the phytophagous beetle *P. cochleariae*. The plants were transferred to the culture chamber the day before to adapt to the environmental conditions. 15 adult beetles or 40 larvae of different age were placed on one plant respectively and removed after 3 days. The leaves were harvested, frozen in liquid nitrogen in 50 ml reaction tubes and stored at -80°C until further use.

6.2.21 Protein extraction from Chinese cabbage

The extraction of proteins was adapted from the protocol of Feiz et. al. (2006) [47].

6.2.21.1 Extraction of cell walls from *B. rapa* ssp. *pekinensis*

Leaves from the PGIP induction experiment (6.2.20) were used for cell wall isolation by centrifugation in increasing sucrose concentrations (0.4 – 1 M sucrose). Approximately 32 g of *B. rapa* ssp. *pekinensis* leaves (fresh weight) were ground in Cell Wall Extraction Buffer I for 15 min in a blender at full speed and 4°C. Approximately 1 ml of Protease Inhibitor Cocktail was added per 30 g of plant material. After 30 min of incubation while stirring at 4°C the mixture was centrifuged (15 min, 4000 x g, 4°C) to separate the cell walls from soluble cytoplasmic components. The supernatant was discarded, the pellet resuspended in Cell Wall Extraction Buffer II, centrifuged again and the supernatant was discarded. The procedure was repeated with Cell Wall Extraction Buffer III. Then the pellet was split up and washed with 3 l of pre-cooled 5 mM sodium acetate buffer, pH 4.6 on Miracloth filtration material (pore size 22 – 25 µm) respectively. The cell wall material was ground in liquid nitrogen in a mortar and lyophilised.

6.2.21.2 Protein extraction from *B. rapa* ssp. *pekinensis* cell walls

Cell wall-associated proteins were extracted from the lyophilised cell wall samples with increasing salt concentrations. 0.65 g of dry material was resuspended in 25 ml of 0.2 M CaCl₂ protein extraction solution by vortexing at room temperature for 10 min and pelleted (15 min, 4000 x g, 4°C). Two extractions were performed with 0.2 M CaCl₂ solution and 1 M NaCl protein extraction solution respectively. The supernatants of the CaCl₂ as well as the NaCl extractions were united respectively and dialysed against

ultrapure water overnight. The cell wall protein extracts were lyophilised and resuspended in AminoLink® Binding/Wash Buffer.

6.2.22 PG-PGIP interaction study

The interaction of PGs from *P. cochleariae* and *S. sclerotiorum* with proteins from *B. rapa* ssp. *pekinensis* was investigated. Purified PGs (PCO_GH28-1, PCO_GH28-3) or total protein from cell culture (SSC_GH28-6, non-transfected SMD1168H) were immobilised on AminoLink® affinity columns (6.2.19). Interaction studies were performed according to the AminoLink® Plus Immobilization Kit manufacturer's instructions [68].

6.2.22.1 Affinity chromatography

The plant cell wall protein CaCl_2 and NaCl extracts (6.2.21) were pooled and pre-treated by incubating it with AminoLink® resin, that has been treated as described in 6.2.19 but with water instead of protein solution, to remove proteins that bind to the resin unspecifically and recovered by centrifugation (1000 x g, 1 min).

After equilibration to room temperature the Storage Buffer was removed from the AminoLink® affinity columns by gravity-flow. The column was equilibrated with 3 CV of AminoLink® Binding/Wash Buffer. Pre-treated plant cell wall protein extracts were added to the column and incubated at 4°C for 45 min while inverting at 25 rpm. Afterwards the flow-through was collected and the column was washed with 6 CV of AminoLink® Binding/Wash Buffer. Elution was achieved in a stepwise manner. 1 CV of AminoLink® Elution Buffer was added to the column and the flow-through, which is still part of the washing fraction, was collected as E0. Then the column was capped and incubated with another 1 CV of AminoLink® Elution Buffer for 5 min. The gravity-driven elution was collected as E1 and elution was repeated three times. 10 µl of AminoLink® Neutralisation Buffer were added to 2 ml of elution.

The AminoLink® affinity column was regenerated by washing it with 8 CV of AminoLink® Binding/Wash Buffer and equilibrated with 4 CV of Storage Buffer (Coupling Buffer BupH Phosphate Buffered Saline pH 7.2, 0.05% sodium azide). After draining of the liquid from the column 1 CV of Storage Buffer was added on top of the resin and the AminoLink® affinity column was stored at 4°C for further use.

After extended storage the activity of PCO_GH28-1 was confirmed using TLC (6.2.15.3) to ensure that the protein was still active.

6.2.22.2 Trichloroacetic acid (TCA) precipitation and sample preparation

The protein concentration in the elutions of the affinity chromatography was too low to be directly monitored properly with a Coomassie-stained SDS-PAGE gel. Therefore a TCA precipitation was performed for protein enrichment.

Sodium deoxycholate was added to a final concentration of 0.02%. Samples were mixed by vortexing, placed on ice and supplemented with TCA to a final concentration of 10%. After vortexing the samples were incubated on ice for 1 h. Precipitated proteins were pelleted by centrifugation (10 min, 16 000 x g, 4°C). Carefully, the supernatant was removed and the remaining pellet was washed with 100% ice-cold acetone by incubating it on ice for 15 min and subsequent centrifugation (10 min, 6000 x g, 4°C). Washing was repeated once, the pellet was air-dried and boiled in SDS-PAGE Buffer (7.5 µl 4x XT Sample Buffer, 1.5 µl 20x XT Reducing Agent, 1% SDS, ad 30 µl H₂O) at 95°C for 5 min. Proteins were separated on a SDS-PAGE gel as described in 6.2.11.

6.2.22.3 Mass spectrometry (MS) analysis and data evaluation

Plant cell wall protein CaCl₂ and NaCl extracts as well as the elutions from the affinity chromatography separated on a SDS-PAGE gel were analysed and the following three methods (6.2.22.3.1 – 6.2.22.3.3) were described and carried out by the MS in-house service.

6.2.22.3.1 In-gel digestion of proteins

Protein bands of interest were cut out from the Coomassie-stained gels, cut into small pieces, washed several times with 25 mM NH₄HCO₃ and destained with 50% acetonitrile (ACN)/25 mM NH₄HCO₃. The proteins were then reduced with 10 mM DTT at 50°C for 1 h and alkylated with 55 mM iodoacetamide (IAA) at room temperature in the dark for 45 min. Next, destained, washed, dehydrated gel pieces were rehydrated for 1 h in 12 ng/µL solution of porcine trypsin (Promega GmbH, Mannheim) in 25 mM NH₄HCO₃ at 4°C and incubated overnight at 37°C. The tryptic peptides were extracted from gel pieces with 75% ACN/5% formic acid (FA), and dried down in a SpeedVac [70]. For nanoUPLC-MS/MS analysis samples were reconstructed in 10 µL aqueous 1% FA.

6.2.22.3.2 LC-MS/MS analysis

Each sample was injected onto a nanoAcquity nanoUPLC system (Waters, Manchester, UK) online coupled to a Q-ToF HDMS mass spectrometer (Waters). Peptides were initially transferred with 0.1% aqueous FA for desalting onto a Symmetry C18 trap-column (20 x 0.18 mm, 5 µm particle size) at a flow rate of 15 µL/min (0.1% aqueous FA), and subsequently eluted onto a nanoAcquity C18 analytical

column (200 mm×75 µm ID, BEH 130 material, 1.7 µm particle size) at a flow rate of 350 nL/min with the following gradient: 1 – 30% B over 13 min, 30 – 50% B over 5 min, 50 – 95% B over 5 min, isocratic at 95% B for 4 min, and a return to 1% B over 1 min (phases A and B composed of 0.1%FA and 100% ACN in 0.1% FA, respectively). The analytical column was re-equilibrated for 9 min prior to the next injection.

The eluted peptides were transferred to the nanoelectrospray source of a Synapt HDMS tandem mass spectrometer (Waters) that was operated in V-mode with a resolution power of at least 10 000 FWHM. All analyses were performed in positive ESI mode. A 650 fmol/µL human Glu-fibrinopeptide B in 0.1% FA/ACN (1:1 v/v) was infused at a flow rate of 0.5 µL/min through the reference Nano-LockSpray source every 30 s to compensate for mass shifts in MS and MS/MS fragmentation mode. LC-MS data were collected using data-dependent acquisition (DDA). The acquisition cycle consisted of a survey scan covering the range of m/z 400 – 1500 Da followed by MS/MS fragmentation of the four most intense precursor ions collected at 1 s intervals in the range of 50 – 1700 m/z. Dynamic exclusion was applied to minimize multiple fragmentations for the same precursor ions.

6.2.22.3.3 Data processing and protein identification

DDA raw files were collected using MassLynx v4.1 software and processed using ProteinLynx Global Server Browser (PLGS) v2.5 software (Waters) under baseline subtraction, smoothing, deisotoping, and lockmass-correction.

The peptide fragment spectra were searched against a subdatabase containing common contaminants (human keratins and trypsin). The following searching parameters were applied: fixed precursor ion mass tolerance of 10 ppm for survey peptide, fragment ion mass tolerance of 0.03 Da, estimated calibration error of 0.003 Da, 1 missed cleavage, fixed carbamidomethylation of cysteines and possible oxidation of methionine.

Spectra that remained unmatched by database searching were interpreted *de novo* to yield peptide sequences. A 0.002 Da mass deviation for *de novo* sequencing was allowed and sequences with a ladder score (percentage of expected y- and b-ions) exceeding 40 were subjected for homology-based searching using the MS BLAST program [71] installed on an in-house server. MS BLAST searches were performed against the viridiplantae and insecta databases (both downloaded from NCBI nr database on September 09, 2015) using the following settings: scoring Table, 100; Filter, none; Expect, 100; matrix, PAM30MS; advanced options, no-gap-hsppmax100-sort_by_totalscore-span1. Statistical significance of the matched hits was evaluated according to the MS BLAST scoring scheme [71].

In parallel, pkl-files of MS/MS spectra were generated and searched against the NCBI nr database (updated on September 09, 2015) using Mascot software version 2.5 (searching parameters as described above). Hits were considered as confident if at least three peptides were matched with ion scores above 30, or proteins were identified by one or two peptides with score of 55 or better.

6.2.22.3.4 Data Evaluation

Each lane of the SDS-PAGE gel was cut into slices of approximately the same width, processed and measured independently. One dataset of protein hits was acquired per gel piece. Peptides match proteins of a similar size as the cut gel piece, but also proteins of considerably higher and lower predicted mass. Within one dataset hits were pre-filtered and selected in a certain range of size. The centre protein size of each gel slice $\pm 10\%$ were included in the hits and used for further data evaluation. For slices twice the average size a range of $\pm 20\%$ was covered, for pieces half the size $\pm 5\%$. For protein sizes of 90 kDa or more the respective range was increased to $\pm 20\%$ to ensure the complete coverage of the lane. Only Brassicaceae hits were considered that contained at least one significant peptide match. If the same set of peptides matched multiple proteins the protein hit was selected that derived from the species that was closest related to *B. rapa* ssp. *pekinensis* [72], [73], [74]. To determine whether a hit was significant Mascot uses probability based scoring [75]. The total score of a protein hit expresses the probability that the matching of the peptide was random. It is displayed as $-10 \cdot \log_{10}(P)$, with P being the absolute probability. Thus a high score indicates a low probability of a random peptide match. Additionally for each protein the total number of peptides matching the protein hit is displayed and thereof those which have an expectation value below the significance threshold of $p < 0.05$.

For peptides matching different proteins of the same species the first hit was chosen from the list of results. The protein hits were annotated as in the NCBI nr database, which was used for protein identification by Mascot analysis. Additionally, a BLAST search was performed for the protein hits from the interaction study elutions against the *B. rapa* genome using the Ensembl Plants BLAST Search online tool [76], [77] and a comparative alignment with the characterised *B. napus* PGIP BnPGIP1 using BLAST bl2seq [78]. Furthermore, all proteins were checked for the presence of a signal peptide for the secretory pathway using SignalP 4.1 to predict the probable localisation. Proteins containing a predicted signal peptide were considered as being localised in the extracellular space, proteins lacking a signal peptide were assumed to be intracellular.

7 Results

7.1 Identification of *B. rapa* ssp. *pekinensis* cell wall proteins

Polygalacturonase-inhibiting proteins (PGIPs) are extracellular, cell wall-bound proteins that are known to inhibit several fungal [17], [34], [35] and some insect polygalacturonases (PGs) [79], [46]. To elucidate if *P. cochleariae* PGs are also inhibited by plant PGIPs, those and other potential extracellular interaction partners were enriched and used for interaction studies (6.2.22). Therefore plant cell walls followed by plant cell wall-associated proteins were extracted from *B. rapa* ssp. *pekinensis* (6.2.21). To validate that extracellular proteins were enriched with this method and PGIPs in particular were present, proteins extracted with CaCl_2 and NaCl were analysed with mass spectrometry (DDA, Mascot, 6.2.22.3). The resulting protein hits were screened for their predicted localisation with SignalP 4.1. A full list of all 377 protein hits identified in the mass spectrometry (MS) analysis can be found in the Supplementary Data (Table 8). The total number and ratio of extra- and intracellular proteins from the cell wall protein extraction are displayed in Table 1.

Extraction	Total protein number	Signal peptide (%)	
		yes	no
$\text{CaCl}_2 \cup \text{NaCl}$	377	71	29
$\text{CaCl}_2 \cap \text{NaCl}$	133	86	14
CaCl_2	328	73	27
NaCl	175	79	21

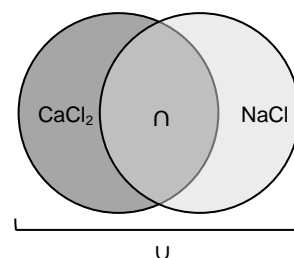


Table 1: Total number of protein hits in the MS analysis of *B. rapa* ssp. *pekinensis* cell wall protein extractions and their predicted localisation. The two extractions with CaCl_2 and NaCl were analysed separately. Proteins that were present in both extractions were shown as the intersection ($\text{CaCl}_2 \cap \text{NaCl}$). The whole protein pool of CaCl_2 and the NaCl extraction was displayed as the union ($\text{CaCl}_2 \cup \text{NaCl}$) of the two extractions. Localisation of the proteins was predicted with SignalP 4.1.

The enrichment of cell wall-associated proteins was performed by the isolation of plant cell wall and its subsequent extraction with 0.2 M CaCl_2 followed by 1 M NaCl buffer. For the CaCl_2 extraction 73% were predicted to be extracellular proteins and 27% intracellular ones. In the NaCl extraction 79% of proteins were predicted to be localised extracellular and 21% intracellular. The enrichment of extracellular proteins was successful for both extractions.

In the union of both extractions 71% and 29% of extra- and intracellular proteins were identified respectively. Even though a higher number of intracellular proteins was found as “contaminants” in the CaCl_2 extraction compared to the NaCl extraction, a pool of both extractions was used for the interaction assays. The first reason for this strategy

was that the protein concentration was notably higher in the CaCl₂ compared to the NaCl extraction (2.6 – 10fold). Secondly, the set of proteins differed with some only present in one of the two samples. To find potential interaction partners for the PGs it is essential to have a **high** concentration of **various** proteins.

The proteins were separated on a SDS-PAGE gel and bands excised at a certain size were used for a MS-based identification. Peptides that derive from the proteins of the excised band match proteins with a similar size, but also those whose predicted mass is considerably higher or lower. Since mostly only proteins of a predicted molecular mass close to the size range of the excised band represent good hits, the protein hits were pre-filtered in the MS analysis according to their size as described in 6.2.22.3.4. Exceptions are proteins with many post-translational modifications resulting in a higher molecular mass than the predicted one, which only takes the amino acid sequence into account.

Extraction	Protein	Mass [Da]	Species	CaCl ₂		NaCl	
				P	S	P	S
CaCl ₂	polygalacturonase inhibitor-like protein*	40475	<i>A. thaliana</i>	10(3)	416		
CaCl ₂ ∪ NaCl	polygalacturonase inhibitor protein 15	39183	<i>B. napus</i>	1(1)	101	1(1)	93
CaCl ₂ ∪ NaCl	polygalacturonase-inhibiting protein 1	38690	<i>B. rapa</i> ssp. <i>pekinensis</i>	20(11)	919	11(7)	573
CaCl ₂ ∪ NaCl	PREDICTED: polygalacturonase inhibitor 1-like	38048	<i>B. rapa</i>	8(5)	453	7(2)	249
CaCl ₂	PREDICTED: polygalacturonase inhibitor 1-like	38036	<i>B. rapa</i>	2(1)	73		
CaCl ₂ ∪ NaCl	PREDICTED: polygalacturonase inhibitor 2-like	37930	<i>B. rapa</i>	6(1)	233	9(2)	356
CaCl ₂	polygalacturonase inhibiting protein*	37930	<i>B. rapa</i> ssp. <i>pekinensis</i>	4(1)	178		
CaCl ₂	PREDICTED: polygalacturonase inhibitor 2*	37795	<i>Camelina sativa</i>	2(1)	108		
NaCl	polygalacturonase-inhibiting protein 3	37620	<i>B. rapa</i> ssp. <i>pekinensis</i>			6(3)	268
CaCl ₂ ∪ NaCl	polygalacturonase inhibitor protein 17	37229	<i>B. napus</i>	18(6)	753	9(7)	486
CaCl ₂ ∪ NaCl	polygalacturonase inhibitor protein 14	37122	<i>B. napus</i>	14(5)	659	9(6)	428
CaCl ₂	polygalacturonase inhibitor protein 7	36994	<i>B. napus</i>	10(4)	462		
NaCl	polygalacturonase inhibitory protein	36344	<i>B. rapa</i> ssp. <i>oleifera</i>			6(2)	270
CaCl ₂	PREDICTED: polygalacturonase inhibitor 1-like	36324	<i>B. rapa</i>	14(10)	736		
CaCl ₂ ∪ NaCl	PREDICTED: polygalacturonase inhibitor 2-like*	15094	<i>Camelina sativa</i>	2(2)	67	1(1)	67

Table 2: PGIPs found in MS data for CaCl₂ and NaCl cell wall protein extractions from *B. rapa* ssp. *pekinensis*. For each protein hit the top number of peptides (P) was shown that match the protein sequence of which the significant ones are shown in brackets. A significance threshold of 0.05 was used. Furthermore the top Mascot score (S) was displayed for each predicted protein. Proteins marked with an asterisk were found outside of the pre-filtered size range.

Of great interest for this study were the PGIPs as they are, based on literature, the most potential interaction partners for the PGs [17], [34], [35]. Several hits for PGIPs were found in the *B. rapa* ssp. *pekinensis* cell wall protein extracts (Table 2), all of which correspond to PGIPs from plants of the Brassicaceae family. Like other proteins, PGIPs can be glycosylated [80], [81] and thus differ from their predicted mass. Therefore all MS analysis protein hits were also searched for PGIPs outside of the pre-filtered size range (marked with asterisk in Table 2).

7.2 Inhibition of PGs by *B. rapa* ssp. *pekinensis* cell wall protein extracts

The pectin polymers of plant cell walls are cleaved by PGs, glycosyl hydrolases of the GH28 family (CAZy nomenclature [9]). The activity of PGs can be quantified with a 3,5-dinitrosalicylic acid (DNS) method as described in 6.2.15.2. Hydrolysis of polygalacturonic acid leads to an increase of reducing sugar acid. In the presence of free carbonyl groups 3,5-dinitrosalicylic acid is reduced, which can be quantified by measurement of the absorption at 575 nm.

PGs can be inhibited by PGIPs [82], [83]. PGIPs, cell wall-associated proteins, were enriched by cell wall isolation and sequential extraction of cell wall proteins from *B. rapa* ssp. *pekinensis* (6.2.21, 7.1). Incubation of the heterologously expressed PGs of *P. cochleariae* (PCO_GH28-1, PCO_GH28-5 and PCO_GH28-9 from Sf9 insect cells, provided by Dr. Roy Kirsch) and *S. sclerotiorum* (SSC_GH28-6 from the yeast *P. pastoris*, see 7.4) with increasing amounts of this plant cell wall protein extract led to a reduced activity of all these enzymes (Figure 1). Interestingly, the total PG activity of the gut content of *P. cochleariae* was also inhibited by the cell wall protein extract.

The activities of non-inhibited PGs were set to 100% and the hydrolysis rates of the respective PGs incubated with plant cell wall protein extracts were expressed as relative activities.

All PGs showed a gradual decrease in activity to 14% (PCO_GH28-1), 13% (PCO_GH28-5), 18% (PCO_GH28-9) and 12% (gut content). The activity of SSC_GH28-6 increased upon incubation with 0.1 and 0.3 µg plant cell wall protein extract to 108% and 111% respectively and then declined, like the beetle PGs, to 12% of the initial activity.

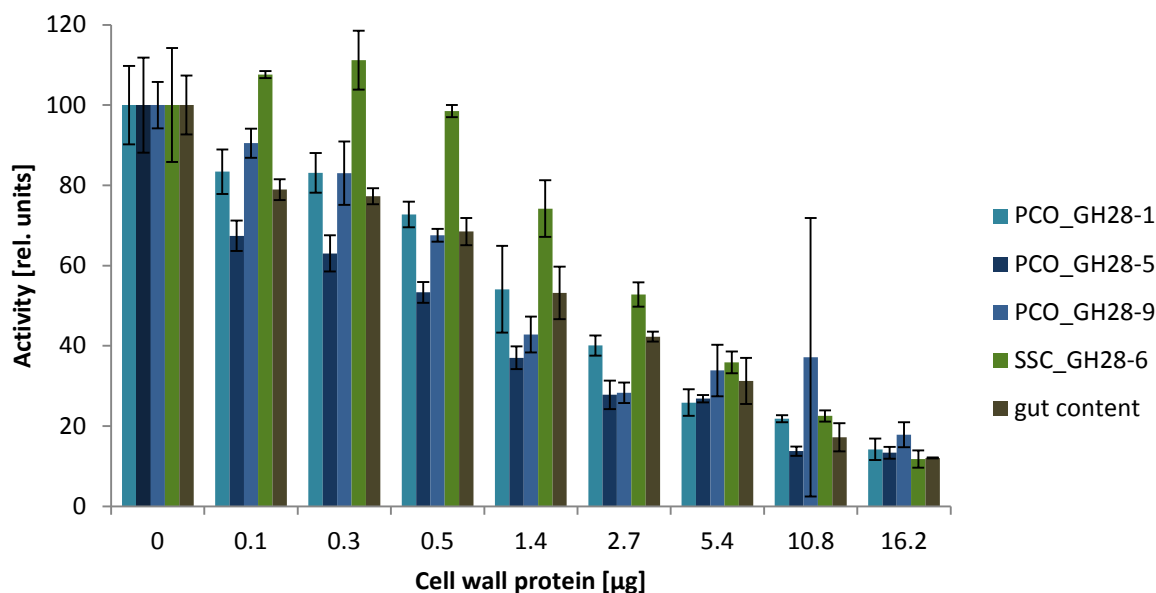


Figure 1: Activities of PGs PCO_GH28-1, PCO_GH28-5, PCO_GH28-9 and SSC_GH28-6 as well as *P. cochleariae* gut content with and without co-incubation with cell wall protein extracts from *B. rapa* ssp. *pekinensis*. The PG activities were determined by a DNS method. A decreasing activity for PCO_GH28-1, PCO_GH28-5, PCO_GH28-9, the *P. cochleariae* gut content and the SSC_GH28-6 from *S. sclerotiorum* was observed when incubated with increasing amounts of plant cell wall protein extracts.

The inhibition of all tested PGs by the plant cell wall protein extract indicates the presence of one or multiple plant-derived inhibiting factors.

7.3 Co-incubation of active and inactive PGs

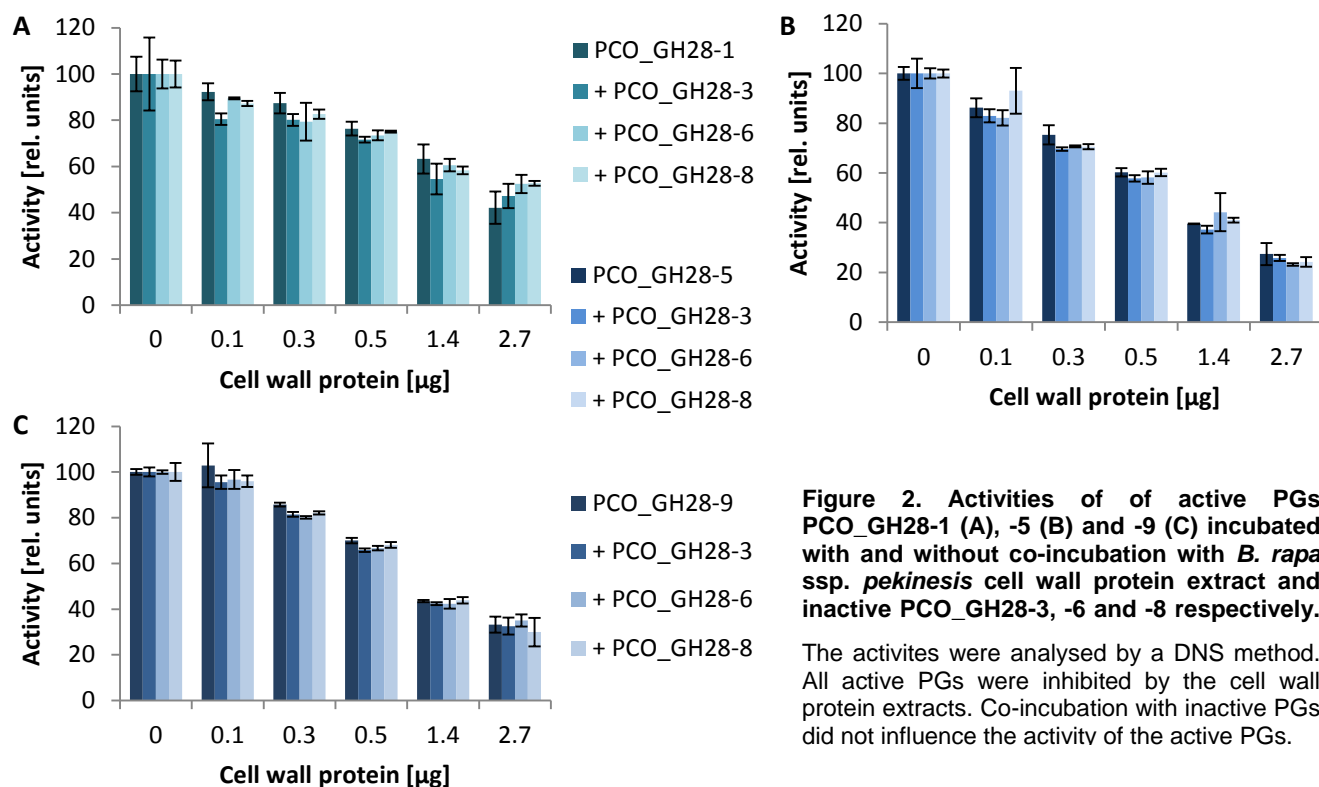
All active PGs from *P. cochleariae*, PCO_GH28-1, PCO_GH28-5 and PCO_GH28-9, were inhibited by *B. rapa* ssp. *pekinensis* cell wall protein extracts (Figure 1). Inactive PGs, such as PCO_GH28-3, -6 and -8, are found at equally high expression levels as active PGs in qPCR analysis [23]. Kirsch et al. (2014) stated that “catalytically inactive proteins may act as “decoy” targets for PGIPs, thus protecting the active PGs from inhibition” [11].

To test this hypothesis the catalytically active PGs were incubated with different concentrations of cell wall proteins, analogous to the previous experiment (7.2), but this time the inactive PCO_GH28-3, -6 and -8 were added individually. The pectinolytic activities were measured again with the DNS method (Figure 2, 6.2.15.2).

All PGs were inhibited by the *B. rapa* ssp. *pekinensis* cell wall protein extract, which confirmed the findings from 7.1. Co-incubation with inactive PGs did not lead to less inhibition. Instead, like without inactive PGs, the activity of the three beetle PGs was inhibited by the cell wall protein extracts, arguing against the “decoy” hypothesis.

However, crude protein mixtures were used in case of the PG solutions as well as plant cell wall protein extracts. Therefore the “decoy” hypothesis cannot be rejected and it cannot be concluded from this experiment that inactive PGs have no effect on the

active PG activity but demonstrate the necessity of additional experiments with purified proteins for direct interaction studies.



7.4 Expression of PGs PCO_GH28-1, PCO_GH28-3 and SSC_GH28-6

The PGs PCO_GH28-1 and PCO_GH28-3 from *P. cochleariae* as well as SSC_GH28-6 from *S. sclerotiorum* were expressed in the yeast *P. pastoris*. The respective open reading frames were amplified from pIB/V5-His-TOPO[®] vectors, that were used for expression in Sf9 insect cells beforehand. PCR products, including the V5 and the His₆ epitope from the pIB/V5-His-TOPO[®] vector, were cloned into pPICZα A vectors and positive clones were selected by sequencing after plasmid preparation of *E. coli* transformants. Vectors of positive clones were further transfected into *P. pastoris* and the integration of the linearised pPICZα A inserts into the genome at the AOX1 locus of the alcohol oxidase was checked by PCR as well as test restriction. Positive clones were used for protein expression. The addition of methanol induces the expression of the recombinant proteins, which were secreted into the culture medium, due to their α-factor signal peptide. The presence of proteins was monitored by Western Blot with an anti-V5-HRP antibody (6.2.11, 6.2.12).

All three proteins, PCO_GH28-1, PCO_GH28-3 and SSC_GH28-6, were successfully expressed. This is exemplarily shown for the PG PCO_GH28-1 in Figure 3 (for PCO_GH28-3 and SSC_GH28-6 expression see Supplementary Data Figure 13 and Figure 14). The expression of recombinant protein was observed in the Western Blot already after 12 h and increased over time. Protein bands were observed at approximately 55 kDa (PCO_GH28-1), between 50 and

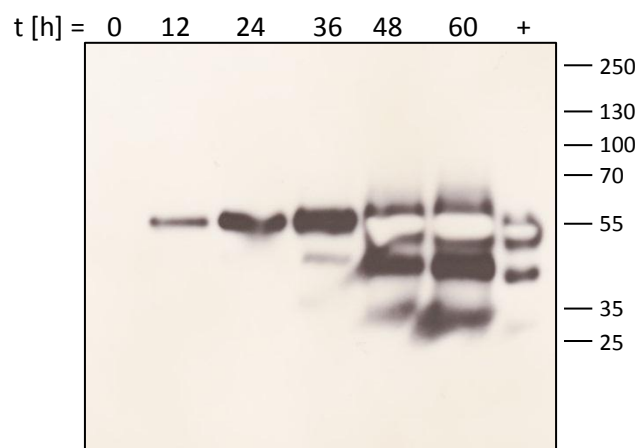


Figure 3: Expression of PCO_GH28-1. The Western Blot shows the time-dependent expression of PCO_GH28-1. The white protein bands (last three lanes) were caused by the high intensity of the HRP signal, which led to a bleaching of the luminescence substrate. PageRuler Plus Prestained Protein Ladder was used as size standard. +: positive control (PCO_GH28-1 expressed in Sf9 insect cells)

70 kDa (PCO_GH28-3) and between 70 and 100 kDa (SSC_GH28-6). This differed from the predicted sizes of 42 kDa, 43 kDa and 40 kDa respectively due to post-translational modifications (7.5.2).

7.5 Protein characterisation

7.5.1 Activity assay for PCO_GH28-1, PCO_GH28-3 and SSC_GH28-6

PCO_GH28-1 and SSC_GH28-6 are known to be active PGs [11], [83]. To test the PG activity of the proteins expressed in *P. pastoris* an agarose diffusion assay was performed (6.2.15.1). The culture medium collected during the expression was applied to agarose plates containing a pectin substrate, incubated and stained with Ruthenium Red. This dye binds the pectin polymer, but not its hydrolytic breakdown products. Endo-PG activity is therefore visible in unstained, clear zones around the application spot. Hydrolysis of terminal galacturonic acid monomers by exo-PGs cannot be detected with this method, because long, stainable polysaccharide chains are left intact in the activity area.

The yeast *P. pastoris* possesses no inherent PG activity. Accordingly, no PG activity was detected at $t = 0$ h. PG activity against demethylated and highly methylated pectin substrate was observed for PCO_GH28-1 and SSC_GH28-6 already after the first 12 h of expression (Figure 4). PCO_GH28-3 showed no PG activity against the tested substrates. This is consistent with previous findings by Kirsch et al. (2014) [11] and the replacement of a catalytic aspartate by an asparagine residue in PCO_GH28-3 [23].

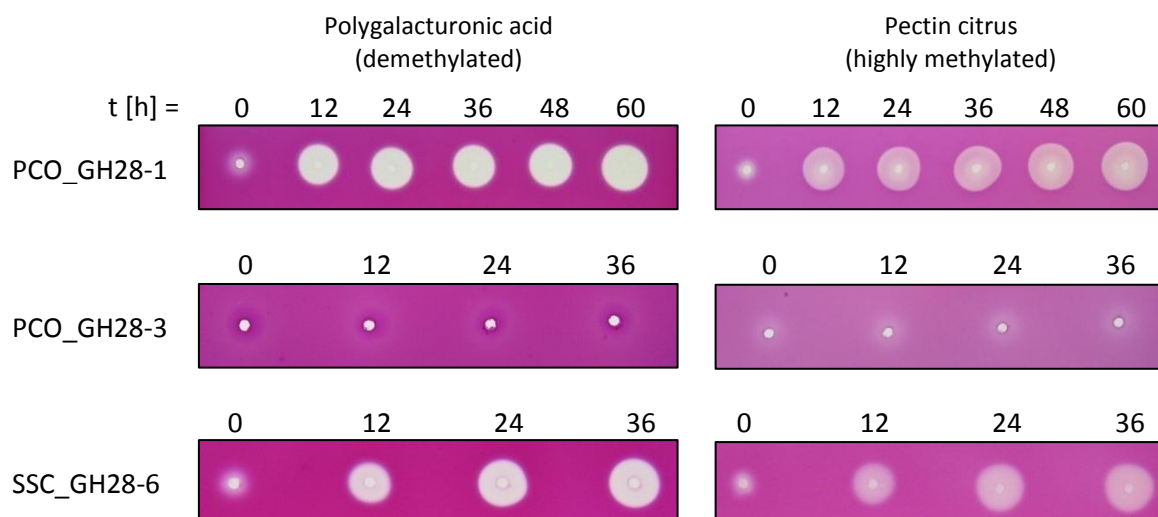


Figure 4: Agarose diffusion assay for PCO_GH28-1, PCO_GH28-3 and SSC_GH28-6. The PGs were incubated at 40°C for 2 h on agarose plates containing demethylated polygalacturonic acid as well as highly methylated pectin and stained with 0.1% Ruthenium Red. PG activity was observed already after 12 h of expression for PCO_GH28-1 and SSC_GH28-6 on both pectin substrates. PCO_GH28-3 exhibited no pectinolytic activity against the tested substrates.

7.5.2 Glycosylation of PCO_GH28-1, PCO_GH28-3 and SSC_GH28-6

Some yeast, like *Saccharomyces cerevisiae*, tend to hyperglycosylate recombinantly expressed proteins. Excess of glycosylation can influence function, folding, transport and interaction of the proteins [84]. The oligosaccharide chains added to the proteins are supposed to be much shorter in *P. pastoris* than in *S. cerevisiae* [57]. Nevertheless a comparison between the amount of glycosylation of proteins expressed in *P. pastoris* and Sf9 insect cells was performed to see if differences were detectable between the two expression systems. Peptide-N-Glycosidase F (PNGase F) cleaves the glycosylation between the innermost N-Acetylglucosamine and the asparagine residue leaving a deglycosylated protein [85]. O-glycosylations are rarely observed in *P. pastoris* and insect cells [57]. Using the NetNGlyc 1.0 tool from the Technical University of Denmark 4, 5 and 11 potential N-glycosylation sites were predicted for PCO_GH28 1, PCO_GH28-3 and SSC_GH28-6 respectively. Deglycosylation of the proteins (6.2.16) led to a reduced mass and therefor to a down-shift of the protein band in the Western Blot. According to their predicted number of glycosylation sites the shift increases from PCO_GH28-1 via PCO_GH28-3 to SSC_GH28-6, with a large difference in size observed between the glycosylated and the deglycosylated form of the latter (Figure 5). The protein bands of the deglycosylated PGs were located below 55 kDa. This was close to their predicted molecular mass of 42 kDa (PCO_GH28-1), 43 kDa (PCO_GH28-3) and 40 kDa (SSC_GH28-6) respectively and indicated that most of the post-translational modifications (PTMs) were N-glycosylations.

The PTMs of the heterologously expressed proteins are likely more similar to those in the beetle host organism when using an insect cell expression system like Sf9 cells. But the comparison of proteins expressed in *P. pastoris* and Sf9 insect cells revealed no significant difference in size (Figure 5), allowing to conclude that glycosylations were carried out in a comparable amount in both systems. In summary, as no hyper-glycosylations were observed and N-glycosylations were found to be of a similar size in both

expression systems, *P. pastoris* is adequate to express not only the fungal PG SSC_GH28-6 but also the beetle PGs PCO_GH28-1 and PCO_GH28-3.

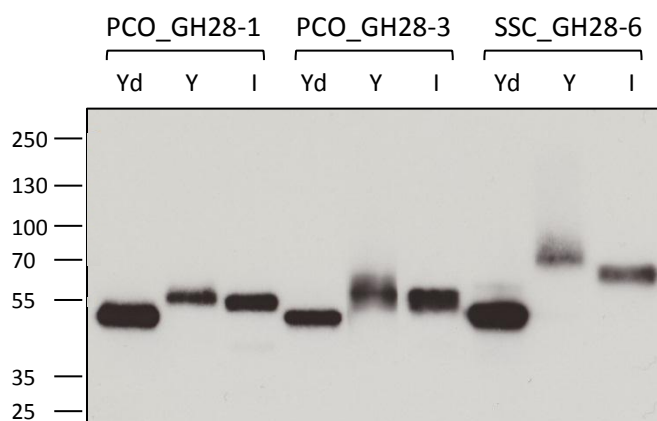


Figure 5: Comparison between PCO_GH28-1, PCO_GH28-3 and SSC_GH28-6 expressed in Sf9 insect cells (I), the *P. pastoris* (Y) as well as deglycosylated proteins from yeast expression (Yd). Proteins were deglycosylated with PNGase F. Upon deglycosylation a down-shift of the bands can be observed due to the decreased molecular weight. The extent of band shifting correlates with the number of predicted glycosylation sites within the protein. No major size difference can be seen between the PGs expressed in Sf9 insect cells and *P. pastoris* respectively. PageRuler Plus Prestained Protein Ladder was used as size standard.

7.6 Protein purification of PCO_GH28-1 and PCO_GH28-3

PCO_GH28-1 and PCO_GH28-3 were purified under native conditions by immobilised metal ion affinity chromatography (IMAC) using both the FPLC and batch standard protocol (6.2.17.1). The culture medium containing secreted proteins was harvested and dialysed against IMAC Binding Buffer. In case of precipitation the sample was centrifuged and the supernatant was used for further protein purification. The recombinant proteins contain a His₆ tag that forms chelate complexes with the IMAC resin's cobalt ions and thus bind to the IMAC column. Proteins were eluted with an excess of free imidazole that competes with the proteins for cobalt ions.

Two images of Coomassie-stained SDS-PAGE gels are displayed exemplarily in Figure 6 for batch and FPLC purification of PCO_GH28-1 (A) and PCO_GH28-3 (B), respectively. Two exemplary chromatograms of successful FPLC purification of PCO_GH28-1 and PCO_GH28-3 are displayed in the Supplementary Data (Figure 16).

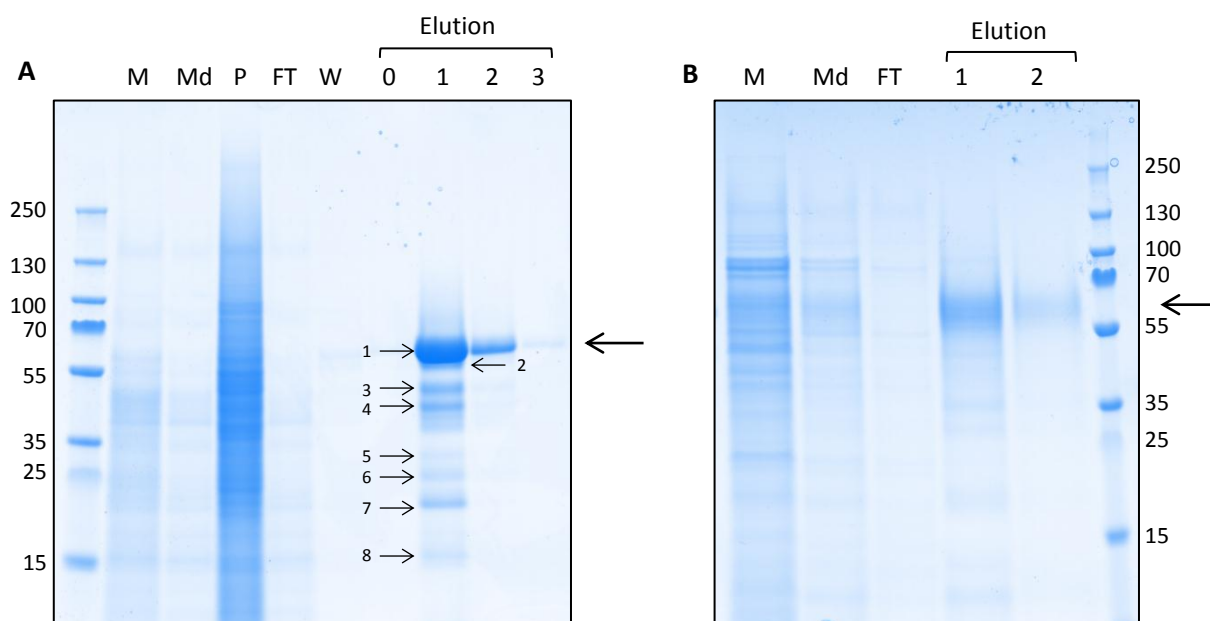


Figure 6: Coomassie-stained SDS-PAGE gel of IMAC-based purification of PGs PCO_GH28-1 and PCO_GH28-3 using IMAC. A: Batch purification of PCO_GH28-1, B: FPLC purification of PCO_GH28-3. Enrichment and purification of PCO_GH28-1 and PCO_GH28-3 could be observed in the elution fractions. Some additional minor bands with less amounts of protein compared with the main PG bands were visible. PageRuler Plus Prestained Protein Ladder was used as size standard. M: medium, Md: medium dialysed, P: pellet, FT: flow-through, W: wash.

A variety of proteins were present in the medium, the potential pellet, which corresponds to precipitated proteins after buffer exchange for IMAC, and the flow-through. In the elution fractions of both PCO_GH28-1 and PCO_GH28-3 one major band between 55 and 70 kDa was present (indicated with arrows in Figure 6). For both PGs additional bands of less intensity were visible. Those can be explained in case of PCO_GH28-1 by the sample treatment prior to gel loading. In the Western Blot (Figure 7) a temperature-dependent fragmentation of the protein was observed, giving rise to two reproducible additional bands. In the Coomassie-stained gel seven additional bands were detected, indicated with small arrows (2 – 8) in Figure 6. The identity of these bands was checked by MS analysis. For all protein bands the only or by far top hit was a glycosyl hydrolase family 28 protein from *P. cochleariae* (mass: 39404 Da), which corresponds to PCOGH28-1. The number of matching peptides, Mascot score and coverage are displayed in Table 3.

The formation of distinct protein bands in the SDS-PAGE gel bands suggests loss of the deglycosylations and reproducible fragmentation of the protein into smaller peptides rather than a random degradation of PCO_GH28-1. However, highlighting the detected peptides in the protein sequence exhibited no localisation in certain protein areas, which would indicate the detection of different protein fragments, but coverage of the complete protein sequence (Supplementary Data Figure 17). Nevertheless, the

fragmentation hypothesis cannot be rejected (see Discussion) and could be tested using alternative methods such as Edman degradation.

Band	Peptides	Score	Coverage [%]
1	86 (47)	1308	43
2	42 (26)	1024	33
3	38 (19)	1047	37
4	28 (16)	794	33
5	19 (9)	684	33
6	28 (18)	992	34
7	35 (18)	1034	39
8	17 (9)	738	33

Table 3: Number of peptides, Mascot score and coverage of MS analysis hits for PCO_GH28-1 degradation products. All peptides match the glycosyl hydrolase family 28 protein from *P. cochleariae* (mass: 39404 Da). The number of peptides above a significance threshold of 0.05 was displayed in brackets respectively. The corresponding protein bands were marked with small arrows in Figure 6.

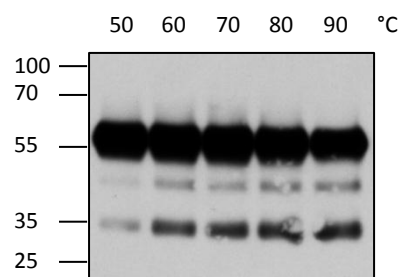


Figure 7: Western Blot of PCO_GH28-1 with different temperature treatments.

Prior to gel loading the samples were incubated at 50 – 90°C. A decrease in the major PCO_GH28-1 (top band) was observed. This correlated with an increase of the intensity of two smaller bands below the main band indicating a temperature-dependent fragmentation of PCO_GH28-1. PageRuler Plus Prestained Protein Ladder was used as size standard.

Temperature-dependent breakdown was also observed for PCO_GH28-3 but less compared to PCO_GH28-1 (Supplementary Data Figure 15).

Although the Coomassie-stained gel revealed more than one protein band, all of those were assigned to PCO_GH28-1. The IMAC elutions were considered as pure and were used for further interaction studies (6.2.22).

7.7 Purification and characterisation of SSC_GH28-6

SSC_GH28-6 is known to be inhibited by BnPGIP1 from *B. napus* [83]. The allopolyploid *B. napus* evolved by hybridisation of its progenitors *B. rapa* and *B. oleracea* and subsequent chromosome doubling [86] [87]. Due to this close relationship it can be hypothesised that a *B. rapa* ssp. *pekinensis* PGIP that is homologous to BnPGIP1 also inhibits SSC_GH28-6. Thus I used SSC_GH28-6 as a positive control for the interaction studies between *P. cochleariae* PGs and *B. rapa* ssp. *pekinensis* PGIPs described below (7.8).

Unfortunately, all attempts to purify SSC_GH28-6 failed. Nevertheless, in the context of troubleshooting regarding the failed purification, I functionally characterised this protein. The results together with the purification strategies are described below.

7.7.1 IMAC approaches

SSC-GH28-6, as the other recombinantly expressed PGs PCO_GH28-1 and PCO_GH28-3, contains a His₆ tag and should therefore bind to IMAC resin. Both batch

and FPLC standard method (6.2.17.1) were applied to purify SSC_GH28-6, but in neither case it bound to the IMAC material in significant amounts but was instead predominantly detected in the flow-through. Nickel ions can have a different affinity and specificity in protein purifications compared to cobalt, but using nickel instead of cobalt IMAC resin did not improve the purification. In general, the His₆ tag does not bind to bivalent metal ions when being in a protonated state and protonation is suppressed at alkaline pH. Increasing the pH from 7.4 (recommended in the manufacturer's instructions [88]) to pH 8.0 in the IMAC Binding Buffer had no effect on the SSC_GH28-6 binding. To exclude the possibility that bivalent metal ions (e.g. from the expression medium) were already masking the His₆ tag when the sample was applied onto the column, and thereby prevented efficient binding to the IMAC resin, the protein solutions were treated with EDTA beforehand. EDTA was removed after incubation by dialysis prior to the loading of protein sample to the IMAC column. Nonetheless, binding could not be improved by this treatment.

To validate that the His₆ tag was expressed with the protein, a Western Blot was performed with an anti-His(C-term)-HRP antibody. A signal was detected for SSC_GH28-6 verifying that the His₆ tag was fused with the protein. To prevent potential degradation of the His₆ tag during expression 1% Protease Inhibitor Cocktail was added during cell culture. It did not have any beneficial effects on the protein purification. Also 10% glycerol was added to saturate hydrophobic interaction sites in the proteins and thereby reduce protein precipitation. No effect on protein purification was observed.

Although the His₆ tag was proven to be expressed with SSC_GH28-6, a purification using the IMAC method was not successful. Besides bivalent metal ions from the expression medium, affinity tags can also be masked by the protein conformation or glycosylation shielding it from the stationary phase. If a masking of the His₆ tag was responsible for the non-successful binding it would be exposed once the protein is denatured. Some proteins are not able to renature in their native conformation thus losing their activity. Since activity assays and interaction studies should be performed with the purified protein, it is important to study the renaturation abilities beforehand.

SSC_GH28-6 is an enzyme with remarkably efficient renaturing properties. The protein solution (previously dialysed against H₂O) was boiled for 15 min to 1 h at 99°C and an assay including the DNS method (6.2.15.2) was performed incubating the samples at 40°C overnight with polygalacturonic acid. 91% of initial activity was restored for SSC_GH28-6 while the activity for PCO_GH28-1 and *P. cochleariae* gut content were reduced by more than 70% compared with the non-denatured samples (Figure 8A). By repeating the assay and incubating SSC_GH28-6 at 30 – 100°C with polygalacturonic

acid, it was shown that SSC_GH28-6 activity decreased with the increase of the incubation temperatures (Figure 8B). Similar results were observed with a guanidine hydrochloride treatment. 6 M guanidine hydrochloride was used to denature SSC_GH28-6 and was subsequently removed by dialysis against water. 68% of initial activity was recovered in case of SSC_GH28-6 and 58% by PCO_GH28-1 (Figure 8C). But when 1 to 5 M guanidine hydrochloride was directly added to the reaction solution the activity of SSC_GH28-6 and PCO_GH28-1 dropped down to 13 – 17% and 22 – 25% respectively (Figure 8D). These experiments clearly demonstrated that SSC_GH28-6 is able to renature and regain most of its activity after denaturation by heating or guanidine hydrochloride treatment.

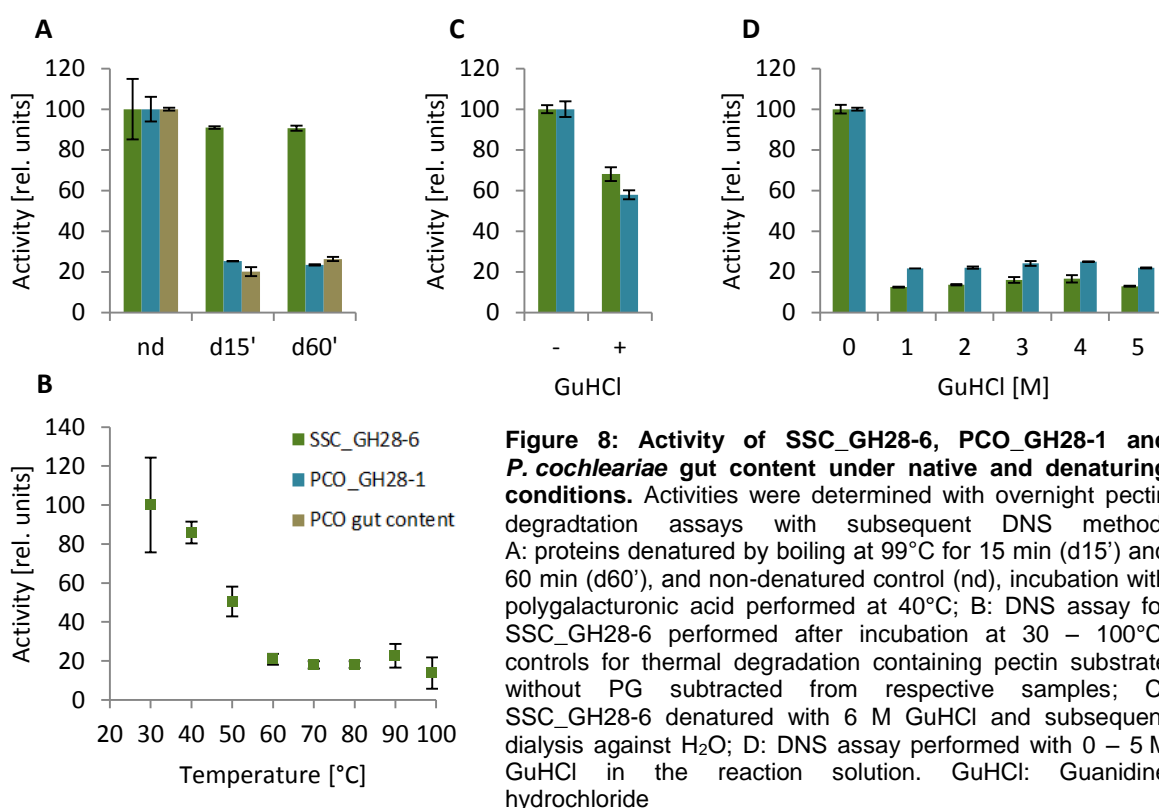


Figure 8: Activity of SSC_GH28-6, PCO_GH28-1 and *P. cochleariae* gut content under native and denaturing conditions. Activities were determined with overnight pectin degradation assays with subsequent DNS method. A: proteins denatured by boiling at 99°C for 15 min (d15') and 60 min (d60'), and non-denatured control (nd), incubation with polygalacturonic acid performed at 40°C; B: DNS assay for SSC_GH28-6 performed after incubation at 30 – 100°C, controls for thermal degradation containing pectin substrate without PG subtracted from respective samples; C: SSC_GH28-6 denatured with 6 M GuHCl and subsequent dialysis against H₂O; D: DNS assay performed with 0 – 5 M GuHCl in the reaction solution. GuHCl: Guanidine hydrochloride

This renaturation property of SSC_GH28-6 enabled protein purification under denaturing conditions. Therefore the fungal PG was denatured with 6 M guanidine hydrochloride as well as 3 M urea followed by the IMAC-based purification strategy. However, SSC_GH28-6 still did not bind to the column in considerable amounts.

7.7.2 Other chromatography strategies

Since it was not possible to purify SSC_GH28-6 using the IMAC method, alternative purification strategies were applied.

PGs, such as SSC_GH28-6, are highly glycosylated proteins (Figure 5). Glycoproteins can be purified by columns with immobilised lectins. A Concanavalin A B4 column was used for SSC_GH28-6 purification (6.2.17.2). Irrespective of the fact that more than one third of the molecular mass of SSC_GH28-6 accounts for sugar moieties the protein was not bound by the lectin column but was detected mainly in the flow-through.

Hydrophobic interaction chromatography (6.2.17.3) facilitates the adsorption of proteins to a hydrophobic matrix in the presence of anti-chaotropic salts such as ammonium sulphate. SSC_GH28-6 did not bind to the HiTrap™ Phenyl FF (high sub) column and was again only detected in the flow-through.

The same result was achieved when a cation exchange chromatography (CEC) was performed using a RESOURCE S column (6.2.17.4). Proteins bind to ion exchange columns depending on their charge and the pH of the buffer. Negatively charged matrices are used for CEC whereas positively charged stationary phases are applied for anion exchange chromatography (AEC, 6.2.17.5). In contrast to the CEC, SSC_GH28-6 was bound by the anion exchange column (RESOURCE Q), indicated by its presence in the fractions eluted with low salt concentrations. But the agarose diffusion assay of all the fractions of the AEC revealed SSC_GH28-6 activity not only in the elution fractions but also in the flow-through. Overloading of the column was excluded by determining the total amount of loaded protein, which was below the saturation limit. Moreover, many protein bands in addition to the one corresponding to SSC_GH28-6 were visible in a Coomassie-stained SDS-PAGE gel of the elution fractions that showed PG activity. Thus SSC_GH28-6 did not bind to the AEC column efficiently and was not pure and concentrated enough to be used for further interaction studies.

Furthermore an anti-V5 column was made by immobilizing 40 µg of anti-V5-HRP antibody on AminoLink® Superflow resin according to 6.2.19. Affinity chromatography was performed with SSC_GH28-6 as described in 6.2.22. However, no recombinant protein was detected in the elution fractions.

7.7.3 Interaction of PGs with insoluble pectin

As shown in 7.5.1 SSC_GH28-6 is an active PG. The halozones in the agarose diffusion assays indicate that SSC_GH28-6, like PCO_GH28-1, is an endo-PG. To cleave the pectin substrate the PGs need to bind it. This binding, like for other enzymes, is reversible and as soon as a galacturonic acid linkage is hydrolysed, the PG either moves forward on the same polymer (processive mode) or detaches from the polymer (non-processive mode) [89]. It has been shown that cross-linked co-polymers

of pectin can be bound by endo-PGs and enable their purification [90], [91]. The galacturonic acid linkages cannot be hydrolysed efficiently leading to PGs trapped on the non-soluble pectin due to missing leaving groups. Cross-linked pectin is insoluble and allows the separation of pectin with potentially bound PGs from the supernatant by centrifugation. To test if cross-linked pectin can be used to purify SSC_GH28-6, binding assays with non-methylated and methylated cross-linked pectin were performed (6.2.17.6) including PCO_GH28-1 and PCO_GH28-3 (Figure 9).

The volumes applied to the gel were adjusted in such a way that the fractions of supernatant (S), wash (W) and pellet (P) sum up to the initially used protein amount (M).

The strongest signal on the Western Blot for PCO_GH28-1 was detected in the pellet fractions, verifying that it bound to the insoluble pectins. Some protein was also found in the supernatant and the wash fractions. For PCO_GH28-3 no protein was detectable in the pellet, some in the wash and the majority in the supernatant fraction, showing that PCO_GH28-3 did not bind to the pectin substrate, neither to the non-methylated nor the methylated form. Unfortunately, SSC_GH28-6 was also found mostly in the supernatant. Some minor signals were detected in the wash and pellet fraction for the non-methylated pectin, but not for the methylated one. Therefore, the insoluble pectin could be used to purify PCO_GH28-1 but not PCO_GH28-3 and SSC_GH28-6. To gain some insights into why SSC_GH28-6 did not bind to the insoluble pectin further functional studies were performed.

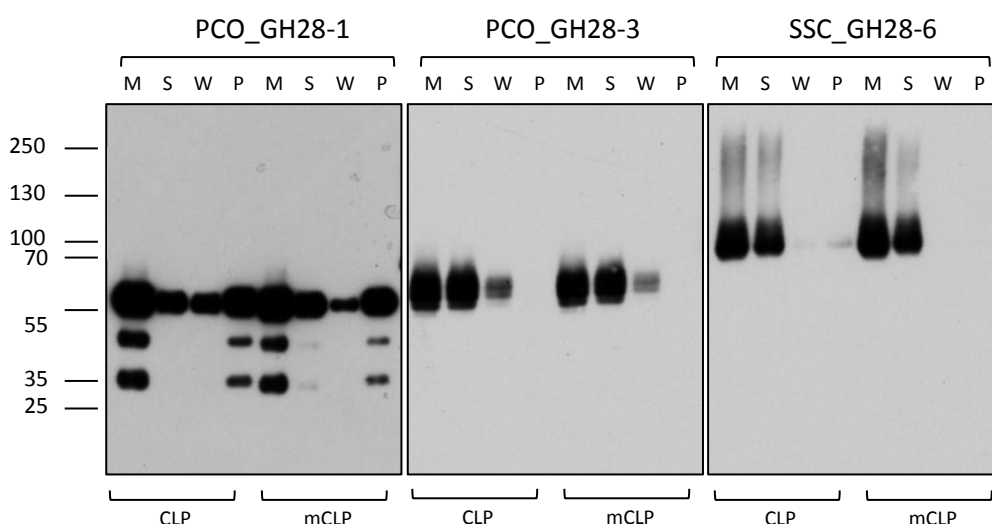


Figure 9: Binding assay of PCO_GH28-1, PCO_GH28-3 and SSC_GH28-6 to cross-linked pectin. The PGs were incubated with the cross-linked pectin substrate (non-methylated and methylated) and centrifuged to separate the substrate from non-bound PGs in the supernatant (S). After washing and subsequent separation of wash fraction (W) proteins were released from the pellet (P) by boiling it in SDS-PAGE sample buffer. The volumes applied to the gel were adjusted in such a way that the fractions of supernatant, wash and pellet sum up to the initially used protein amount (displayed in lanes M). CLP: cross-linked pectin, mCLP: methylated cross-linked pectin.

In a thin layer chromatography (TLC) for SSC_GH28-6 using pectin substrates of different degree of methylation as well as tri- and di-galacturonic acid (Figure 10) SSC_GH28-6 exhibited an inverse correlation of activity and degree of methylation. The lower the degree of methylation of the substrate was the better the hydrolysis by SSC_GH28-6. During the reaction galacturonic acid oligomers of different length as well as trimer (TGA), dimer (DGA) and monomer (MGA) were formed. Endo-PGs cleave polygalacturonic acid to oligomers, tri- and di-galacturonic acid, whereas exo-PGs hydrolyse the substrate from the ends, releasing galacturonic acid monomers. For SSC_GH28-6 in addition to TGA and DGA the formation of MGA was detected. TGA was further cleaved to DGA and MGA and also the DGA was hydrolysed. This suggests an endo-exo-mixed mode of action for SSC_GH28-6 leading to the complete breakdown of pectin to MGA.

The immobilisation by cross-linked pectin might be incomplete because the exo-PG activity enables a release of the enzyme from the insoluble substrate as non-cross-linked ends can be attacked. In conclusion, a purification of SSC_GH28-6 using cross-linked pectin is probably not possible.

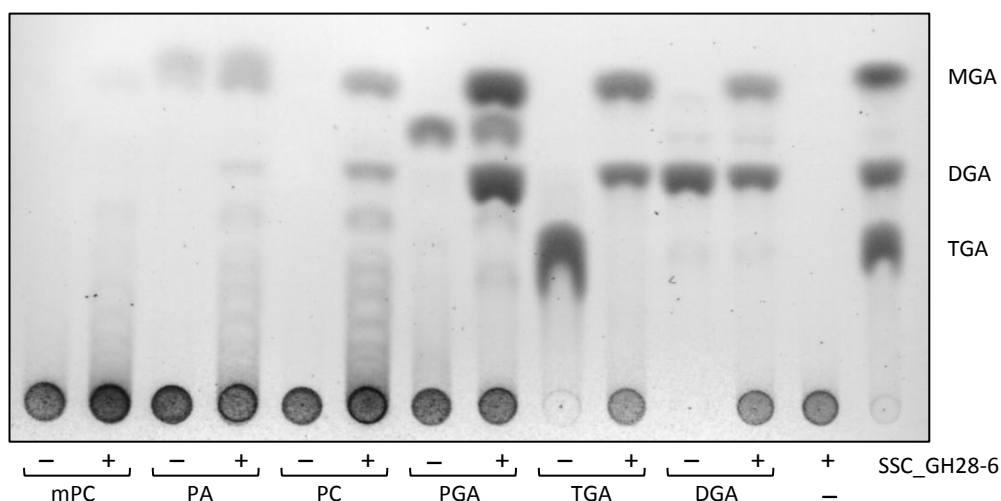


Figure 10: Thin Layer Chromatogram for SSC_GH28-6 activity towards pectin substrates. SSC_GH28-6 was incubated with pectin substrates with decreasing degree of methylation: methylated pectin from citrus (mPC) > pectin from apple (PA) > pectin from citrus (PC) > demethylated polygalacturonic acid (PGA). SSC_GH28-6 showed an increase of activity the lower the degree of methylation of the pectin substrate was. Galacturonic acid oligomers of various lengths as well as TGA, DGA and MGA were released. TGA was cleaved to DGA and MGA, DGA was hydrolysed to MGA. A standard of TGA, DGA and MGA was used for size comparison. TGA: tri-galacturonic acid, DGA: di-galacturonic acid, MGA: mono-galacturonic acid.

7.7.4 Alternative treatment for SSC_GH28-6

No purification of SSC_GH28-6 was achieved with the methods described above. Due to its special function as positive control in the PG-PGIP interaction assay, an alternative treatment was performed to elucidate potential SSC_GH28-6-PGIP interactions. The total secreted proteins were collected from non-transfected SMD1169H *P. pastoris* as well as from transfected SSC_GH28-6-expressing yeast. The culture medium was approximately 10fold concentrated and the dialysed protein mixtures were immobilised on two AminoLink® columns for PG-PGIP interaction studies.

7.8 Affinity chromatography: PG-PGIP interaction study

The PGs PCO_GH28-1 and SSC_GH28-6 were inhibited by *B. rapa* ssp. *pekinensis* cell wall protein extracts, as shown in 7.1. To find the interaction partners for the PGs and to test the “decoy” hypothesis the purified proteins PCO_GH28-1 and PCO_GH28-3 were immobilised on AminoLink® columns and cell wall protein extracts were applied (see below). SSC_GH28-6 is known to be inhibited by BnPGIP1 from *B. napus* [83] and thereby functions as a positive control for the PG-PGIP interaction study. Due to the close relationship of *B. napus* and *B. rapa* ssp. *pekinensis* it is likely that a potential PGIP that is homologous to BnPGIP1 is present in *B. rapa* ssp. *pekinensis*. Despite several tested methods (7.7) no purification was achieved for SSC_GH28-6. Therefore, the total secreted proteins of non-transfected SMD1168H *P. pastoris* cells (WT) as well as SSC_GH28-6 expressing cells (SSC6) were immobilised on an AminoLink® column to identify potential SSC_GH28-6 interaction partners by comparing the eluted protein band profiles of the two. The proteins of the WT and SSC6 sample used for this immobilisation were displayed in Figure 11 (last two lanes). Theoretically, both protein profiles should only differ in the recombinantly expressed SSC_GH28-6. Indeed, both cell lines showed a similar protein expression pattern but with different band intensities. SMD1168H exhibited four major bands that were of lower intensity in the SSC_GH28-6-expressing yeast. In the latter sample only two main bands were visible of which one was only present in the SSC_GH28-6 sample. This band was assumed to be SSC_GH28-6 (arrow with closed arrowhead in Figure 11). Identity of the band was verified with MS analysis. Amongst other proteins (see Discussion), the neutral endopolygalacturonase SSPG6 from *S. sclerotiorum* was detected (peptides 2(2), score 165), which corresponds to SSC_GH28-6 and thus allows the use of the SSC_GH28-6 column for affinity chromatography.

Before their application for the affinity chromatography, pooled cell wall protein extracts were pre-treated by passing them over an empty instead of PG-bound AminoLink™

column to remove proteins binding unspecifically to the resin. Aliquots of non-treated (nt) and pre-treated (pt) samples loaded on a SDS-PAGE gel showed no difference (Figure 12, first two lanes).

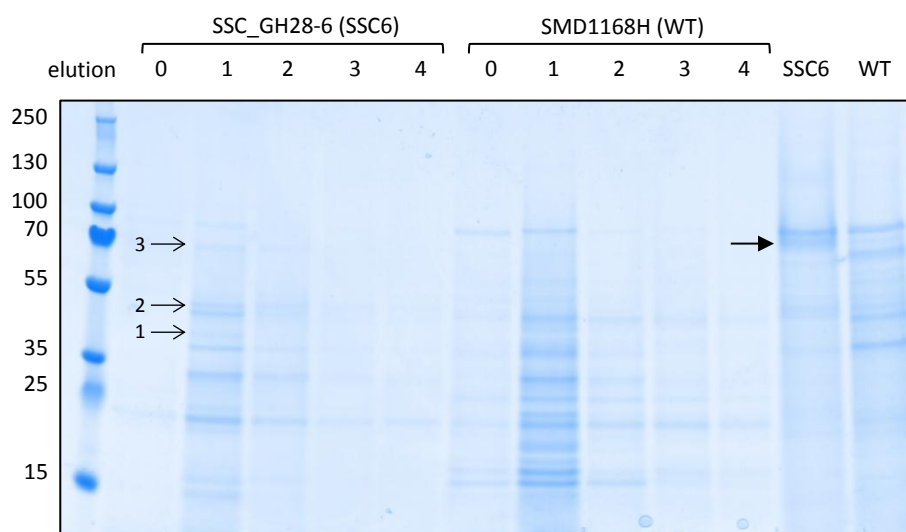


Figure 11: Coomassie-stained SDS-PAGE gel of the interaction study of SSC_GH28-6 with *B. rapa* ssp. *pekinensis* cell wall protein extracts. Affinity chromatography elutions 0 – 4 exhibited different band patterns of eluted proteins for SSC_GH28-6 and SMD1168H total proteins respectively. The total secreted proteins of SSC_GH28-6-expressing (SSC6) and wild-type (WT) that was immobilised on affinity columns was displayed in the last two lanes.

The cell wall protein extract was divided and 0.4 mg of protein was applied onto the column with immobilised SSC_GH28-6 and SMD1168H wild type total protein respectively. Affinity chromatography was performed as described in 6.2.22; the complete elutions were used for TCA precipitation and separated on a SDS-PAGE gel (Figure 11). A variety of proteins were detected in the elution fractions of both columns. But only proteins that were exclusively present in the SSC_GH28-6 elution are potential interaction partners. Those differing bands were excised and analysed by MS/MS. (Figure 11, arrows in lane 2).

Protein hits are annotated based on the NCBI nr database, which was used for protein identification by Mascot analysis. Additionally a BLAST search was performed for the protein hits against the *B. rapa* genome using the Ensembl Plants BLAST Search online tool [77]. Proteins matching PGIPs or leucine-rich repeat (LRR) proteins in general were displayed in Table 4. A full table of all protein hits is provided in the Supplementary Data (Table 9).

Two protein hits for LRR proteins from *Brassica oleracea* var. *oleracea* and *Camelina sativa* were detected that showed the highest similarity to same *B. rapa* gene (Bra035741) allowing to conclude the peptides matching this protein originated from one protein as well. The proteins were not measurable in the cell wall protein extract

(7.1) indicating an enrichment by interaction with SSC_GH28-6 above the detection limit. Aligning the LRR amino acid sequences with BnPGIP1, a PGIP from *B. napus*, that was characterised to have a PG-inhibiting property [83], using BLAST (bl2seq) [78] resulted in 30 and 31% similarity of the sequence. Additionally the polygalacturonase-inhibiting protein 3 (*B. rapa* ssp. *pekinensis*) was detected, which exhibited 89% similarity with the known PGIP.

In the following, the proteins interacting with the PGs were divided into three categories: 1) LRR proteins that were not characterised as PGIPs or PGIP-like proteins and exhibit low similarity (0 – 40%) with BnPGIP1, a *B. napus* PGIP known to have PG-inhibiting property [83], 2) LRR proteins that were annotated as PGIPs and PGIP-like proteins but share medium sequence identity (40 – 70%) with BnPGIP1, 3) proteins that share high similarity (70 – 100%) with BnPGIP1.

Alltogether, SSC_GH28-6 interacted with PGIP3, a category 3 protein, from *B. rapa* ssp. *pekinensis* and one not characterised LRR protein (category 1).

Protein	Mass [Da]	Species	P	S	SP	C	E	Gene	ID%	BS	Cat.	ID% ^B
1 PREDICTED: DNA-damage-repair/toleration protein DRT100	40527	<i>B. oleracea</i> var. <i>oleracea</i>	2(1)	106	y	6	n	Bra035741	99.1	1779	1	31
1 PREDICTED: DNA-damage-repair/toleration protein DRT100-like	40507	<i>Camelina sativa</i>	2(1)	102	y	6	n	Bra035741	92.3	1732	1	30
2 polygalacturonase-inhibiting protein 3*	37620	<i>B. rapa</i> ssp. <i>pekinensis</i>	1(1)	89	y	4	y	Bra005919	100	724	3	89

Table 4: MS results for interaction study of SSC_GH28-6 with *B. rapa* ssp. *pekinensis* cell wall protein extracts. Protein bands were indicated in Figure 11 with arrows. Only proteins annotated as PGIPs or proteins with hits for LRR proteins were shown. For each protein hit the top number of peptides (P) was shown that match the protein sequence of which the significant ones are shown in brackets. A significance threshold of 0.05 was used. Furthermore the Mascot score (S), coverage (C), BLAST score (BS) and identity with the best hit of the *B. rapa* genome (Gene) in BLAST analysis (ID%) and with BnPGIP1 in BLAST alignment (ID%^B) was displayed for each predicted protein. Proteins marked with an asterisk were found outside of the pre-filtered size range. Localisation of the proteins was predicted by searching for a signal peptide (SP) with SignalP 4.1. Moreover, it is displayed if the proteins were detected in the cell wall protein extracts beforehand (E). y: yes, n: no.

For PCO_GH28-1 and PCO_GH28-3 2.2 mg of proteins of the same cell wall protein extract were incubated with the respective affinity columns; half of the elutions were used for TCA precipitation and were separated on a SDS-PAGE gel (Figure 12).

In the elution one major band was visible for PCO_GH28-1 at approximately 24 kDa. Additionally, four minor bands were detected, two between 40 and 50 kDa, one at approximately 30 and 35 kDa respectively.

The band pattern in the elutions looked different for PCO_GH28-3, pointing to the presence of other interaction partners compared to PCO_GH28-1. Two main bands were present at approximately 24 and 45 kDa. Two fainter bands were visible at approximately 35 kDa and slightly below the 45 kDa band. The background of maybe unspecific binding proteins was lower compared to PCO_GH28-1.

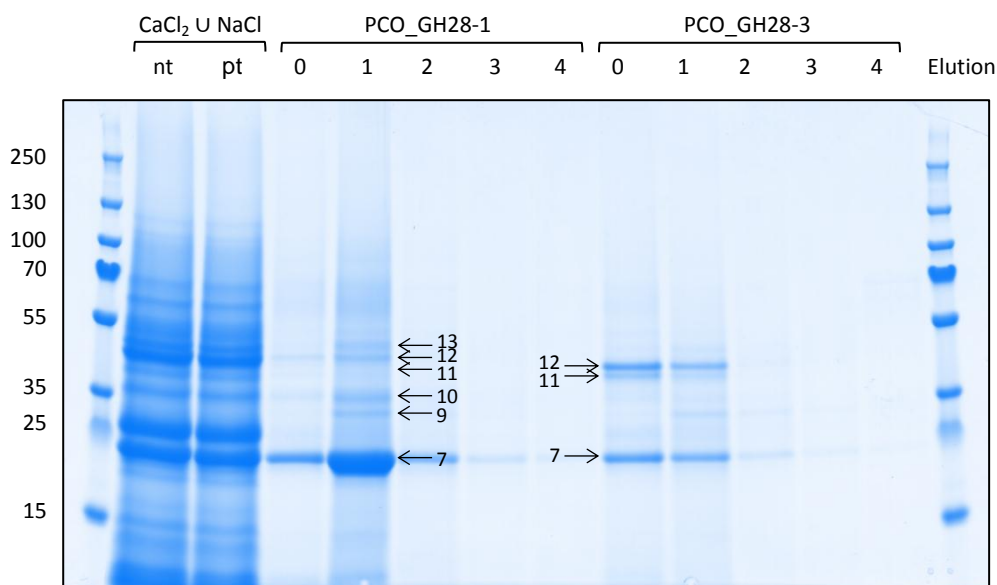


Figure 12: Coomassie-stained SDS_PAGE gel from the interaction study of the PGs PCO_GH28-1 and PCO_GH28-3 with *B. rapa* ssp. *pekinensis* cell wall protein extracts. Cell wall protein extracts (CaCl₂ U NaCl) were pre-treated (pt) to reduce unspecific binding to the AmnoLink[®] resin (non-treated (nt)). Affinity chromatography elutions 0 – 4 exhibit different band patterns of eluted proteins for PCO_GH28-1 and PCO_GH28-3.

Protein bands that were visible in the Coomassie-stained SDS-PAGE gel from the elutions E1 (PCO_GH281) and E0 (PCO_GH28-3) were analysed by MS/MS (Figure 12, arrows). Again, like for SSC_GH28-6 (see above), an additional BLAST search against the *B. rapa* genome was performed to identify the genes coding for the protein hits. Furthermore, an alignment for the Mascot-acquired protein hits with BnPGIP1, a characterised PGIP from *B. napus*, was performed. Protein hits for band 7 (Table 5) as well as proteins annotated as PGIPs and LRR proteins were displayed in Table 6 (PCO_GH28-1) and Table 7 (PCO_GH28-3). A full table of all protein hits can be found in the Supplementary Data (PCO_GH28-1 Table 10, PCO_GH28-3 Table 11).

For proteins that showed highest similarity to the same *B. rapa* gene, it was assumed that the matching peptides originated from the same corresponding *B. rapa* protein in the sample.

As already visible in the gel a more diverse set of proteins was detected for PCO_GH28-1 (90 protein hits), indicating more specific binding of proteins to PCO_GH28-3 (13 protein hits).

One main protein band (Figure 12, band 7) was visible for PCO_GH28-1 slightly below 25 kDa. Two of the detected proteins (Table 5) were annotated as “germin-like” (Bra006567, Bra003874). Furthermore, the other proteins were predicted to be a serine protease inhibitor family protein (Bra016073) and a STS14 protein (Bra037162). None

of the proteins were characterised yet. Despite their annotation, which are named based on sequence similarities, their function and activity remains unknown.

	Protein	Mass [Da]	Species	P	S	SP	C	E	Gene	ID%	BS
7	PREDICTED: kunitz-type serine protease inhibitor DrT1	24024	<i>B. rapa</i>	2(2)	79	y	4	y	Bra016073	100	1070
7	PREDICTED: germin-like protein subfamily 3 member 3	22029	<i>B. rapa</i>	3(1)	123	y	17	y	Bra006567	100	1065
7	germin-like protein	22023	<i>A. thaliana</i>	3(1)	102	y	17	y	Bra006567	95.3	879
7	PREDICTED: germin-like protein 1	21767	<i>B. rapa</i>	4(2)	89	y	21	n	Bra003874	100	985
7	PREDICTED: STS14 protein	20388	<i>B. rapa</i>	2(1)	108	y	13	n	Bra037162	100	745

Table 5: MS results for interaction study of PCO_GH28-1 with *B. rapa* ssp. *pekinensis* cell wall protein extracts, protein band 7.

The protein band was indicated with an arrow in Figure 12. For each protein hit the top number of peptides (P) was shown that match the protein sequence of which the significant ones are shown in brackets. A significance threshold of 0.05 was used. Furthermore the Mascot score (S), coverage (C), BLAST score (BS) and identity with the best hit of the *B. rapa* genome (Gene) in BLAST analysis (ID%) is displayed for each predicted protein. Localisation of the proteins was predicted by searching for a signal peptide (SP) with SignalP 4.1. Moreover, it is displayed if the proteins were detected in the cell wall protein extracts beforehand (E). y: yes, n: no.

For PCO-GH28-3 a protein band 7 was also visible, but no protein hits were found. In the protein bands 9 and 10 only uncharacterised proteins were detected as hits and their function still need to be elucidated. The protein bands 11 – 13 exhibited an overlap of protein hits, of which predicted LRR proteins and potential PGIPs and PGIP-like proteins were displayed in Table 6 (PCO_GH28-1) and Table 7 (PCO_GH28-3). For proteins detected in more than one protein band, the top hit was named, resulting in the preference of hits from protein band 11 and 12 over those from band 13. Even though no clear protein band 11 was visible for PCO_GH28-1, it was analysed as a comparison to the distinct band for PCO_GH28-3.

	Protein	Mass [Da]	Species	P	S	SP	C [%]	E	Gene	ID%	BS	Cat.	ID% ^B
12	leucine-rich repeat-containing protein	40475	<i>A. thaliana</i>	10(4)	415	y	21	y	Bra035741	93.8	1747	1	26
12	PREDICTED: DNA-damage-repair/toleration protein DRT100	40461	<i>B. rapa</i>	19(8)	791	y	40	y	Bra035741	100	1808	1	31
12	BnaA01g36810D	40377	<i>B. napus</i>	11(4)	449	y	23	y	Bra035741	92.0	1728	1	31
12	polygalacturonase inhibitor protein 15	39183	<i>B. napus</i>	1(1)	83	y	5	y	Bra005916	97.1	879	3	82
12	PREDICTED: polygalacturonase inhibitor 2-like	38737	<i>B. oleracea var. oleracea</i>	6(3)	354	y	21	n	Bra005917	95.5	896	3	99
11	BnaC03g02770D	38730	<i>B. napus</i>	6(3)	265	y	19	y	Bra005917	95.5	899	3	99
12	polygalacturonase inhibitor protein	38729	<i>B. napus</i>	6(3)	346	y	19	n	Bra005917	95.5	899	3	100
11	polygalacturonase-inhibiting protein 1	38690	<i>B. rapa ssp. pekinensis</i>	6(3)	284	y	20	y	Bra005917	99.4	929	3	96
11	PREDICTED: polygalacturonase inhibitor 1-like	38048	<i>B. rapa</i>	8(3)	366	y	27	y	Bra034774	100	1705	2	50
11	PREDICTED: polygalacturonase inhibitor 2-like	37930	<i>B. rapa</i>	4(1)	154	y	10	y	Bra009238	100	1587	3	76
11	PREDICTED: polygalacturonase inhibitor 2	37795	<i>C. sativa</i>	3(1)	98	y	5	y	Bra009235	71.0	600	3	71
11	polygalacturonase-inhibiting protein 3	37620	<i>B. rapa ssp. pekinensis</i>	7(3)	332	y	25	y	Bra005919	100	724	3	89
11	polygalacturonase inhibitor protein 14	37122	<i>B. napus</i>	5(3)	280	y	18	y	Bra005918	93.2	795	3	92
11	BnaA05g26870D	37094	<i>B. napus</i>	8(3)	360	y	25	y	Bra034774	98.2	1675	2	50
11	polygalacturonase inhibiting protein 2	37091	<i>A. thaliana</i>	2(1)	86	y	5	n	Bra009238	74.1	1088	3	72
11	hypothetical protein CARUB_v10014170mg	36644	<i>C. rubella</i>	3(1)	113	y	9	y	Bra038700	90.3	1427	2	51
11	polygalacturonase inhibitory protein	36344	<i>B. rapa ssp. oleifera</i>	17(10)	641	y	49	y	Bra038700	99.4	1626	2	52

Table 6: MS results for interaction study of PCO_GH28-1 with *B. rapa ssp. pekinensis* cell wall protein extracts. Protein bands were indicated in Figure 12 with arrows. Only proteins annotated as PGIPs or proteins with hits for LRR proteins were shown. For each protein hit the top number of peptides (P) was displayed that match the protein sequence of which the significant ones were shown in brackets. A significance threshold of 0.05 was used. Furthermore the Mascot score (S), coverage (C), BLAST score (BS) and identity with the best hit of the *B. rapa* genome (Gene) in BLAST analysis (ID%) and with BnPGIP1 in BLAST alignment (ID%^B) was displayed for each predicted protein. Localisation of the proteins was predicted by searching for a signal peptide (SP) with SignalP 4.1. Moreover, it was displayed if the proteins were detected in the cell wall protein extracts beforehand (E). Proteins highlighted with grey are found in both PCO_GH28-1 and PCO_GH28-3 elutions. y: yes, n: no.

	Protein	Mass [Da]	Species	P	S	SP	C [%]	E	Gene	ID%	BS	Cat.	ID% ^B
12	leucine-rich repeat-containing protein	40475	<i>A. thaliana</i>	6(1)	270	y	15	y	Bra035741	93.8	1747	1	26
12	PREDICTED: DNA-damage-repair/toleration protein DRT100	40461	<i>B. rapa</i>	13(5)	597	y	33	y	Bra035741	100	1808	1	31
12	BnaA01g36810D	40377	<i>B. napus</i>	7(1)	298	y	17	y	Bra035741	92.0	1728	1	31
11	PREDICTED: polygalacturonase inhibitor 1-like	38048	<i>B. rapa</i>	18(9)	735	y	48	y	Bra034774	100	1705	2	50
11	PREDICTED: polygalacturonase inhibitor 1-like	38046	<i>B. oleracea</i> var. <i>oleracea</i>	15(9)	666	y	37	n	Bra034774	98.8	1690	2	51
11	BnaA05g26870D	37094	<i>B. napus</i>	18(8)	681	y	47	y	Bra034774	98.2	1675	2	50
11	hypothetical protein CARUB_v10014170mg	36644	<i>C. rubella</i>	10(4)	185	y	13	y	Bra038700	90.3	1427	2	51
11	polygalacturonase inhibitory protein	36344	<i>B. rapa</i> ssp. <i>oleifera</i>	40(19)	897	y	59	y	Bra038700	99.4	1626	2	52
11	PREDICTED: polygalacturonase inhibitor 1-like	36118	<i>B. oleracea</i> var. <i>oleracea</i>	31(15)	663	y	50	n	Bra038700	97.2	1583	2	52

Table 7: MS results for interaction study of PCO_GH28-3 with *B. rapa* ssp. *pekinensis* cell wall protein extracts. Protein bands were indicated in Figure 12 with arrows. Only proteins annotated as PGIPs or proteins with hits for LRR proteins were shown. For each protein hit the top number of peptides (P) was displayed that match the protein sequence of which the significant ones were shown in brackets. A significance threshold of 0.05 was used. Furthermore the Mascot score (S), coverage (C), BLAST score (BS) and identity with the best hit of the *B. rapa* genome (Gene) in BLAST analysis (ID%) and with BnPGIP1 in BLAST alignment (ID%^B) was displayed for each predicted protein. Localisation of the proteins was predicted by searching for a signal peptide (SP) with SignalP 4.1. Moreover, it was displayed if the proteins were detected in the cell wall protein extracts beforehand (E). Proteins highlighted with grey are found in both PCO_GH28-1 and PCO_GH28-3 elutions. y: yes, n: no.

Again, the proteins interacting with the PGs were divided into three categories: 1) uncharacterised LRR proteins that were not annotated as PGIPs or PGIP-like proteins and exhibit low similarity (0 – 40%) with BnPGIP1, 2) LRR proteins that were annotated to be PGIPs or PGIP-like proteins but share medium sequence identity (40 – 70%) with BnPGIP1, 3) proteins that share high similarity (70 – 100%) with BnPGIP1.

All detected non-PGIP LRR protein sequences showed highest sequence similarity with one *B. rapa* gene (Bra035741), indicating the presence of one single category 1 protein interacting with PCO_GH28-1 and PCO_GH28-3.

For PCO_GH28-1 five category 3 proteins were detected that share 82 – 96% sequence identity with BnPGIP1 (Bra009238, Bra005919, Bra005918, Bra005916, Bra005917). Furthermore, two other category 3 proteins were identified that were 76 and 71% identical with BnPGIP1. Thus several proteins that share a high sequence similarity with BnPGIP1, which was characterised to have PGIP activity, were detected by MS analysis strongly indicating their interaction with PCO_GH28-1. No category 3 proteins were detected for PCO_GH28-3.

The same two category 2 proteins (Bra034774, Bra038700) were detected in the case of PCO_GH28-1 and PCO_GH28-3 that were annotated as PGIPs (NCBI nr) or LRR proteins (EnsemblPlant *B. rapa*), but shared only 50 – 52% sequence identity with BnPGIP1.

Compared to the distinct bands visible for PCO_GH28-3 (Figure 12, protein bands 12 and 11), only a faint (12) and no protein band (11) could be identified for PCO_GH28-1 at the size range of putative PGIPs. This was consistent with the detected number of peptides matching the protein hits. For PCO_GH28-1 an average number of peptide hits of 13.3 (category 1), 9.0 (category 2), and 4.6 (category 3) was detected, whereas 8.7 (category 1) and 22 (category 2) peptide hits were found for PCO_GH28-3. Considerably more peptide matches were measured for category 2 proteins annotated as PGIPs and PGIP-like proteins from PCO_GH28-3, allowing the assumption that those proteins interact stronger with PCO_GH28-3 than PCO_GH28-1.

In summary, a clear differential interaction of *B. rapa* ssp. *pekinensis* cell wall proteins with the PGs PCO_GH28-1 and PCO_GH28-3 could be observed. PCO_GH28-1 bound a larger set of different proteins, including one LRR protein (category 1) and proteins annotated as PGIPs with high sequence similarity to the characterised BnPGIP1 (category 3). PCO_GH28-3 did not interact with those category 3 proteins. For both PGs LRR proteins were found that were annotated as PGIPs or PGIP-like proteins but shared poor sequence identity with the known BnPGIP1 (category 2).

8 Discussion

The mustard leaf beetle *P. cochleariae* feeds on leaves of various plants of the Brassicaceae family. The plant cells, that the beetle encounters during herbivory, are encased by plant cell walls, a complex mixture of polysaccharides, e.g. pectin and cellulose, and proteins [6]. PGs, enzymes of the glycoside hydrolase family 28, degrade homogalacturonan, the major pectin component [3]. Kirsch et al. (2012) found nine PG genes in *P. cochleariae*, whereof five expressed proteins were detected in the gut content [23]. Activity assays and qPCR analysis revealed that active as well as inactive PGs were expressed specifically in the gut in comparable abundance [11], [23]. The physiological relevance of the inactive PGs still needs to be elucidated. Interestingly, also plant-derived PGIPs were detected in the same protein fractions as *P. cochleariae* PGs after anion exchange chromatography and SDS-PAGE. Since the high similarity of their physico-chemical properties is unlikely, a potential interaction of beetle PGs and plant PGIPs has been hypothesised as a reason for their co-elution. Kirsch et al. (2014) stated that “catalytically inactive proteins may act as “decoy” targets for PGIPs, thus protecting the active PGs from inhibition” [11].

PGIPs are extracellular glycoproteins known to inhibit several fungal PGs [17], [34], [35] and some insect pectolytic activities [79], [46]. Kirsch et al. (2012) found the *B. rapa* polygalacturonase-inhibiting protein 3 in the same protein band as the *P. cochleariae* PGs PCO_GH28-1 and PCO_GH28-3, making it a good candidate for a beetle PG inhibiting protein [23]. But instead of expressing this PGIP heterologously and testing its inhibitory effect on the beetle PGs, a more unbiased approach was chosen in my Master’s thesis to identify plant-derived interaction partners. Since more than a single protein could be involved in the potential interaction with beetle PGs, crude protein extracts from *B. rapa* ssp. *pekinensis* cell walls containing a large set of different plant proteins were used for PG inhibition and interaction assays. It has been demonstrated before that crude plant protein extracts successfully inhibit PGs [92], [93].

Constitutively expressed PGIPs are localised in the plant cell wall, “molecular sentinels” [94] ready to inhibit PGs. Upon abiotic or biotic stimuli, the expression of further PGIPs can be induced [69], [40], [38]. PGIPs exhibit functional redundancy and sub-functionalisation and are differentially regulated depending on environmental cues [37], [34], [38]. To trigger the expression of a preferably large set of different PGIPs, *B. rapa* ssp. *pekinensis* plants were infested with juvenile and adult mustard leaf beetles.

PGIPs have been shown to interact *in vitro* with completely and partially demethylated stretches of homogalacturonan via a pectin binding site composed of a regular cluster of positively charged amino acids [95]. Being ionically bound to the plant cell wall,

these proteins can be extracted with buffers of high ionic strength [47], [95]. Plant cell walls followed by cell wall-associated proteins were extracted with CaCl_2 and NaCl and analysed by MS/MS and their localisation was predicted by the presence of a signal peptide for the secretory pathway. The enrichment of extracellular proteins was successful with 71% extracellular and 29% intracellular proteins in a pool of both extractions ($\text{CaCl}_2 \cup \text{NaCl}$, Table 1). A simplification for the evaluation of the MS results was applied to cope with the magnitude of data. For MS analysis protein bands are excised from the SDS-PAGE gel at a certain size and further analysed. The detected peptides match to proteins of a similar, but also considerably larger or smaller predicted mass. Therefore, the protein hits were pre-filtered in the MS analysis according to their size as described in 6.2.22.3. This reduces the protein hits to proteins with a mass corresponding to the size range of the excised band. But pre-filtering the MS results in such a way probably leads to the exclusion of some proteins with a large number of post-translational modifications (PTMs). This fact should be taken into account if the data generated here will be used for further studies on post-translationally modified proteins. An alternative would be to consider all proteins with a similar or smaller predicted mass, which would result in a much larger dataset, but does not distinguish between proteins with and without PTMs. Since most extracellular plant proteins are glycosylated, this filter could include more proteins but also increases the risk for false-positives. However, the chosen selection of the protein hits was sufficient for the addressed question, yet not completely unbiased. The interaction of plant-derived cell wall proteins with beetle PGs was studied by affinity chromatography (see below). Of special interest were PGIPs, that are the most potential interaction partners of PGs, based on the literature [17], [34], [35]. Therefore special attention was paid to their detection, searching for their presence also outside of the pre-filtered size range. This privilege was applied only for proteins that were annotated as PGIPs or PGIP-like proteins in the NCBI nr database (Table 2).

In summary, the extraction of plant cell wall proteins, based on the protocol of Feiz et al. (2006) [47] was successfully adapted for *B. rapa* ssp. *pekinensis* and was sufficient to enrich extracellular proteins, which contain PGIPs, the most potential interaction partners for beetle PGs. Therefore, the plant cell wall protein extracts met all the requirements to be used for the interaction studies.

To investigate if *P. cochleariae* PGs were inhibited by *B. rapa* ssp. *pekinensis* cell wall proteins, the active PGs PCO-28-1, -5 and -9 (expressed in Sf9 insect cells), SSC_GH28-6 from *S. sclerotiorum* (expressed in *P. pastoris*, 7.4) as well as the *P. cochleariae* gut content were incubated with different concentrations of *B. rapa* ssp. *pekinensis* cell wall protein extract. A decrease of the activity of all PGs as well as the

gut content was observed with increasing concentrations of plant cell wall protein extract. At the highest protein amount of 16.2 µg the hydrolysis rates were reduced to 12 – 18% of initial activity. This observation strongly indicates the existence of one or multiple plant-derived proteins that inhibit the PG activity, not only of the fungal SSC_GH28-6, but also of the beetle PGs PCO_GH28-1, -5 and -9 and the *P. cochleariae* gut content. In the gut content plant-derived proteins, such as PGIPs, were found by Kirsch et al. (2012), indicating their resistance to proteolysis in the beetle's gut [23]. Thus the proteins are likely to be present intact in the gut and could potentially interact with gut proteins such as PGs. Nevertheless, the gut content showed PG activity when incubated without additional plant cell wall proteins, allowing three possible explanations. First, the plant-derived proteins present intact in the gut content do not inhibit the beetle PGs. Secondly, the inhibiting proteins might not be abundant enough to completely inhibit the PGs. On the one hand, this might be due to a considerably lower concentration compared to a potential excess of PGs. On the other hand, according to the “decoy” hypothesis, catalytically inactive PGs might bind inhibiting proteins and thereby protect the active PGs from inhibition [11]. Also, a combination of the latter two explanations is possible.

The incubation of the beetle gut content with *B. rapa* ssp. *pekinensis* cell wall protein extracts, mimicking the ingestion of a subset of the proteins normally taken up by *P. cochleariae* while feeding, led to a reduction of PG activity. This could suggest that inhibiting proteins might not survive the digestive environment in the beetle gut and are degraded by proteases, but act *in vitro* in the inhibition assay. This is unlikely, since intact proteins were detected in the gut by Kirsch et al. (2012) [23]. Furthermore, several host plant proteins, e.g. an endo-glucanase inhibitor protein or PR protein P2 from tomato (*Solanum lycopersicum*), have been identified to occur intact and be active in the gut and frass of herbivorous insects [96], [97]. By rearing the beetles on plants with a reduced or increased PGIP expression the survival of PG-inhibiting proteins in the insect gut could be tested. If plant-derived inhibitors stay intact in the beetle gut and partly inhibit the PG activity, a change of gut PG activity should be observable compared to beetles on wild type plant diet. A down-regulation of PGIPs was performed e.g. for *A. thaliana* (AtPGIP1) [98] or *Vitis vinifera* L. (VvPGIP1) [99]. AtPGIP1 and -2 [37] as well as BnPGIP1 and -2 [83] for example were overexpressed in *A. thaliana* and a high abundance of PGIPs might be sufficient to overcome the beetle's pectin hydrolysis activity.

To test the “decoy” hypothesis the catalytically active beetle PGs were incubated with different concentrations of cell wall proteins, analogous to the previous experiment, but this time the inactive PCO_GH28-3, -6 and -8 were added individually. This co-

incubation did not lead to less reduction of pectinolytic activity, but, as observed before, the PGs were inhibited by the plant cell wall protein extracts in the same concentration-dependent manner. Superficially considered, this argues against the “decoy” hypothesis, but it cannot be concluded from this experiment that inactive PGs have no effect on the active PG activity, because crude protein mixtures were used for the PGs as well as the plant cell wall protein extracts. The concentrations of PGs and interaction partners remain unknown. A potential overloading of the system with plant proteins may prevent the inactive PGs in this co-incubation experiment as well in the inhibition assay of the gut content (see above) to intercept all inhibiting proteins from the active PGs. Protein extracts were used in the experiments that derive from 0 – approx. 2.7 g of *B. rapa* ssp. *pekinensis* plant material. The applied volume of gut content solution was equivalent to approximately 10% of the gut content of one larva. According to these rough calculations one larva would have to ingest 27 g of plant material at once to encounter this amount of cell wall proteins, arguing for a likely overload of the system at least for the gut content. The experiments should be repeated using dilution series of plant cell wall protein extracts. Also, if inhibitors of beetle PGs were known, they could be expressed heterologously and the effect of inactive PGs on the inhibition of active PGs could be studied with purified proteins. Therefore, potential interaction partners for the beetle PGs were identified during this Master’s thesis project.

Both PGs PCO_GH28-1 and PCO_GH28-3 were found in the same protein band in the proteomics study of Kirsch et al. (2012) together with a PGIP from *B. rapa* [23], thus representing promising candidates for studying PG-PGIP interactions. These PGs were favored for the interaction studies over the other pair of active (PCO_GH28-9) and inactive (PCO_GH28-6) PGs, also found in the same protein band as a PGIP, due to an amino acid exchange in the catalytic centre of PCO_GH28-3. A conserved, catalytically important aspartate is replaced by an asparagine, being the putative reason for the loss of activity [23]. Such amino acid exchange is not present in PCO_GH28-6 making an activity towards another substrate as likely as acting as a “decoy” molecule.

SSC_GH28-6 is known to be inhibited by the *B. napus* BnPGIP1 [83]. Due to the close relationship of *B. napus* and *B. rapa* ssp. *pekinensis* it is likely that a *B. rapa* ssp. *pekinensis* PGIP, that is homologous to BnPGIP1, might interact with and inhibit SSC_GH28-6 as well. Therefore this fungal PG functions as a positive control in the PG-PGIP interaction study.

Since for affinity chromatography milligrams of pure PGs were needed, a yeast expression system was used instead of the established Sf9 insect cells, which allows the production of proteins in considerably higher amounts [57]. The PGs PCO_GH28-1,

PCO_GH28-3 and SSC_GH28-6 were expressed in the yeast *P. pastoris* and the secreted recombinant proteins were detected in the culture medium after 12 h already (PCO_GH28-1 Figure 3, PCO_GH28-3 and SSC_GH28-6 Supplementary Data Figure 13 and Figure 14 respectively).

PCO_GH28-1 and SSC_GH28-6 are known to be active PGs [11], [83], whereas PCO_GH28-3 did not show any pectinolytic activity against the tested substrates in previous experiments [11]. Accordingly, PCO_GH28-1 and SSC_GH28-6 degraded demethylated and partly methylated polygalacturonic acid, whereas no pectin hydrolysis was achieved by PCO_GH28-3 (Figure 4), confirming the results of Kirsch et al. (2014) [11]. The functional integrity of PGs expressed in *P. pastoris* was thus demonstrated for PCO_GH28-1 and SSC_GH28-6.

PGs are glycosylated proteins. When using an insect cell expression system the PTMs added to the proteins are more similar to those in the beetle host organism. Some yeast tend to hyperglycosylate recombinantly expressed proteins, which can influence function, folding, transport and interaction of the proteins [84]. A comparison of PCO_GH28-1, PCO_GH28-3 and SSC_GH28-6 expressed in *P. pastoris* and Sf9 insect cells showed no significant difference in the amount of PTMs (Figure 5). Due to the similarity of glycosylations in insect cells and yeast and the functional integrity (demonstrable for PCO_GH28-1 and SSC_GH28-6) *P. pastoris* was confirmed to be an adequate expression system not only for the fungal PG SSC_GH28-6 but also for the beetle PGs PCO_GH28-1 and PCO_GH28-3. SSC_GH28-6 has been demonstrated to be expressed in “large amounts” [83] in *P. pastoris*. Also, other proteins of insect or even plant origin have been successfully expressed in *P. pastoris* before [100]. For example, a β -fructofuranosidase from the sugarcane weevil (*Sphenophorus levis*) or α -amylases from the cotton bollworm *Helicoverpa armigera* were expressed in *P. pastoris* and purified using nickel IMAC with a yield of 16 (SI- β -fruct), 2.5 (HaAmy1) and 8.5 (HaAmy2) mg/l of culture respectively [101], [102], supporting the assumption of *P. pastoris* being an appropriate expression system for insect proteins.

The PGs PCO_GH28-1, PCO_GH28-3 and SSC_GH28-6 contain a His₆ tag, theoretically allowing purification by IMAC. Unfortunately, all strategies to purify SSC_GH28-6 failed. A variety of the protein's characteristics were taken into account for the purification, including the presence of affinity tags (His₆ and V5), glycosylation, charge and hydrophobicity. During these numerous approaches I had the opportunity to characterise SSC_GH28-6. A particularly special characteristic of SSC_GH28-6 was its mode of action. Like other PGs it showed an increase of the pectin hydrolysis correlating with the decrease of methylation. But unlike any other PG described so far it was able to release galacturonic acid oligomers as well as trimers, dimers and

monomers. Even di-galacturonic acid was degraded by SSC_GH28-6, indicating endo- as well as exo-PG activity. Usually PGs are characterised to be either endo- or exo-active. The intrinsic property to cleave the homogalacturonan either randomly into oligomers or terminally hydrolysing galacturonic acid monomers is defined by the substrate binding site of the enzymes. In endo-PGs the polygalacturonic acid backbone fits into an open-ended cleft, allowing internal cleavage, whereas in exo-PGs the substrate binding by a closed pocket restricts the enzyme to the exclusive hydrolysis of terminal galacturonic acid residues [103]. To my knowledge, no structure of a PG with mixed endo-exo-mode of action has been reported. Thus it would be interesting to identify the structural properties that enable SSC_GH28-6 to bind to pectin both internally as well as terminally, allowing the breakdown of the complete homogalacturonan to the galacturonic acid monomer by a single enzyme. Besides, this endo-exo-mixed mode of action could be an explanation why SSC_GH28-6 did not bind to and could probably not be purified using insoluble pectin. Endo-active PGs (e.g. PCO_GH28-1) are immobilised to cross-linked pectin due to a lacking leaving group in the hydrolysis reaction and can thus be separated from the supernatant by centrifugation. The ability to hydrolyse terminal galacturonic acid residues might result in the incomplete binding of SSC_GH28-6 to the substrate. No binding at all to insoluble pectin was observed for PCO_GH28-3. Additional to the catalytic amino acid replacement, this could be another reason for its inactivity, since binding of the substrate is one important prerequisite for the hydrolysis reaction.

PCO_GH28-1 and PCO_GH28-3 were purified by IMAC. At best 0.77 mg/ml were detected in the elution fraction after purification, which corresponds to 0.015 g/l of culture. This is in the range of 0.004 – 2.5 g/l that were obtained expressing enzymes according to the EasySelect™ Pichia Expression Kit manual [57]. For insect proteins comparable yields of e.g. 0.016 or 0.0085 g/l culture were obtained (see above). But most of the time the yield of *P. cochleariae* PGs was below 0.1 mg/ml purified protein and even though enough protein was obtained for further studies, the yield was not satisfying. Western Blots showed that the proteins did not bind quantitatively to the column and some protein was detected in the flow-through. A saturation of the column can be excluded by measuring the applied protein which never reached the binding capacity. This indicates a general problem of PG purification by His₆ tag and IMAC not only in case of SSC_GH28-6 but also for the beetle PGs. To improve the yield, purification efficiencies should be tested using different affinity tags. Only few reports about successful purification of PGs with specific affinity tags were published so far (e.g. expression in *P. pastoris* [104] or *E. coli* [105], purification by Ni²⁺ IMAC).

The purity of PCO_GH28-1 and PCO_GH28-3 was monitored by SDS-PAGE (Figure 6). In addition to the main PCO_GH28-1 protein band seven other bands of lower intensity were detected. This indicates the presence of proteins other than PCO_GH28-1 in the sample and thus an insufficient purification. But surprisingly, the MS/MS analysis of these bands revealed PCO_GH28-1 as the only or by far major protein hit. Additionally, a temperature-dependent degradation of the enzyme was observed in the Western Blot. This reproducible band pattern indicates a fragmentation of the protein into distinct peptides rather than random decay. Due to the high abundance of the matching peptides (17 – 42 peptides per protein band) all protein bands were assigned to PCO_GH28-1. But a mapping of the respective protein bands onto distinct parts of PCO_GH28-1, using the resulting peptides from the MS analysis (Figure 17), was not possible, because the detected peptides of each band covered the same protein regions (Supplementary Data Figure 17). This can be explained by the loss of glycosylations as well as different protein fragments of the same size in one protein band. Detection of potential pre-determined breaking points in the protein could be achieved by e.g. Edman degradation. A temperature-dependent fragmentation was also observed for PCO_GH28-3 (Supplementary Data Figure 15), but less compared to PCO_GH28-1. The observation of a PG fragmentation is of great relevance for future purifications, since it demonstrates that multiple bands in a SDS-PAGE gel do not necessarily indicate the presence of impurities but can derive from a single, purified protein.

The purified proteins PCO_GH28-1 and PCO_GH28-3 were immobilised on affinity columns. For SSC_GH28-6 no purification was achieved and thus total proteins from the medium of non-transfected and SSC_GH28-6-expressing yeast cells were concentrated and used for the interaction studies. Theoretically, these secreted proteins should only differ in the recombinant SSC_GH28-6 and differences in the eluted plant protein patterns might indicate potential interaction partners which are specific for SSC_GH28-6. Indeed, the expression pattern observed for transfected and non-transfected cells was similar, except for one band (Figure 11, arrow with closed arrowhead). In this protein band SSC_GH28-6, amongst other protein hits, was detected by MS analysis. But the top hits were an ATPase (mass 74226, peptides 16(11), score 1013) and an alcohol oxidase (AOX, mass 74489, peptides 16(8), score 751) both from *P. pastoris* GS115. Comparing their number of detected peptides with that of SSC_GH28-6 (peptides 2(2), score 165) allows the conclusion that the PG is present in considerably lower abundance. Linearised pPICZ α A-SSC_GH28-6 integrates at the AOX1 locus and thus both SSC_GH28-6 and AOX are induced simultaneously by methanol during expression. Assuming that a higher number of

peptides correspond to a higher expression level of the AOX, there have likely been problems during the expression of SSC_GH28-6, which also might have influenced its purification. Compared to PCO_GH28-1 and PCO_GH28-3, SSC_GH28-6 contains notably more glycosylations (Figure 5). Since no sugars are present in the expression medium, this excessive demand might influence the metabolic pathways and expression of the glycosylated protein. This problem might be circumvented by the supplementation of other carbon sources, e.g. trehalose, sorbitol or mannitol, to the expression medium in addition to methanol that can be utilised by the yeast but do not repress the AOX1 promotor [106]. It has also been demonstrated that continuously releasing glucose enzymatically from a glucose polymer (enzymatic glucose feed) may avoid starvation of the yeast in between methanol pulses and at the same time keep the glucose level below an AOX promotor-repressing concentration, consequently increasing the yield of the recombinantly expressed protein [107]. These methods could be tested to improve SSC_GH28-6 but also beetle PG expression in the future. Nevertheless, since SSC_GH28-6 was detected by MS/MS, the protein mixture was used for interaction studies. According to the complex mixture of total protein extracts immobilised on the column, a variety of different protein bands were visible in the elutions (Figure 11). Three bands were exclusively detected for the SSC_GH28-6 and not the yeast wild type column, making them potential specific interaction partners. The respective protein bands were analysed by MS/MS. SSC_GH28-6 interacted with the polygalacturonase inhibiting protein 3 from *B. rapa* ssp. *pekinensis* (category 3, see below) and one not characterised LRR protein (category 1) (Table 4). The LRR protein was not detected in the plant cell wall protein extract, indicating enrichment up to the detection limit by interaction with the PG. It can be concluded from this single experiment that, if SSC_GH28-6 could be purified successfully, it could be used as a positive control for such PG-PGIP interaction assays.

But even without SSC_GH28-6 as positive control, the results obtained from the interaction study of PCO_GH28-1 and PCO_GH28-3 with plant cell wall protein extracts revealed that the establishment of the affinity chromatography method in general was successful. Two different protein band patterns were observed in the elution fractions of the beetle PGs (Figure 12), indicating a divergent set of interacting partners for the active and inactive PG. A more intense background in the SDS-PAGE gel was detected for PCO_GH28-1. This is reflected by a more diverse set of proteins detected for PCO_GH28-1 (90 protein hits), suggesting a more specific binding of proteins to PCO_GH28-3 (13 protein hits). But the columns used for the experiment differ in their date of manufacturing as well as the amount of immobilised protein (PCO_GH28-1: 1.72 g, PCO_GH28-3: 0.91 g). The PCO_GH28-3 column was used

shortly after immobilisation of the proteins, whereas the PCO_GH28-1 column was stored at 4°C before use. However, a positive activity assay, using an aliquot of immobilised PCO_GH28-1, excluded loss of conformational changes or degradation and thus enabled the use for interaction studies. Nevertheless, if this interaction study would be repeated, it should be performed with two columns of the same age that were loaded with the same amount of protein.

One main protein band was detected for PCO_GH28-1 at approximately 22 kDa (band 7, Table 5). Two of the detected proteins are annotated as “germin-like” proteins. Germins and germin-like proteins (GLPs) have been found to be usually associated with the plant cell wall and are involved in e.g. germination, developmental processes, fruit ripening, and, most interestingly, also in plant defence [108]. Like PGIPs, their expression can be upregulated upon pathogen infection [109], [110] and their hydrogen peroxide-generating activity is thought to have an anti-microbial effect [108]. Additionally, hydrogen peroxide has been hypothesised to be involved in the cross-linking of cell wall components, e.g. pectin or proteins, in order to strengthen the plant cell wall upon pathogen attack [111], [112], [108]. To my knowledge, nothing is known about PG-germin interactions. Further research on germin and GLP interaction with PGs might elucidate their potential contribution to plant defence against herbivores.

Moreover, one protein of protein band 7 was predicted to be an STS14 protein. STS14 is similar to pathogen-related PR1-proteins, also involved in plant defence [113]. The fourth protein detected in this band is a predicted serine protease inhibitor family protein. Many proteases and protease inhibitors were found in this interaction study. This is not surprising, since proteases degrade and thus need to bind other proteins. Those were usually only listed in the complete tables (Supplementary Data Table 9, Table 10, Table 11).

The analysis of protein band 7 also present in PCO_GH28-3 revealed no protein hits within the corresponding size range. The proteins from band 7 might be glycosylated proteins that are missed due to the size filter or their peptides were difficult to ionise. PGIPs belong to the superfamily of LRR proteins. In Brassicaceae their number of detected genes ranges from two in *A. thaliana* [37] to 16 in *B. napus* [38]. In *B. rapa* ssp. *pekinensis* nine PGIPs were found by Dr. Roy Kirsch (personal communication). But only one PGIP has been functionally characterised in the genus *Brassica*: BnPGIP1 from *B. napus* inhibits the PG SSC_GH28-6 from *S. sclerotiorum* [83]. Since *B. napus* and *A. thaliana* as well as characterised legume and grass PGIPs share a common ancestry in phylogenetic analyses, a PG-inhibiting property, like for BnPGIP1, can be assumed for the related *Brassica* proteins [114].

Usually PGIPs possess a molecular mass around 40 kDa. Between 25 and 55 kDa four protein bands of low intensity were visible for PCO_GH28-1, two of them around 40 kDa (Table 6, Figure 12, lane 4). One major and one fainter band were detected for PCO_GH28-3 at approximately 40 kDa (Table 7, Figure 12 lane 8). The proteins found and potentially interacting with the two PGs were assigned to three categories: 1) uncharacterised LRR proteins that were not annotated as PGIPs or PGIP-like proteins and exhibit low similarity (0 – 40%) with BnPGIP1, for which the PG-inhibiting property has been demonstrated [83], 2) LRR proteins that were annotated to be PGIPs or PGIP-like proteins but share medium sequence identity (40 – 70%) with BnPGIP1, 3) proteins that share high similarity (70 – 100%) with BnPGIP1.

PCO_GH28-1 and PCO_GH28-3 interacted with the same category 1 protein, which was also detected for SSC_GH28-6, and same two category 2 proteins. For PCO_GH28-1 five category 3 proteins were detected that shared a high sequence similarity with BnPGIP1. Interestingly, no category 3 proteins were detected for PCO_GH28-3. The close sequence similarity of category 3 proteins with the characterised BnPGIP1 indicates that they might be PGIPs as well, making them good candidates for heterologous expression and subsequent inhibition assays with beetle PGs.

More peptides matching category 2 proteins were found for PCO_GH28-3 than for PCO_GH28-1, assuming their higher abundance, which is consistent with intensity of the protein bands. But other proteins from the crude cell wall protein mixture might influence the interaction of PG inhibitors with the column. A different binding pattern might also be the result of the interaction of PGs with other proteins (e.g. abundant proteins from protein band 7 for PCO_GH28-1), which might outcompete PGIP and PGIP-like proteins for binding sites. Again, the heterologous expression and incubation of purified proteins could elucidate the different binding affinities of PGIPs and PGIP-like proteins to beetle PGs and their inhibitory potential. This affinity chromatography identified good candidates of PGIPs and PGIP-like proteins to use in such direct interaction studies, especially because none of the PGIP-like proteins has been tested for PG-inhibiting properties.

Doubts about contribution of category 2 proteins to PG-inhibition might arise from their medium sequence identity to the characterised BnPGIP1. By incubating PCO_GH28-1 with the elutions from PCO_GH28-3, lacking category 3 PGIPs but are enriched in category 2 PGIP-like proteins, their PG-inhibiting ability could be tested. If the plant cell wall proteins that bound to PCO_GH28-3 would inhibit pectinolytic activity of PCO_GH28 1, the “decoy” hypothesis would be supported, since the inactive would shield the active PG from inhibiting proteins.

In addition to the direct protective function of inactive PGs, another mechanism is conceivable how these proteins contribute to a pectin breakdown by active PGs. PGIPs do not only function by directly binding PGs and thus inhibiting their hydrolytic activity. They have been shown to bind homogalacturonan and thereby interfere with the action of attacking PGs [95]. A binding to inactive PGs without the ability to inhibit active PGs could be evidence for such polysaccharide-protective PGIPs. A detachment of those PGIPs from the cell wall through binding of inactive PGs may support active PGIPs in their pectinolytic activity by liberation of the substrate for hydrolysis.

Category 2 proteins are annotated to be PGIPs or PGIP-like proteins, but Brassicaceae counterparts share only approximately 50% sequence identity with the characterised BnPGIP1. But there is some evidence from the literature that there are PGIPs that structurally vary from the conserved PGIP motifs.

Plant extracellular LRR (eLRR) proteins, amongst them PGIPs, share the conserved motif of 24 residues LxxLxxLxLxxNxLT/SGxIPxxLGx, tandemly repeated 10 times [115]. It is suggested that protein-protein interaction is enabled by the eLRR domain, but the structural basis of the recognition ability remains elusive [115], [116]. Plant proteins containing eLRRs can be divided into four classes, including not only PGIPs and PGIP-like proteins, but also leucine-rich repeat extensins (LRXs) and LRX-like proteins as well as the transmembrane receptor-like proteins and receptor-like kinases [116], [44]. In PGIPs the LRRs form a curved superhelix, whose concave face is made of parallel β -sheets and involved in PG binding [44].

OsPGIP1 from *Oryza sativa* L. was demonstrated to be an active PGIP, even though an entire LRR motif is missing from its amino acid sequence [117]. Furthermore, a PGIP was identified, TaPGIP3 from *Triticum aestivum*, that deviates from the conserved structure of PGIPs, containing nine instead of 10 LRR motifs, of which 3 – 7 are relatively conserved compared to other PGIPs, as well as an additional 91 amino acid insert. A potential role in plant defence, analogous to other PGIPs, is suggested for the cell wall-associated TaPGIP3, since silencing enhanced the plant's susceptibility towards *Fusarium graminearum* infection [118].

Another *Brassica* PGIP, BcMF19, from *Brassica campestris* L. ssp. *chinensis* Makino, was recently analysed and exhibits the usual structural characteristics of a PGIP, but no PG-inhibiting activity was tested for BcMF19 so far. Instead, a contribution to germination and pollen development was suggested [119], [120].

Alltogether, only a few of the numerous plant PGIPs and PGIP-like proteins have been characterised to really inhibit PGs and the function of most proteins remains elusive. During this Master's thesis a protein categorisation was used according to their similarity with a characterised PGIP, but a phylogenetic analysis would provide insight

into the real relationship of PGIPs and PGIP-like proteins from an evolutionary point of view. Moreover, mapping the known activities onto the tree could suggest functions for the so far uncharacterised members.

Besides the potential inhibition of insect PGs, uncharacterised PGIP-like proteins, which differ from conserved PGIP structures, could be involved in the regulation of plant PGs. This putative novel class of PGIP-like proteins might be good candidates in the search for plant PG-targeting PGIPs.

In summary, all of these experiments were performed to test the “decoy” hypothesis stated by Kirsch et al. (2014) [11] and to identify beetle PG-interacting, plant-derived proteins by an approach as unbiased as possible. Still, no definite answer can be provided concerning the role of inactive beetle PGs in the interaction of active PGs with plant-derived inhibiting proteins. But a variety of new insights in the interaction of *P. cochleariae* PGs with *B. rapa* ssp. *pekinensis* cell wall proteins was obtained in the course of my Master’s thesis that lay the foundation for a wide range of further experiments to address these open questions.

First of all, the protocol for the enrichment of plant cell wall-associated proteins of Feiz et al. (2006) [47] was successfully adapted for *B. rapa* ssp. *pekinensis*. Using this method PGIPs and PGIP-like proteins, the most promising candidates for the interaction with beetle PGs, were detected by MS analysis in these plant cell wall protein extracts.

Activity assays demonstrated that beetle PGs, namely PCO_GH28-1, -5 and -9 as well as the pectinolytic activity of the total *P. cochleariae* gut content, and the fungal SSC_GH28-6 were inhibited by *B. rapa* ssp. *pekinensis* cell wall protein extracts.

The heterologous expression of beetle PGs (PCO_GH28-1 and PCO_GH28-3) and a fungal PG (SSC_GH28-6) was established for the *P. pastoris* yeast expression system. Purification of PGs was studied intensively and succeeded for the two beetle PGs.

Interaction studies performed by affinity chromatography of purified PGs with plant cell wall protein extracts and subsequent MS analysis of the elutions enabled the identification of plant-derived interaction partners of the active PCO_GH28-1 and the catalytically inactive PCO_GH28-3. A differential interaction of the two beetle PGs with the cell wall proteins was observed. Category 3 proteins, that share a high sequence similarity with the characterised BnPGIP1, only interacted with the active PCO_GH28-1. Uncharacterised LRR proteins (category 1) and category 2 proteins, PGIP-like proteins that share only medium sequence similarity with BnPGIP1, were found to interact with both PGs, but in case of the category 2 proteins predominantly with the inactive PCO_GH28-3.

PGIP-like proteins might be involved in plant developmental processes [119], [120] or defence [118] by inhibiting PGs or shielding the pectin from attacking proteins [95]. But their function in all of these mechanisms is still elusive.

The “decoy” hypothesis remains unproven. But the plant proteins identified as interaction partners for beetle PGs limit the complex set of plant proteins to a small number of good candidates for the heterologous expression of PGIPs and PGIP-like proteins and their application in a variety of upcoming experiments. In one-to-one interaction studies the inhibitory properties of candidate proteins could be tested individually, potentially revealing different specificities and affinities towards active and inactive beetle PGs. This could be the key to confirm or falsify the “decoy” hypothesis by Kirsch et al. (2014) [11] and could help to elucidate the function of catalytically inactive, yet expressed beetle PGs.

The discovery of novel PGIP-like proteins, sharing low sequence similarity with Brassicaceae LRR proteins previously categorised as PGIPs, allows speculation about their potential function in plant defence, development and/or plant PG regulation. The results obtained in this Master’s thesis provide first evidence that herbivorous beetles such as *P. cochleariae* encounter plant-derived PG-inhibiting proteins and need to circumvent this plant defence mechanism to ensure the efficient pectinolytic activity of their PGs. The underlying adaptations remain elusive but represent an exciting subject in the completely undiscovered field of beetle PG-PGIP research and could contribute to the understanding of herbivorous insect evolution in general.

9 Future perspectives

The “decoy” hypothesis by Kirsch et al. (2014) [11] remains unproven. During this Master’s thesis differential interactions of the active *P. cochleariae* PG PCO_GH28-1 and the inactive PCO_GH28-3 with *B. rapa* ssp. *pekinensis* cell wall proteins were observed. This study provides good candidates to further investigate PG-PGIP interactions in general and to disentangle the putative role of inactive beetle PGs in the interaction of active PGs with plant-derived inhibiting proteins.

The plant PGIPs and PGIP-like proteins identified here could be heterologously expressed and used in one-to-one interaction experiments with beetle PGs. Category 3 proteins, that show high sequence similarity with the characterised BnPGIP1 and interacted only with PCO_GH28-1, could be tested for their PG-inhibiting property and affinity towards active and inactive beetle PGs. Testing category 2 proteins, that share medium sequence similarity with BnPGIP1, for PGIP activity would be of special interest, as no such protein has been characterised yet and their function remains unknown. These experiments could be the key to confirm or falsify the “decoy” hypothesis.

In addition, a phylogenetic analysis could shed light on the evolutionary relationships of category 2 and category 3 proteins.

Proteins annotated as “germin-like”, suggested to be involved in plant development and defence, showed a high affinity towards PCO_GH28-1. Nothing is known so far about germin-like protein-PG interactions. This raises the question, which function these proteins have and why they interacted with the beetle PG.

All in all, nothing is known about how herbivorous beetles might circumvent plant inhibitors to ensure the pectin hydrolysis. This study provided the first insight into this topic and also enables to address questions about the complex interaction of beetle PGs with plant defence proteins and herbivorous insect evolution in general.

10 Summary

The mustard leaf beetle *P. cochleariae* feeds on various plants of the Brassicaceae family. The plant cells are encased by plant cell walls, a complex mixture of polysaccharides (e.g. pectin) and proteins [6]. Polygalacturonases (PGs), enzymes of the glycoside hydrolase family 28, degrade homogalacturonan, the major pectin component [3]. Nine PG genes were previously identified in *P. cochleariae*, of which active and catalytically inactive PGs were expressed in the gut in comparable abundance [11], [23]. Interestingly, also plant-derived polygalacturonase-inhibiting proteins (PGIPs) co-eluted with *P. cochleariae* PGs, indicating a potential interaction of beetle PGs and plant PGIPs. The function of inactive PGs remains elusive, and it has been hypothesised that they “may act as “decoy” targets for PGIPs, thus protecting the active PGs from inhibition” [11].

During my Master’s thesis plant cell wall proteins from *B. rapa* ssp. *pekinensis*, a *P. cochleariae* host plant, were extracted. These inhibited the PG activity of the beetle’s PCO_GH28-1, -5 and -9, total gut content and the fungal SSC_GH28-6, indicating the presence of proteinaceous plant PG inhibitors. To find PG interaction partners and to test the “decoy” hypothesis the active PCO_GH28-1 and the inactive PCO_GH28-3 were expressed in *P. pastoris*, purified and used for interaction studies with plant cell wall proteins. Analysis of interacting proteins by MS/MS showed differential interaction of the active and inactive PG with plant proteins. Of special interest were PGIPs and PGIP-like proteins and of those three categories of proteins were detected to interact with the PGs. 1) One uncharacterised LRR protein interacted with both PGs. 2) Several proteins were detected that were annotated as PGIPs or PGIP-like proteins, but shared medium sequence similarity with BnPGIP1, a characterised PG inhibitor. These novel PGIP-like proteins differing from conserved PGIP structures were found for both PGs, but predominantly for PCO_GH28-3. 3) Proteins that shared a high sequence similarity with BnPGIP1, also suggesting PGIP activity for these proteins, were found to interact only with PCO_GH28-1. Since only one of the numerous *Brassica* spp. PGIPs has been characterised so far, the role of PGIPs and PGIP-like proteins remains elusive. Besides plant defence (e.g. inhibition of PGs or shielding of homogalacturonan), functions in developmental processes or regulation of plant PGs might be conceivable. The results obtained in this Master’s thesis provide first evidence that herbivorous beetles such as *P. cochleariae* encounter plant-derived PG-inhibiting proteins and need to circumvent this plant defence mechanism to ensure an efficient pectin breakdown. The underlying adaptations remain elusive but represent an exciting subject in the completely undiscovered field of beetle PG-PGIP research and could contribute to the understanding of herbivorous insect evolution in general.

11 Zusammenfassung

Der herbivore Meerrettichblattkäfer *P. cochleariae* lebt ektophytisch auf Pflanzen der Kreuzblütengewächse (Brassicaceae) und ernährt sich von deren Blättern. Die beim Fraß aufgenommenen Pflanzenzellen sind von einer pflanzlichen Zellwand umgeben. Hierbei handelt es sich um eine komplexe Struktur aus Polysacchariden, wie z.B. Pektin, und Proteinen [6]. Polygalacturonasen (PGs) gehören zur Familie 28 der Glycosylhydrolasen (GH28) und hydrolysieren Homogalacturonan, welches den Hauptbestandteil von Pektin darstellt [3]. *P. cochleariae* besitzt neun PG-Gene, von denen sowohl die aktiven als auch katalytisch inaktiven Proteine spezifisch im Darm des Käfers exprimiert werden [11], [23]. Die Co-Elution von pflanzlichen Polygalacturonase-inhibierenden Proteinen (PGIPs) mit Käfer-PGs in einem 2D-Proteomics-Versuch von Kirsch et al. (2012) lässt eine potentielle Interaktion von Käfer-PGs mit pflanzlichen PGIPs vermuten [23]. Kirsch et al. stellten 2014 die Hypothese auf, dass katalytisch inaktive PGs als „Köder“ für PGIPs, dienen könnten, die diese binden und so zum Schutz von aktiven PGs beitragen könnten [11].

Während meiner Masterarbeit habe ich Zellwandproteine aus *B. rapa* ssp. *pekinensis*, einer der Wirtspflanzen von *P. cochleariae*, extrahiert und nachgewiesen, dass diese die Käfer-PGs PCO_GH28-1, -5 und -9, sowie die pektinolytische Aktivität des Darminhalts und eine pilzliche PG, SSC_GH28-6, inhibierten. Um Proteine zu identifizieren, für diese Inhibition verantwortlich sein könnten und die „Köder“-Hypothese zu untersuchen, wurden die aktive PG PCO_GH28-1 und die inaktive PCO_GH28-3 in *P. pastoris* exprimiert, aufgereinigt und für Interaktionsstudien mit pflanzlichen Zellwandextrakten verwendet. Die an die PGs gebundenen Proteine wurden mittels MS/MS analysiert. Für PCO_GH28-1 und PCO_GH28-3 konnte eine unterschiedliche Interaktion mit pflanzlichen Zellwandproteinen nachgewiesen werden. Unter den detektierten Interaktionspartnern waren vor allem PGIPs und PGIP-ähnliche Proteine von besonderem Interesse. Diese wurden in drei Kategorien eingeteilt. 1) Für beide PGs wurde ein bislang noch nicht charakterisiertes *leucine-rich repeat* (LRR)-Protein detektiert. 2) Proteine, die als PGIPs oder PGIP-ähnliche Proteine benannt wurden, jedoch nur geringe Ähnlichkeit mit BnPGIP1, einem charakterisierten PG-inhibierenden Protein, aufwiesen, interagierten mit beiden PGs. Diese neuartigen PGIP-ähnlichen Proteine, die von der konservierten Struktur bisher bekannter PGIPs abweichen, wurden vorwiegend für PCO_GH28-3 gefunden. 3) Nur für PCO_GH28-1 wurde die Interaktion mit Proteinen nachgewiesen, die eine hohe Sequenzähnlichkeit mit BnPGIP1 aufweisen, was ebenfalls eine PG-inhibierende Funktion dieser Proteine vermuten lässt.

Da von den zahlreichen PGIPs der Brassica spp. bisher nur ein einziges Protein, BnPGIP1, als PG-inhibierendes Protein charakterisiert wurde, ist über die Funktion der PGIPs und PGIP-ähnlichen Proteine nur wenig bekannt. Außer für die Abwehr der Pflanze (z.B. durch Inhibition von PGs oder protektive Bindung an Homogalacturonan) könnten diese eine Rolle bei Entwicklungsprozessen oder sogar der Regulation von pflanzeneigenen PGs spielen.

Die Ergebnisse dieser Masterarbeit liefern erste Hinweise darauf, dass herbivore Insekten wie *P. cochleariae* Proteine mit der Nahrung zu sich nehmen, die ihre PGs inhibieren. Um die effiziente Hydrolyse von Pektin zu gewährleisten, müssen diese pflanzlichen Abwehrmechanismen umgangen werden. Die dazu notwendigen Adaptionen des Käfers sind nicht bekannt, stellen aber ein interessantes Thema in dem bislang unerforschten Gebiet der Interaktionen zwischen Käfer-PGs und pflanzlichen PGIPs dar und könnte zum Verständnis der Evolution von herbivoren Insekten im Allgemeinen beitragen.

12 Literature

1. Dettner, K. and Peters, W., *Lehrbuch Der Entomologie*. 2011: Spektrum Akademischer Verlag.
2. Brett, C. and Waldron, K., *Physiology and Biochemistry of Plant Cell Walls*. Topics in Plant Physiology. Vol. 2. 1990: Springer Netherlands.
3. Caffall, K.H. and Mohnen, D., *The structure, function, and biosynthesis of plant cell wall pectic polysaccharides*. Carbohydr Res, 2009. 344(14): p. 1879-900.
4. Northcote, D.H., *Chemistry of the Plant Cell Wall*. Annual Review of Plant Physiology, 1972. 23(1): p. 113-132.
5. Cosgrove, D.J., *Growth of the plant cell wall*. Nat Rev Mol Cell Biol, 2005. 6(11): p. 850-61.
6. Mohnen, D., *Pectin structure and biosynthesis*. Curr Opin Plant Biol, 2008. 11(3): p. 266-77.
7. Lombard, V., et al., *A hierarchical classification of polysaccharide lyases for glycogenomics*. Biochem J, 2010. 432(3): p. 437-44.
8. Davies, G. and Henrissat, B., *Structures and mechanisms of glycosyl hydrolases*. Structure, 1995. 3(9): p. 853-859.
9. *Carbohydrate-active enzymes database (CAZy)*. Available from: <http://www.cazy.org/>. Cited: 21.9.2015
10. Pelloux, J., Rustérucchi, C., and Mellerowicz, E.J., *New insights into pectin methylesterase structure and function*. Trends in Plant Science, 2007. 12(6): p. 267-277.
11. Kirsch, R., et al., *Horizontal gene transfer and functional diversification of plant cell wall degrading polygalacturonases: Key events in the evolution of herbivory in beetles*. Insect Biochem Mol Biol, 2014. 52: p. 33-50.
12. Benen, J.A., Kester, H.C., and Visser, J., *Kinetic characterization of Aspergillus niger N400 endopolygalacturonases I, II and C*. Eur J Biochem, 1999. 259(3): p. 577-85.
13. André-Leroux, G., Tessier, D., and Bonnin, E., *Action pattern of Fusarium moniliforme endopolygalacturonase towards pectin fragments: Comprehension and prediction*. Biochimica et Biophysica Acta (BBA) - Proteins and Proteomics, 2005. 1749(1): p. 53-64.
14. Bordenave, M., *Analysis of Pectin Methyl Esterases*, in *Plant Cell Wall Analysis*, Linskens, H. and Jackson, J., Editors. 1996, Springer Berlin Heidelberg. p. 165-180.
15. Jolie, R.P., et al., *Pectin methylesterase and its proteinaceous inhibitor: a review*. Carbohydrate Research, 2010. 345(18): p. 2583-2595.
16. Jayani, R.S., Saxena, S., and Gupta, R., *Microbial pectinolytic enzymes: A review*. Process Biochemistry, 2005. 40(9): p. 2931-2944.
17. De Lorenzo, G., D'Ovidio, R., and Cervone, F., *The role of polygalacturonase-inhibiting proteins (PGIPs) in defense against pathogenic fungi*. Annu Rev Phytopathol, 2001. 39: p. 313-35.
18. Watanabe, H., et al., *A cellulase gene of termite origin*. Nature, 1998. 394(6691): p. 330-331.
19. Consortium, T.G.S., *The genome of the model beetle and pest Tribolium castaneum*. Nature, 2008. 452(7190): p. 949-955.
20. Consortium, T.I.S.G., *The genome of a lepidopteran model insect, the silkworm Bombyx mori*. Insect Biochem Mol Biol, 2008. 38(12): p. 1036-45.
21. Pauchet, Y., et al., *Diversity of Beetle Genes Encoding Novel Plant Cell Wall Degrading Enzymes*. PLoS ONE, 2010. 5(12): p. e15635.

22. Girard, C. and Jouanin, L., *Molecular cloning of cDNAs encoding a range of digestive enzymes from a phytophagous beetle, Phaeton cochleariae*. Insect Biochemistry and Molecular Biology, 1999. 29(12): p. 1129-1142.
23. Kirsch, R., et al., *Combining proteomics and transcriptome sequencing to identify active plant-cell-wall-degrading enzymes in a leaf beetle*. BMC Genomics, 2012. 13: p. 587.
24. Shen, Z., et al., *Polygalacturonase from Sitophilus oryzae: Possible horizontal transfer of a pectinase gene from fungi to weevils*. Journal of Insect Science, 2003. 3: p. 24.
25. Shelomi, M., et al., *Differential expression of endogenous plant cell wall degrading enzyme genes in the stick insect (Phasmatodea) midgut*. BMC Genomics, 2014. 15: p. 917.
26. Danchin, E.G.J., et al., *Multiple lateral gene transfers and duplications have promoted plant parasitism ability in nematodes*. Proceedings of the National Academy of Sciences of the United States of America, 2010. 107(41): p. 17651-17656.
27. Jaubert, S., et al., *A polygalacturonase of animal origin isolated from the root-knot nematode Meloidogyne incognita1*. FEBS Letters, 2002. 522(1–3): p. 109-112.
28. Marvaldi, A.E., et al., *Structural alignment of 18S and 28S rDNA sequences provides insights into phylogeny of Phytophaga (Coleoptera: Curculionoidea and Chrysomeloidea)*. Zoologica Scripta, 2009. 38(1): p. 63-77.
29. Marvaldi, A.E., et al., *Molecular and Morphological Phylogenetics of Weevils (Coleoptera, Curculionoidea): Do Niche Shifts Accompany Diversification?* Systematic Biology, 2002. 51(5): p. 761-785.
30. McKenna, D.D. and Farrell, B.D., *The Timetree of Life*. 2009: OUP Oxford.
31. *Phaeton cochleariae* (Fabricius, 1792). Available from: <http://www.thewcg.org.uk/chrysomelidae/0186G.htm>. Cited: 5.11.2015
32. *Phaeton cochleariae* Fabricius - Mustard Leaf Beetle. Available from: http://www.agroatlas.ru/en/content/pests/Phaeton_cochleariae/. Cited: 5.11.2015
33. *Der Meerrettichblattkäfer (Phaeton cochleariae Fbr.)*. Anzeiger für Schädlingkunde, 1929. 5(7): p. 84-85.
34. D'Ovidio, R., et al., *Characterization of the Complex Locus of Bean Encoding Polygalacturonase-Inhibiting Proteins Reveals Subfunctionalization for Defense against Fungi and Insects*. Plant Physiology, 2004. 135(4): p. 2424-2435.
35. Manfredini, C., et al., *Polygalacturonase-inhibiting protein 2 of Phaseolus vulgaris inhibits BcPG1, a polygalacturonase of Botrytis cinerea important for pathogenicity, and protects transgenic plants from infection*. Physiological and Molecular Plant Pathology, 2005. 67(2): p. 108-115.
36. Kalunke, R.M., et al., *An update on polygalacturonase-inhibiting protein (PGIP), a leucine-rich repeat protein that protects crop plants against pathogens*. Frontiers in Plant Science, 2015. 6.
37. Ferrari, S., et al., *Tandemly duplicated Arabidopsis genes that encode polygalacturonase-inhibiting proteins are regulated coordinately by different signal transduction pathways in response to fungal infection*. Plant Cell, 2003. 15(1): p. 93-106.
38. Hegedus, D., et al., *Brassica napus possesses an expanded set of polygalacturonase inhibitor protein genes that are differentially regulated in response to Sclerotinia sclerotiorum infection, wounding and defense hormone treatment*. Planta, 2008. 228(2): p. 241-253.
39. Powell, A.L.T., et al., *Transgenic Expression of Pear PGIP in Tomato Limits Fungal Colonization*. Molecular Plant-Microbe Interactions, 2000. 13(9): p. 942-950.
40. Li, R., et al., *Two Brassica napus polygalacturonase inhibitory protein genes are expressed at different levels in response to biotic and abiotic stresses*. Planta, 2003. 217(2): p. 299-308.

41. Cervone, F., et al., *The Interaction between Fungal Endopolygalacturonase and Plant Cell Wall PgiP (Polygalacturonase-Inhibiting Protein)*, in *Mechanisms of Plant Defense Responses*, Fritig, B. and Legrand, M., Editors. 1993, Springer Netherlands. p. 64-67.
42. Federici, L., et al., *Structural requirements of endopolygalacturonase for the interaction with PGIP (polygalacturonase-inhibiting protein)*. *Proc Natl Acad Sci U S A*, 2001. 98(23): p. 13425-30.
43. King, D., et al., *Use of amide exchange mass spectrometry to study conformational changes within the endopolygalacturonase II-homogalacturonan-polygalacturonase inhibiting protein system*. *Biochemistry*, 2002. 41(32): p. 10225-33.
44. Federici, L., et al., *Polygalacturonase inhibiting proteins: players in plant innate immunity?* *Trends in Plant Science*, 2006. 11(2): p. 65-70.
45. Leckie, F., et al., *The specificity of polygalacturonase-inhibiting protein (PGIP): a single amino acid substitution in the solvent-exposed beta-strand/beta-turn region of the leucine-rich repeats (LRRs) confers a new recognition capability*. *Embo j*, 1999. 18(9): p. 2352-63.
46. Doostdar, H., McCollum, T.G., and Mayer, R.T., *Purification and Characterization of an endo-Polygalacturonase from the Gut of West Indies Sugarcane Rootstalk Borer Weevil (Diaprepes abbreviatus L.) Larvae**. *Comparative Biochemistry and Physiology Part B: Biochemistry and Molecular Biology*, 1997. 118(4): p. 861-867.
47. Feiz, L., et al., *Evaluation of cell wall preparations for proteomics: a new procedure for purifying cell walls from Arabidopsis hypocotyls*. *Plant Methods*, 2006. 2: p. 10.
48. Wu, S. and Letchworth, G.J., *High efficiency transformation by electroporation of Pichia pastoris pretreated with lithium acetate and dithiothreitol*. *Biotechniques*, 2004. 36(1): p. 152-4.
49. Invitrogen. *pIB/V5-His TOPO TA Expression Kit*. Available from: https://tools.lifetechnologies.com/content/sfs/manuals/insectselectpibtopo_man.pdf. Cited: 25.10.2015
50. Invitrogen. *pIB/V5-His TOPO vector map*. Available from: https://tools.lifetechnologies.com/content/sfs/vectors/pibv5histopo_map.pdf. Cited: 25.10.2015
51. Qiagen. *Taq PCR Handbook*. Available from: <http://www.qiagen.com/resources/download.aspx?id=c73208eb-a83e-40c4-a9b6-ea5c4c94b9f4&lang=en>. Cited: 25.10.2015
52. Zymo Research Corporation. *DNA Clean & Concentrator-5 Kit*. Available from: <http://www.zymoresearch.com/downloads/dl/file/id/35/d4003i.pdf>. Cited: 25.10.2015
53. Zymo Research Corporation. *Zymoclean Gel DNA Recovery Kit*. Available from: <http://www.zymoresearch.com/downloads/dl/file/id/34/d4001i.pdf>. Cited: 25.10.2015
54. Promega. *Ligafast™ Rapid DNA Ligation System*. Available from: <https://www.promega.de/~media/files/resources/protocols/product%20information%20sheets/g/ligafast%20rapid%20dna%20ligation%20system%20protocol.pdf>. Cited: 25.10.2015
55. Thermo Scientific. *GeneJET Plasmid Miniprep Kit*. Available from: <http://www.thermoscientificbio.com/uploadedfiles/resources/k0502-product-information.pdf>. Cited: 25.10.2015
56. Invitrogen. *PureLink HiPure Plasmid Filter Midiprep Kit*. Available from: https://tools.lifetechnologies.com/content/sfs/manuals/purelink_hipure_plasmid_filter_purification_man.pdf. Cited: 25.10.2015
57. Invitrogen. *EasySelect™ Pichia Expression Kit*. Available from: http://tools.lifetechnologies.com/content/sfs/manuals/easyselect_man.pdf. Cited: 25.10.2015

58. Zymo Research Corporation. *ZR Fungal/Bacterial DNA MiniPrep™ Kit*. Available from: <http://www.zymoresearch.com/downloads/dl/file/id/88/d6005i.pdf>. Cited: 25.10.2015
59. Li, Z., et al., *Secretion and proteolysis of heterologous proteins fused to the Escherichia coli maltose binding protein in Pichia pastoris*. *Protein Expr Purif*, 2010. 72(1): p. 113-24.
60. Miller, G.L., *Use of Dinitrosalicylic Acid Reagent for Determination of Reducing Sugar*. *Analytical Chemistry*, 1959. 31(3): p. 426-428.
61. GmbH, N.E.B., *PNGase F Protocol*.
62. GE Healthcare Life Sciences. *HiTrap™ Con A 4B, 1 ml and 5 ml*. Available from: https://www.gelifesciences.com/gehcls_images/GELS/Related%20Content/Files/1314787424814/litdoc28954901_20140526232723.pdf. Cited: 25.10.2015
63. GE Healthcare Life Sciences. *HiTrap™ HIC columns*. Available from: https://www.gelifesciences.com/gehcls_images/GELS/Related%20Content/Files/1314742967685/litdoc11003452_20150424102314.pdf. Cited: 25.10.2015
64. Rombouts, F.M., Wissenburg, A.K., and Pilnik, W., *Chromatographic separation of orange pectinesterase isoenzymes on pectates with different degrees of cross-linking*. *Journal of Chromatography A*, 1979. 168(1): p. 151-161.
65. Heri, W., Neukom, H., and Deuel, H., *Chromatographische Fraktionierung von Pektinstoffen an Diäthylaminoäthyl-Cellulose. 15. Mitteilung über Ionenaustauscher*. *Helvetica Chimica Acta*, 1961. 44(7): p. 1939-1945.
66. Thermo Scientific. *Pierce^(R) Concentrator 9K MWCO, 20 mL*. Available from: https://tools.thermofisher.com/content/sfs/manuals/MAN0011685_Pierce_Concentrator_9K_20K_MWCO_20mL_UG.pdf. Cited: 25.10.2015
67. Thermo Scientific. *Zeba™ Spin Desalting Columns*. Available from: https://tools.thermofisher.com/content/sfs/manuals/MAN0011529_Zeba_Spin_Desalt_Col_UG.pdf. Cited: 25.10.2015
68. Thermo Scientific. *AminoLink^(R) Plus Immobilization Kit*. Available from: https://tools.thermofisher.com/content/sfs/manuals/MAN0011263_AminoLnk_Plus_Immobil_UG.pdf. Cited: 25.10.2015
69. D'Ovidio, R., et al., *Characterization of the complex locus of bean encoding polygalacturonase-inhibiting proteins reveals subfunctionalization for defense against fungi and insects*. *Plant Physiol*, 2004. 135(4): p. 2424-35.
70. Shevchenko, A., et al., *In-gel digestion for mass spectrometric characterization of proteins and proteomes*. *Nat. Protocols*, 2007. 1(6): p. 2856-2860.
71. Shevchenko, A., et al., *Charting the proteomes of organisms with unsequenced genomes by MALDI-quadrupole time-of-flight mass spectrometry and BLAST homology searching*. *Anal Chem*, 2001. 73(9): p. 1917-26.
72. *Taxonomy Database*. Available from: <http://www.ncbi.nlm.nih.gov/taxonomy>. Cited: 23.10.2015
73. Beilstein, M.A., et al., *Brassicaceae phylogeny inferred from phytochrome A and ndhF sequence data: tribes and trichomes revisited*. *Am J Bot*, 2008. 95(10): p. 1307-27.
74. Bailey, C.D., et al., *Toward a global phylogeny of the Brassicaceae*. *Mol Biol Evol*, 2006. 23(11): p. 2142-60.
75. *Mascot Database Search Scoring*. Available from: http://www.matrixscience.com/search_form_select.html. Cited: 3.11.2015
76. *EnsemblPlants Brassica rapa BLAST search*. Available from: http://plants.ensembl.org/Brassica_rapa/Tools/Blast?db=core. Cited: 13.11.2015
77. Wang, X., et al., *The genome of the mesopolyploid crop species Brassica rapa*. *Nat Genet*, 2011. 43(10): p. 1035-1039.

78. BLAST *bl2seq*. Available from: http://blast.ncbi.nlm.nih.gov/Blast.cgi?PROGRAM=blastp&PAGE_TYPE=BlastSearch&BLAST_SPEC=blast2seq&LINK_LOC=blasttab&LAST_PAGE=blastn&BLAST_INIT=blast2seq. Cited: 28.11.2015
79. Frati, F., et al., *Activity of endo-polygalacturonases in mirid bugs (Heteroptera: Miridae) and their inhibition by plant cell wall proteins (PGIPs)*. European Journal of Entomology, 2006. 103 (3): p. 515-522.
80. Bergmann, C.W., et al., *The effect of glycosylation of Endopolygalacturonases and polygalacturonase inhibiting proteins on the production of oligogalacturonides*, in *Progress in Biotechnology*, Visser, J. and Voragen, A.G.J., Editors. 1996, Elsevier. p. 275-282.
81. Lim, J.-M., et al., *Mapping glycans onto specific N-linked glycosylation sites of *Pyrus communis* PGIP redefines the interface for EPG-PGIP interactions*. Journal of proteome research, 2009. 8(2): p. 673-680.
82. Giulia De Lorenzo, D'Ovidio, R., and Cervone, F., *THE ROLE OF POLYGALACTURONASE-INHIBITING PROTEINS (PGIPS) IN DEFENSE AGAINST PATHOGENIC FUNGI*. Annual Review of Phytopathology, 2001. 39(1): p. 313-335.
83. Bashi, Z.D., et al., *Brassica napus polygalacturonase inhibitor proteins inhibit *Sclerotinia sclerotiorum* polygalacturonase enzymatic and necrotizing activities and delay symptoms in transgenic plants*. Can J Microbiol, 2013. 59(2): p. 79-86.
84. A, V. and JB, L., *Essentials of Glycobiology*, Varki A, C.R., Esko JD, Editor. 2009, Cold Spring Harbor (NY): Cold Spring Harbor Laboratory Press.
85. Maley, F., et al., *Characterization of glycoproteins and their associated oligosaccharides through the use of endoglycosidases*. Anal Biochem, 1989. 180(2): p. 195-204.
86. U, N., *Genome analysis in Brassica with special reference to the experimental formation of *B. napus* and peculiar mode of fertilization*. Japan Journal of Botany, 1935(7): p. 389-452.
87. Chalhoub, B., et al., *Early allopolyploid evolution in the post-Neolithic Brassica napus oilseed genome*. Science, 2014. 345(6199): p. 950-953.
88. GE Healthcare Life Sciences. *HiTrap™ TALON® crude, 1 ml and 5 ml TALON Superflow™*. Available from: https://www.gelifesciences.com/gehcls_images/GELS/Related%20Content/Files/1326706518989/litdoc28957496_20150223004640.pdf. Cited: 25.10.2015
89. D'Ovidio, R., et al., *Polygalacturonases, polygalacturonase-inhibiting proteins and pectic oligomers in plant-pathogen interactions*. Biochimica et Biophysica Acta (BBA) - Proteins and Proteomics, 2004. 1696(2): p. 237-244.
90. Rexová-Benková, L. and Tibenský, V., *Selective purification of *Aspergillus niger* endopolygalacturonase by affinity chromatography on cross-linked pectic acid*. Biochimica et Biophysica Acta (BBA) - Enzymology, 1972. 268(1): p. 187-193.
91. Rexová-Benková, L., *On the character of the interaction of endopolygalacturonase with cross-linked pectic acid*. Biochimica et Biophysica Acta (BBA) - Enzymology, 1972. 276(1): p. 215-220.
92. Schacht, T., et al., *Endo- and exopolygalacturonases of *Ralstonia solanacearum* are inhibited by polygalacturonase-inhibiting protein (PGIP) activity in tomato stem extracts*. Plant Physiol Biochem, 2011. 49(4): p. 377-87.
93. Albersheim, P. and Anderson, A.J., *Proteins from plant cell walls inhibit polygalacturonases secreted by plant pathogens*. Proc Natl Acad Sci U S A, 1971. 68(8): p. 1815-9.
94. Bellincampi, D., et al., *Potential physiological role of plant glycosidase inhibitors*. Biochimica et Biophysica Acta (BBA) - Proteins and Proteomics, 2004. 1696(2): p. 265-274.

95. Spadoni, S., et al., *Polygalacturonase-Inhibiting Protein Interacts with Pectin through a Binding Site Formed by Four Clustered Residues of Arginine and Lysine*. Plant Physiology, 2006. 141(2): p. 557-564.
96. Chen, H., et al., *Stability of plant defense proteins in the gut of insect herbivores*. Plant Physiol, 2007. 143(4): p. 1954-67.
97. Howe, G.A. and Herde, M., *Interaction of plant defense compounds with the insect gut: new insights from genomic and molecular analyses*. Current Opinion in Insect Science, 2015. 9: p. 62-68.
98. Ferrari, S., et al., *Antisense Expression of the Arabidopsis thaliana AtPGIP1 Gene Reduces Polygalacturonase-Inhibiting Protein Accumulation and Enhances Susceptibility to Botrytis cinerea*. Molecular Plant-Microbe Interactions, 2006. 19(8): p. 931-936.
99. Bertazzon, N., et al., *Transient silencing of the grapevine gene VvPGIP1 by agroinfiltration with a construct for RNA interference*. Plant Cell Rep, 2012. 31(1): p. 133-43.
100. Wang, W., et al., *Functional properties of a cysteine proteinase from pineapple fruit with improved resistance to fungal pathogens in Arabidopsis thaliana*. Molecules, 2014. 19(2): p. 2374-89.
101. Peduzzi, R., et al., *A novel β -fructofuranosidase in Coleoptera: Characterization of a β -fructofuranosidase from the sugarcane weevil, Sphenophorus levis*. Insect Biochemistry and Molecular Biology, 2014. 55: p. 31-38.
102. Bhide, A.J., et al., *Biochemical, structural and functional diversity between two digestive α -amylases from Helicoverpa armigera*. Biochimica et Biophysica Acta (BBA) - General Subjects, 2015. 1850(9): p. 1719-1728.
103. Abbott, D.W. and Boraston, A.B., *The structural basis for exopolygalacturonase activity in a family 28 glycoside hydrolase*. J Mol Biol, 2007. 368(5): p. 1215-22.
104. Cho, I.J., et al., *Heterologous expression of polygalacturonase genes isolated from Galactomyces citri-aurantii IJ-1 in Pichia pastoris*. J Microbiol, 2012. 50(2): p. 332-40.
105. Chen, Y., et al., *Cloning, expression and characterization of a novel thermophilic polygalacturonase from Caldicellulosiruptor bescii DSM 6725*. Int J Mol Sci, 2014. 15(4): p. 5717-29.
106. Inan, M. and Meagher, M.M., *Non-repressing carbon sources for alcohol oxidase (AOX1) promoter of Pichia pastoris*. Journal of Bioscience and Bioengineering, 2001. 92(6): p. 585-589.
107. Panula-Perälä, J., et al., *Small-scale slow glucose feed cultivation of Pichia pastoris without repression of AOX1 promoter: towards high throughput cultivations*. Bioprocess and Biosystems Engineering, 2014. 37(7): p. 1261-1269.
108. Patnaik, D. and Khurana, P., *Germins and germin like proteins: an overview*. Indian J Exp Biol, 2001. 39(3): p. 191-200.
109. Zhang, Z., Collinge, D.B., and Thordal-Christensen, H., *Germin-like oxalate oxidase, a H₂O₂-producing enzyme, accumulates in barley attacked by the powdery mildew fungus*. The Plant Journal, 1995. 8(1): p. 139-145.
110. Dunwell, J.M., Purvis, A., and Khuri, S., *Cupins: the most functionally diverse protein superfamily?* Phytochemistry, 2004. 65(1): p. 7-17.
111. Caliskan, M. and Cuming, A.C., *Spatial specificity of H₂O₂-generating oxalate oxidase gene expression during wheat embryo germination*. Plant J, 1998. 15(2): p. 165-71.
112. Bradley, D.J., Kjellbom, P., and Lamb, C.J., *Elicitor- and wound-induced oxidative cross-linking of a proline-rich plant cell wall protein: A novel, rapid defense response*. Cell, 1992. 70(1): p. 21-30.
113. Van Eldik, G.J., et al., *Molecular analysis of a pistil-specific gene expressed in the stigma and cortex of Solanum tuberosum*. Plant Mol Biol, 1996. 30(1): p. 171-6.

114. Prabhu, S.A., et al., *Experimental and bioinformatic characterization of a recombinant polygalacturonase-inhibitor protein from pearl millet and its interaction with fungal polygalacturonases*. Journal of Experimental Botany, 2014.
115. Kobe, B. and Kajava, A.V., *The leucine-rich repeat as a protein recognition motif*. Current Opinion in Structural Biology, 2001. 11(6): p. 725-732.
116. van der Hoorn, R.A., et al., *Structure-function analysis of cf-9, a receptor-like protein with extracytoplasmic leucine-rich repeats*. Plant Cell, 2005. 17(3): p. 1000-15.
117. Janni, M., et al., *Characterization of expressed Pgip genes in rice and wheat reveals similar extent of sequence variation to dicot PGIPs and identifies an active PGIP lacking an entire LRR repeat*. Theoretical and Applied Genetics, 2006. 113(7): p. 1233-1245.
118. Hou, W., et al., *Identification of a wheat polygalacturonase-inhibiting protein involved in Fusarium head blight resistance*. European Journal of Plant Pathology, 2015. 141(4): p. 731-745.
119. Huang, L., et al., *A polygalacturonase inhibitory protein gene (BcMF19) expressed during pollen development in Chinese cabbage-pak-choi*. Mol Biol Rep, 2011. 38(1): p. 545-52.
120. Liu, J.-l., et al., *Decreased Pollen Viability and Thicken Pollen Intine in Antisense Silenced Brassica campestris Mutant of BcMF19*. Journal of Integrative Agriculture, 2014. 13(5): p. 954-962.

13 Supplementary Data

13.1 Sequences

The full length polygalacturonase sequences were checked for signal peptides using the SignalP 4.1 tool of the Technical University of Denmark. Amino acids that were predicted to be part of a signal peptide are indicated in small letters and were not amplified. The stop codon, also in small letters, was also excluded to enable addition of tags from the pIB/V5-His TOPO® Vector.

PCO_GH28-1:

```
atgtcgatcagattgatagccgtactctcagctgcatcaattgcagtcacatcagctACCCCGGTTGCTGATTGAGCT
GCACTATTTCCAGCTTCGACCAAGTAGCTTCAGTGTTAGCTGAATGTACAGACATCGTAGT
CTCCAATCTTGAAGTACCTGCTGGCGAAACTCTGAATCTTGAGACCAAGAAAAAAGGAGTA
ACTATAACTTTTCGAGGGTAAGACTACCTTCGCATATAAAGAATGGTCCGGACCTCTTCTGA
GGGTAAAAGGAAAAGCCATCACTGTTGTGGGAGCTAAAGGCTCAGTCCTTGATGGACAAG
GACAGCTCTATTGGGATGGCAAAGGAGGAAACGGAGGAATAACGAAGCCGAAATTTTTCA
AAATAAAGGCAACAGAAGGTTCCCATTTCAAAAATATCAATTTACTGAACTGCCCAGTACAG
TGCACTTCTATTGATCATTCTGGACCACTCACTCTCAGTGGATGGAACATTGATGTTTCCCA
AGGAGACAAAGATGCATTGGGCCACAATACTGATGGATTGACATCAACACCACAGATCAA
CTGACAATCGAAGATACCGTGGTCAAAAACCAAGATGATTGCATCGCAGTCAACCAAGGCA
CAAATTTCTCTTTAACAATTTGGATTGTTCCGGAGGCCATGGTTTGAGTCTGTGAGTTGGC
ACCAGCCATGAAATTATCAAGAACACCGTCAGAAATGTCACCTTTCTCTAATTCAGTTGTTG
CAAATCGAGGAATGGGATCCATATCAAAACACATACCAATTCCGGGGAAGGTATCATCGAG
GATGTTACTTACAGTAACATTGCCATGGAAGGTATCTGGAAGTATGCTGTCAACGTGGAAC
AGGACTATAAGAAGGGCAAACCCACTGGAATCCCCGTTGGTAACATACCCATCAAAGGTCT
ACATCTGGAAAAAGTCACCGGAACCTTGACCGGAGAAGAATCGACTCCGGTGTATATCATT
TGCGCTGATGGTGCTTGACAGCAACTTCAACTGGTCGGGAGTATCATTTGAAGGTGCTTCG
ACGCTAGTAACTGTAGTTACGTACCTACTGGCTATTCTTGTga
```

PCO_GH28-3:

```
atggcttcattgccttactcgtagccttttggcttcaacagccaccattttcgccAAATCTGCCCTTGGAGACAACTGCA
CAATTTACAAGCTATCTGACGCAGCTGATGTCACAGCCAACTGCGACAACATCGTGTTGAA
AGATATCCAGATCGATGCCGGTCAAACCTCTTCAGCTGTTTCTGAAAGACGCAGCTACCTTG
ACATTTCAAGGAACCATCACTTTGACTACGCAGAATGGCTTGGACCGGCTATTTGGATCA
AAGGGAACGCTTTGAAAGTCCAAGGAGCGAAGTTTGATCACCTGATCGACGGTAGGGGAG
CATACTGGTGGGACGGTTTGGGCGGTAGCGGTAAACAAAAGCCCCCTCCTTATGAAAATAG
AGGCTACAGGCGGATCTGTTTTCAATAACATCCACCTCAAAAAGTCCCCCAAGCTTGCGT
CGGCCTGGAAAACAGTGACAGTGTACGTTGACTTACTGGGACATCGATATCATCGACGG
AAATCCTGCCAATGGAAAAGAAGTCGGTGTGAACACTGATGGTTTCTACATTATCGACTCG
```

SSC_GH28-6:

ix

13.2 Western Blots

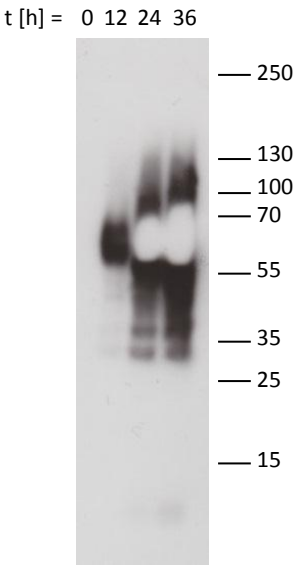


Figure 13: Expression of PCO_GH28-3. The Western Blot showed the time-dependent expression of PCO_GH28-3. PageRuler Plus Prestained Protein Ladder was used as size standard.

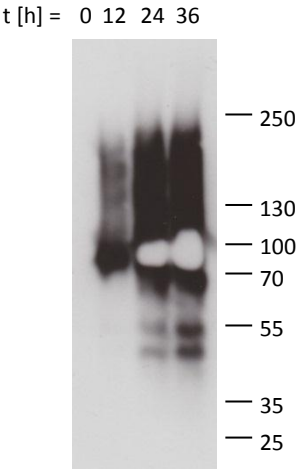


Figure 14: Expression of SSC_GH28-6. The Western Blot showed the time-dependent expression of SSC_GH28-6. PageRuler Plus Prestained Protein Ladder was used as size standard.

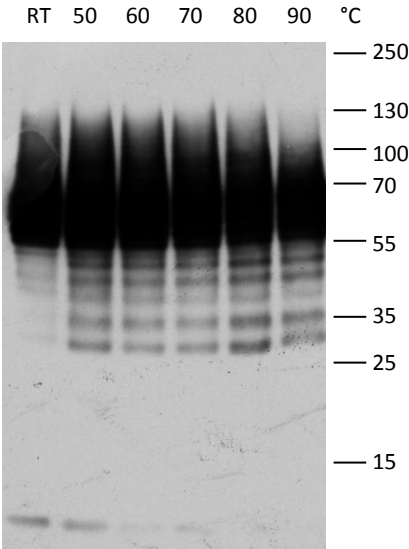


Figure 15: Western Blot of PCO_GH28-3 with different temperature treatments. Prior to gel loading the samples were incubated at RT – 90°C. A decrease in the major PCO_GH28-3 (top band) was observed. Additional bands of lower intensity below the main band indicated a temperature-dependent fragmentation of PCO_GH28-3. PageRuler Plus Prestained Protein Ladder was used as size standard.

13.3 FPLC chromatograms

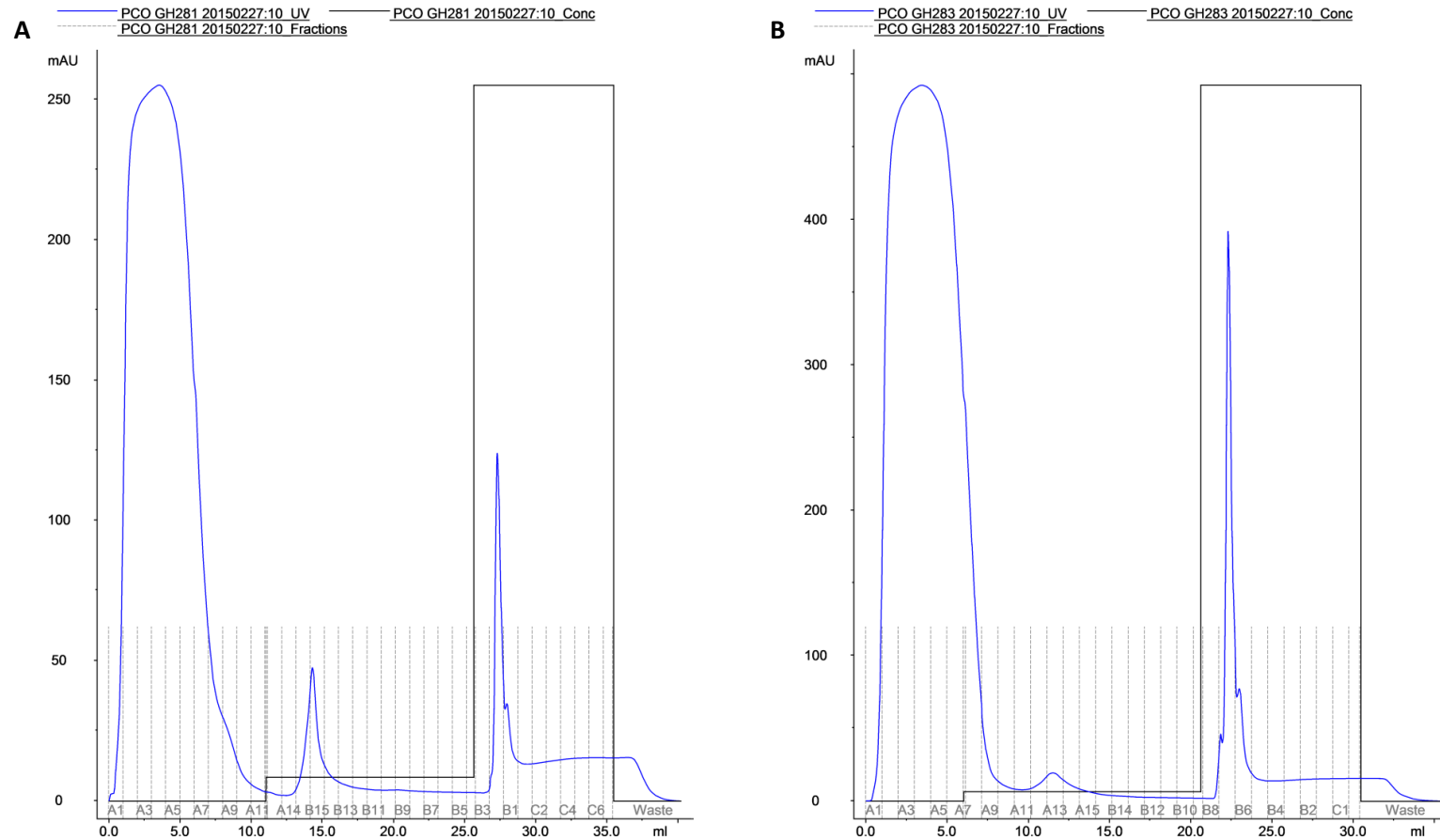


Figure 16: FPLC chromatogram of PCO_GH28-1 (A) and PCO_GH28-3 (B) IMAC purification. PG purification was carried out with an ÄKTA FPLC Protein Purification System using pre-packed HiTrap™ TALON crude 1 ml columns. 5 ml of culture medium, dialysed against IMAC Binding Buffer, were applied onto the column and washed with 10 CV IMAC Wash Buffer. Elution was performed in a stepwise manner by manually pausing the FPLC run every 1 CV of IMAC Elution Buffer and incubating it on the column for 5 min before resuming and draining the elution fraction. The concentration of imidazole in the buffers was displayed in black and increases from 0 M in the IMAC Binding Buffer to 0.3 M in the IMAC Elution Buffer. Protein abundance was measured by absorption at 280 nm and were displayed in blue. Protein peaks of specifically bound proteins were visible in the elution fractions for PCO_GH28-1 and PCO_GH28-3 respectively.

13.4 Distribution of peptides in PCO_GH28-1

		
		5	15	25	35	45	55	65	75	85	95
PCO_GH28-1 (1)	MSIRLIAVLS	AASIAVTSAT	PVADSSCTIS	SFDQVASVLA	ECTDIVVSNL	EVPAGETLNL	ETKKKGVTIT	FEGKTTTFAYK	EWSGPLLRVK	GKAITVVGAK	
PCO_GH28-1 (2)	MSIRLIAVLS	AASIAVTSAT	PVADSSCTIS	SFDQVASVLA	ECTDIVVSNL	EVPAGETLNL	ETKKKGVTIT	FEGKTTTFAYK	EWSGPLLRVK	GKAITVVGAK	
PCO_GH28-1 (3)	MSIRLIAVLS	AASIAVTSAT	PVADSSCTIS	SFDQVASVLA	ECTDIVVSNL	EVPAGETLNL	ETKKKGVTIT	FEGKTTTFAYK	EWSGPLLRVK	GKAITVVGAK	
PCO_GH28-1 (4)	MSIRLIAVLS	AASIAVTSAT	PVADSSCTIS	SFDQVASVLA	ECTDIVVSNL	EVPAGETLNL	ETKKKGVTIT	FEGKTTTFAYK	EWSGPLLRVK	GKAITVVGAK	
PCO_GH28-1 (5)	MSIRLIAVLS	AASIAVTSAT	PVADSSCTIS	SFDQVASVLA	ECTDIVVSNL	EVPAGETLNL	ETKKKGVTIT	FEGKTTTFAYK	EWSGPLLRVK	GKAITVVGAK	
PCO_GH28-1 (6)	MSIRLIAVLS	AASIAVTSAT	PVADSSCTIS	SFDQVASVLA	ECTDIVVSNL	EVPAGETLNL	ETKKKGVTIT	FEGKTTTFAYK	EWSGPLLRVK	GKAITVVGAK	
PCO_GH28-1 (7)	MSIRLIAVLS	AASIAVTSAT	PVADSSCTIS	SFDQVASVLA	ECTDIVVSNL	EVPAGETLNL	ETKKKGVTIT	FEGKTTTFAYK	EWSGPLLRVK	GKAITVVGAK	
PCO_GH28-1 (8)	MSIRLIAVLS	AASIAVTSAT	PVADSSCTIS	SFDQVASVLA	ECTDIVVSNL	EVPAGETLNL	ETKKKGVTIT	FEGKTTTFAYK	EWSGPLLRVK	GKAITVVGAK	
		
		105	115	125	135	145	155	165	175	185	195
PCO_GH28-1 (1)	GSVLDGQGQL	YWDGKGGNGG	ITKPKFFKIK	ATEGSHFKNI	NLLNCPVQCT	SIDHSGPLTL	SGWNIDVSQG	DKDALGHNTD	GFDINTTDQL	TIEDTVVKNO	
PCO_GH28-1 (2)	GSVLDGQGQL	YWDGKGGNGG	ITKPKFFKIK	ATEGSHFKNI	NLLNCPVQCT	SIDHSGPLTL	SGWNIDVSQG	DKDALGHNTD	GFDINTTDQL	TIEDTVVKNO	
PCO_GH28-1 (3)	GSVLDGQGQL	YWDGKGGNGG	ITKPKFFKIK	ATEGSHFKNI	NLLNCPVQCT	SIDHSGPLTL	SGWNIDVSQG	DKDALGHNTD	GFDINTTDQL	TIEDTVVKNO	
PCO_GH28-1 (4)	GSVLDGQGQL	YWDGKGGNGG	ITKPKFFKIK	ATEGSHFKNI	NLLNCPVQCT	SIDHSGPLTL	SGWNIDVSQG	DKDALGHNTD	GFDINTTDQL	TIEDTVVKNO	
PCO_GH28-1 (5)	GSVLDGQGQL	YWDGKGGNGG	ITKPKFFKIK	ATEGSHFKNI	NLLNCPVQCT	SIDHSGPLTL	SGWNIDVSQG	DKDALGHNTD	GFDINTTDQL	TIEDTVVKNO	
PCO_GH28-1 (6)	GSVLDGQGQL	YWDGKGGNGG	ITKPKFFKIK	ATEGSHFKNI	NLLNCPVQCT	SIDHSGPLTL	SGWNIDVSQG	DKDALGHNTD	GFDINTTDQL	TIEDTVVKNO	
PCO_GH28-1 (7)	GSVLDGQGQL	YWDGKGGNGG	ITKPKFFKIK	ATEGSHFKNI	NLLNCPVQCT	SIDHSGPLTL	SGWNIDVSQG	DKDALGHNTD	GFDINTTDQL	TIEDTVVKNO	
PCO_GH28-1 (8)	GSVLDGQGQL	YWDGKGGNGG	ITKPKFFKIK	ATEGSHFKNI	NLLNCPVQCT	SIDHSGPLTL	SGWNIDVSQG	DKDALGHNTD	GFDINTTDQL	TIEDTVVKNO	
		
		205	215	225	235	245	255	265	275	285	295
PCO_GH28-1 (1)	DDCIAVNQGT	NFLFNNLDCS	GGHGLSLSVG	TSHEIIKNTV	RNVTFSNSVV	RKSRNGIHIK	THTNSGEGII	EDVTYSNIAM	EGIWKYAVNV	EQDYKKGKPT	
PCO_GH28-1 (2)	DDCIAVNQGT	NFLFNNLDCS	GGHGLSLSVG	TSHEIIKNTV	RNVTFSNSVV	RKSRNGIHIK	THTNSGEGII	EDVTYSNIAM	EGIWKYAVNV	EQDYKKGKPT	
PCO_GH28-1 (3)	DDCIAVNQGT	NFLFNNLDCS	GGHGLSLSVG	TSHEIIKNTV	RNVTFSNSVV	RKSRNGIHIK	THTNSGEGII	EDVTYSNIAM	EGIWKYAVNV	EQDYKKGKPT	
PCO_GH28-1 (4)	DDCIAVNQGT	NFLFNNLDCS	GGHGLSLSVG	TSHEIIKNTV	RNVTFSNSVV	RKSRNGIHIK	THTNSGEGII	EDVTYSNIAM	EGIWKYAVNV	EQDYKKGKPT	
PCO_GH28-1 (5)	DDCIAVNQGT	NFLFNNLDCS	GGHGLSLSVG	TSHEIIKNTV	RNVTFSNSVV	RKSRNGIHIK	THTNSGEGII	EDVTYSNIAM	EGIWKYAVNV	EQDYKKGKPT	
PCO_GH28-1 (6)	DDCIAVNQGT	NFLFNNLDCS	GGHGLSLSVG	TSHEIIKNTV	RNVTFSNSVV	RKSRNGIHIK	THTNSGEGII	EDVTYSNIAM	EGIWKYAVNV	EQDYKKGKPT	
PCO_GH28-1 (7)	DDCIAVNQGT	NFLFNNLDCS	GGHGLSLSVG	TSHEIIKNTV	RNVTFSNSVV	RKSRNGIHIK	THTNSGEGII	EDVTYSNIAM	EGIWKYAVNV	EQDYKKGKPT	
PCO_GH28-1 (8)	DDCIAVNQGT	NFLFNNLDCS	GGHGLSLSVG	TSHEIIKNTV	RNVTFSNSVV	RKSRNGIHIK	THTNSGEGII	EDVTYSNIAM	EGIWKYAVNV	EQDYKKGKPT	
		
		305	315	325	335	345	355	365			
PCO_GH28-1 (1)	GIPVGNIPK	GLHLEKVTGT	LTGEESTPVY	IICADGACSN	FNWSGVSFEG	ASHASNCYSV	PTGYSC.				
PCO_GH28-1 (2)	GIPVGNIPK	GLHLEKVTGT	LTGEESTPVY	IICADGACSN	FNWSGVSFEG	ASHASNCYSV	PTGYSC.				
PCO_GH28-1 (3)	GIPVGNIPK	GLHLEKVTGT	LTGEESTPVY	IICADGACSN	FNWSGVSFEG	ASHASNCYSV	PTGYSC.				
PCO_GH28-1 (4)	GIPVGNIPK	GLHLEKVTGT	LTGEESTPVY	IICADGACSN	FNWSGVSFEG	ASHASNCYSV	PTGYSC.				
PCO_GH28-1 (5)	GIPVGNIPK	GLHLEKVTGT	LTGEESTPVY	IICADGACSN	FNWSGVSFEG	ASHASNCYSV	PTGYSC.				
PCO_GH28-1 (6)	GIPVGNIPK	GLHLEKVTGT	LTGEESTPVY	IICADGACSN	FNWSGVSFEG	ASHASNCYSV	PTGYSC.				
PCO_GH28-1 (7)	GIPVGNIPK	GLHLEKVTGT	LTGEESTPVY	IICADGACSN	FNWSGVSFEG	ASHASNCYSV	PTGYSC.				
PCO_GH28-1 (8)	GIPVGNIPK	GLHLEKVTGT	LTGEESTPVY	IICADGACSN	FNWSGVSFEG	ASHASNCYSV	PTGYSC.				

Figure 17: Distribution of peptides detected by MS/MS in the amino acid sequence of PCO_GH28-1. After PG purification multiple protein bands were visible in the Coomassie-stained gel, which were subsequently analysed by MS/MS. Detected peptides were highlighted in the amino acid sequence of the full length PCO_GH28-1 for the main protein band of the PG purification (1, blue) as well as the protein bands of lower intensity (2 – 8). The corresponding numbered protein bands are marked with arrows in Figure 6.

13.5 Complete tables of MS analyses containing all protein hits

Extraction	Protein	Mass [Da]	Species	SP	CaCl ₂		NaCl	
					P	S	P	S
NaCl	PREDICTED: probable glycerophosphoryl diester phosphodiesterase 2	148012	<i>Brassica rapa</i>	y			5(2)	218
CaCl ₂	PREDICTED: myrosinase-binding protein-like At1g52030 isoform X1	123983	<i>Brassica rapa</i>	n	11(3) 7(3)	464 444		
CaCl ₂	myrosinase binding protein	104268	<i>Brassica napus</i>	n	3(2)	143		
CaCl ₂ ∪ NaCl	PREDICTED: alpha-xylosidase 1	103893	<i>Brassica rapa</i>	y	16(5)	654	3(1)	144
CaCl ₂	PREDICTED: alpha-xylosidase 1-like	103565	<i>Brassica rapa</i>	y	11(3)	385		
CaCl ₂	PREDICTED: alpha-xylosidase 1-like	102981	<i>Camelina sativa</i>	y	5(1)	185		
CaCl ₂	PREDICTED: probable beta-D-xylosidase 5	86306	<i>Brassica rapa</i>	y	7(1)	212		
CaCl ₂	PREDICTED: probable glycerophosphoryl diester phosphodiesterase 2	83488	<i>Brassica rapa</i>	y	5(2)	235		
CaCl ₂	PREDICTED: subtilisin-like protease	82224	<i>Brassica rapa</i>	y	4(1) 3(1)	187 129		
CaCl ₂	BnaA09g07410D	79777	<i>Brassica napus</i>	y	6(1)	227		
CaCl ₂	PREDICTED: primary amine oxidase	77171	<i>Brassica rapa</i>	y	7(1) 2(1)	220 73		
CaCl ₂	BnaCnng28690D	75215	<i>Brassica napus</i>	y	5(2) 3(2)	248 166		
CaCl ₂	PREDICTED: lysosomal beta glucosidase-like	72931	<i>Brassica rapa</i>	y	1(1)	65		
NaCl	PREDICTED: probable LRR receptor-like serine/threonine-protein kinase At1g56130	70357	<i>Brassica rapa</i>	y			6(3)	266
NaCl	BnaC06g31350D	70297	<i>Brassica napus</i>	y			5(3)	226
CaCl ₂	BnaA03g24520D	68145	<i>Brassica napus</i>	n	19(4)	419		
CaCl ₂	hypothetical protein CARUB_v10000546mg	65847	<i>Capsella rubella</i>	y	9(3)	393		
CaCl ₂ ∪ NaCl	PREDICTED: monocopper oxidase-like protein SKU5	65707	<i>Brassica rapa</i>	y	11(4) 5(3)	483 357	3(3) 3(1)	226 155
NaCl	PREDICTED: pectinesterase/pectinesterase inhibitor 3-like	64882	<i>Brassica rapa</i>	n			3(1) 2(0)	123 100
NaCl	PREDICTED: pectinesterase/pectinesterase inhibitor 3	64226	<i>Brassica rapa</i>	n			5(2) 4(1)	196 168
CaCl ₂ ∪ NaCl	PREDICTED: probable pectinesterase/pectinesterase inhibitor 41	63889	<i>Brassica rapa</i>	y	2(2)	102	1(1)	101
CaCl ₂	BnaA09g08470D	63648	<i>Brassica napus</i>	y	16(2)	368		
CaCl ₂	beta-N-acetylhexosaminidase-like protein	63638	<i>Arabidopsis thaliana</i>	y	4(1)	174		
CaCl ₂ ∪ NaCl	myrosinase	63506	<i>Brassica rapa</i> ssp. <i>pekinensis</i>	y	28(7)	875	13(5)	615
CaCl ₂ ∪ NaCl	myrosinase	63416	<i>Raphanus sativus</i>	y	15(4) 5(1)	493 271	8(4)	440
CaCl ₂ ∪ NaCl	PREDICTED: myrosinase-like	63404	<i>Brassica rapa</i>	y	9(2)	218	4(2)	172
CaCl ₂	PREDICTED: myrosinase-like	63298	<i>Brassica rapa</i>	y	4(2) 2(1)	236 124		
CaCl ₂ ∪ NaCl	Myrosinase	63276	<i>Brassica napus</i>	y	32(7) 9(1)	904 364	13(5)	610
CaCl ₂ ∪ NaCl	myrosinase 2	63261	<i>Brassica napus</i>	y	28(7)	817	12(4)	545
CaCl ₂	myrosinase, thioglucoside glucohydrolase	63228	<i>Brassica juncea</i>	y	10(2)	351		
CaCl ₂	BnaCnng53320D	63163	<i>Brassica napus</i>	y	30(7)	832		
CaCl ₂ ∪ NaCl	PREDICTED: myrosinase-like isoform X2	63072	<i>Brassica rapa</i>	y	19(6)	628	11(3)	418
CaCl ₂ ∪ NaCl	BnaA09g26590D	62983	<i>Brassica napus</i>	y	26(7) 10(1)	754 381	11(2)	435
CaCl ₂ ∪ NaCl	PREDICTED: beta-hexosaminidase 1	62830	<i>Brassica rapa</i>	y	7(3) 2(0)	295 78	5(2)	187

CaCl ₂	PREDICTED: myrosinase MA1	62818	<i>Brassica rapa</i>	y	7(2) 2(1)	168 124		
CaCl ₂ u NaCl	Myrosinase MB3	62765	<i>Sinapis alba</i>	y	17(5) 5(1)	532 219	7(2)	298
CaCl ₂	myrosinase	62760	<i>Brassica oleracea</i>	y	23(5) 6(1)	585 237		
CaCl ₂ u NaCl	myrosinase	62737	<i>Raphanus sativus</i>	y	18(3) 6(0)	511 170	8(2)	328
NaCl	myrosinase	62707	<i>Eutrema japonicum</i>	y			4(2)	182
CaCl ₂	hypothetical protein EUTSA_v10010264mg	62587	<i>Eutrema salsugineum</i>	y	5(2)	197		
CaCl ₂	PREDICTED: myrosinase-like	62557	<i>Brassica rapa</i>	y	19(3) 5(2)	431 261		
CaCl ₂	PREDICTED: uncharacterized protein At4g06744-like	62244	<i>Brassica rapa</i>	y	5(1)	185		
CaCl ₂	PREDICTED: L-ascorbate oxidase homolog	62238	<i>Brassica rapa</i>	y	5(1)	211		
CaCl ₂	hypothetical protein EUTSA_v10016482mg	61946	<i>Eutrema salsugineum</i>	y	5(1)	181		
CaCl ₂ u NaCl	BnaA08g20470D	61910	<i>Brassica napus</i>	n	5(1)	172	4(1)	172
CaCl ₂	PREDICTED: probable pectinesterase/pectinesterase inhibitor 51	61832	<i>Brassica rapa</i>	n	4(1)	126		
CaCl ₂	PREDICTED: L-ascorbate oxidase homolog	61406	<i>Camelina sativa</i>	y	1(1)	89		
CaCl ₂ u NaCl	BnaCnng60730D, partial	61096	<i>Brassica napus</i>	y	9(2)	398	15(4)	552
CaCl ₂	PREDICTED: heparanase-like protein 1 isoform X1	61066	<i>Brassica rapa</i>	y	1(1)	58		
CaCl ₂	PREDICTED: reticuline oxidase-like protein	61049	<i>Brassica rapa</i>	y	9(2)	349		
CaCl ₂	PREDICTED: myrosinase-like	61000	<i>Brassica rapa</i>	y	29(7)	836		
CaCl ₂	PREDICTED: glutathione reductase, chloroplastic	60937	<i>Brassica rapa</i>	n	10(4)	466		
CaCl ₂	BnaC02g40420D	60780	<i>Brassica napus</i>	y	27(6)	663		
CaCl ₂	hypothetical protein AALP_AA5G173600	60656	<i>Arabidopsis thaliana</i>	y	7(1)	271		
CaCl ₂ u NaCl	PREDICTED: probable pectinesterase/pectinesterase inhibitor 51	60649	<i>Brassica rapa</i>	y	12(3)	365	1(1)	67
CaCl ₂	Putative pectinesterase	60583	<i>Arabidopsis thaliana</i>	y	9(4)	531		
CaCl ₂ u NaCl	PREDICTED: beta-hexosaminidase 3	60565	<i>Brassica rapa</i>	y	4(0)	136	3(1)	162
CaCl ₂ u NaCl	PREDICTED: L-ascorbate oxidase homolog isoform X1	60554	<i>Camelina sativa</i>	y	8(3)	446	6(2)	233
CaCl ₂ u NaCl	PREDICTED: L-ascorbate oxidase homolog	60524	<i>Brassica rapa</i>	y	14(5)	744	8(2)	268
CaCl ₂ u NaCl	hypothetical protein CARUB_v10008790mg	60446	<i>Capsella rubella</i>	y	9(4)	517	6(2)	227
CaCl ₂	PREDICTED: probable pectinesterase/pectinesterase inhibitor 51	60355	<i>Brassica rapa</i>	y	6(2)	231		
CaCl ₂ u NaCl	PREDICTED: L-ascorbate oxidase homolog	60347	<i>Brassica rapa</i>	y	10(4)	440	15(5)	605
CaCl ₂ u NaCl	PREDICTED: L-ascorbate oxidase homolog	60323	<i>Camelina sativa</i>	y	7(2)	354	9(1)	281
CaCl ₂ u NaCl	hypothetical protein CARUB_v10020107mg	60228	<i>Capsella rubella</i>	y	7(2)	339	9(1)	280
CaCl ₂ u NaCl	SKU5-like 5 protein	60177	<i>Arabidopsis thaliana</i>	y	7(2)	339	9(1)	280
CaCl ₂ u NaCl	hypothetical protein EUTSA_v10018373mg	60129	<i>Eutrema salsugineum</i>	y	10(6)	522	9(4)	431
CaCl ₂ u NaCl	PREDICTED: L-ascorbate oxidase homolog	60030	<i>Brassica rapa</i>	y	8(4)	345	13(5)	594
CaCl ₂ u NaCl	hypothetical protein AALP_AA5G148000	59929	<i>Arabidopsis thaliana</i>	y	9(6)	508	7(4)	374
CaCl ₂	BnaC05g26270D	58945	<i>Brassica napus</i>	y	4(1)	195		
CaCl ₂ u NaCl	BnaA10g23380D	58391	<i>Brassica napus</i>	y	3(1)	132	3(1)	136
CaCl ₂	PREDICTED: probable pectinesterase/pectinesterase inhibitor 32 isoform X1	57977	<i>Brassica rapa</i>	y	2(1)	81		

CaCl ₂	hypothetical protein AALP_AA7G145400	57099	<i>Arabis alpina</i>	n	4(1)	102		
CaCl ₂	PREDICTED: ectonucleotide pyrophosphatase/phosphodiesterase family member 1	55468	<i>Brassica rapa</i>	n	3(1)	123		
CaCl ₂	PREDICTED: bifunctional purple acid phosphatase 26 isoform X2	55424	<i>Brassica rapa</i>	y	6(2)	228		
CaCl ₂	PREDICTED: probable serine protease EDA2	55041	<i>Brassica rapa</i>	y	3(1)	93		
NaCl	PREDICTED: purple acid phosphatase 10-like isoform X1	54260	<i>Brassica rapa</i>	y			4(1)	197
CaCl ₂	PREDICTED: vacuolar-processing enzyme gamma-isozyme	53755	<i>Brassica rapa</i>	y	1(1)	85		
CaCl ₂	PREDICTED: serine carboxypeptidase-like 25	53694	<i>Brassica rapa</i>	y	1(1)	65		
CaCl ₂	PREDICTED: myrosinase	53559	<i>Brassica rapa</i>	y	1(1)	67		
CaCl ₂	PREDICTED: protein ASPARTIC PROTEASE IN GUARD CELL 2-like	53435	<i>Brassica rapa</i>	n	1(1)	65		
CaCl ₂	PREDICTED: protein ASPARTIC PROTEASE IN GUARD CELL 1	53355	<i>Brassica rapa</i>	y	2(1)	112		
CaCl ₂ u NaCl	PREDICTED: uncharacterized protein At4g06744	53202	<i>Brassica rapa</i>	y	6(1) 2(1)	254 108	5(1)	161
CaCl ₂ u NaCl	PREDICTED: serine carboxypeptidase 24	52875	<i>Brassica rapa</i>	y	3(2)	161	2(2)	190
CaCl ₂ u NaCl	PREDICTED: protein ASPARTIC PROTEASE IN GUARD CELL 2-like isoform X1	52477	<i>Brassica rapa</i>	y	4(3) 2(0)	222 56	3(1)	112
CaCl ₂	PREDICTED: protein ASPARTIC PROTEASE IN GUARD CELL 1-like	52072	<i>Brassica rapa</i>	y	5(2) 5(0)	240 173		
CaCl ₂ u NaCl	PREDICTED: epidermis-specific secreted glycoprotein EP1-like	51034	<i>Brassica rapa</i>	y	17(10) 7(3)	710 476	11(5)	499
CaCl ₂	BnaA07g34420D	50964	<i>Brassica napus</i>	y	15(8)	681		
CaCl ₂	PREDICTED: aspartic proteinase Asp1	50542	<i>Brassica rapa</i>	y	2(1)	142		
CaCl ₂	BnaC08g42010D	50417	<i>Brassica napus</i>	n	3(2)	182		
CaCl ₂	hypothetical protein EUTSA_v10004188mg	50219	<i>Eutrema salsugineum</i>	y	7(2)	343		
CaCl ₂ u NaCl	hypothetical protein CARUB_v10000927mg	49955	<i>Capsella rubella</i>	y	13(6) 5(3)	473 310	5(2)	259
CaCl ₂ u NaCl	PREDICTED: cystine lyase COR13-like	49770	<i>Brassica rapa</i>	n	14(7) 5(4)	663 308	9(4)	474
CaCl ₂	PREDICTED: aspartic proteinase nepenthesin-1	49768	<i>Brassica rapa</i>	y	9(2)	376		
CaCl ₂ u NaCl	hypothetical protein EUTSA_v10013504mg	49690	<i>Eutrema salsugineum</i>	y	11(5)	405	6(1)	233
CaCl ₂	PREDICTED: probable cysteine proteinase At3g19400 isoform X1	49026	<i>Brassica rapa</i>	y	1(1)	73		
NaCl	BnaCnng69940D, partial	48073	<i>Brassica napus</i>	n			1(1)	56
CaCl ₂	unnamed protein product	47843	<i>Thellungiella halophila</i>	n	2(2)	124		
CaCl ₂	PREDICTED: protein ASPARTIC PROTEASE IN GUARD CELL 2-like isoform X1	47796	<i>Camelina sativa</i>	y	6(5)	502		
CaCl ₂	BnaA10g23500D	47730	<i>Brassica napus</i>	y	13(6)	739		
CaCl ₂	PREDICTED: protein ASPARTIC PROTEASE IN GUARD CELL 2	47724	<i>Brassica rapa</i>	y	13(6)	705		
CaCl ₂	nucleoid DNA-binding-like protein	47701	<i>Arabidopsis thaliana</i>	y	5(3)	310		
CaCl ₂	PREDICTED: protein ASPARTIC PROTEASE IN GUARD CELL 2-like	47650	<i>Brassica rapa</i>	y	5(2)	216		
CaCl ₂	BnaC03g51090D	47458	<i>Brassica napus</i>	n	5(1)	187		
CaCl ₂	PREDICTED: probable pectate lyase 20	47111	<i>Brassica rapa</i>	y	5(3)	230		
CaCl ₂ u NaCl	hypothetical protein AALP_AA5G176500	46901	<i>Arabis alpina</i>	y	11(4)	447	7(5)	428
CaCl ₂	PREDICTED: peptidyl-prolyl cis-trans isomerase CYP38, chloroplastic	46889	<i>Brassica rapa</i>	y	9(2)	329		
CaCl ₂	BnaA09g34280D	46879	<i>Brassica napus</i>	y	20(6)	503		

CaCl ₂ u NaCl	PREDICTED: protein ASPARTIC PROTEASE IN GUARD CELL 2-like	46876	<i>Brassica rapa</i>	y	26(11)	630	9(6)	437
CaCl ₂ u NaCl	PREDICTED: protein ASPARTIC PROTEASE IN GUARD CELL 2-like	46743	<i>Brassica rapa</i>	y	6(3)	397	7(3)	372
CaCl ₂	PREDICTED: protein notum homolog	46646	<i>Brassica rapa</i>	y	1(1)	59		
CaCl ₂ u NaCl	aspartyl protease family protein	46258	<i>Arabidopsis thaliana</i>	y	5(2)	224	7(3)	372
CaCl ₂	PREDICTED: probable inactive purple acid phosphatase 29	45614	<i>Brassica rapa</i>	n	8(3)	494		
CaCl ₂	PREDICTED: fructose-1,6-bisphosphatase, chloroplastic	45274	<i>Brassica rapa</i>	n	5(2)	274		
CaCl ₂	PREDICTED: sedoheptulose-1,7-bisphosphatase, chloroplastic-like isoform X1	45116	<i>Brassica rapa</i>	n	13(3)	413		
CaCl ₂	PREDICTED: fasciclin-like arabinogalactan protein 1	44947	<i>Brassica rapa</i>	y	2(1)	100		
CaCl ₂	BnaA02g34830D	43955	<i>Brassica napus</i>	y	36(6)	373		
CaCl ₂	BnaA09g38900D	43841	<i>Brassica napus</i>	y	3(1)	130		
CaCl ₂	BnaC02g08470D	43760	<i>Brassica napus</i>	y	6(4)	344		
CaCl ₂	PREDICTED: fasciclin-like arabinogalactan protein 10	43530	<i>Camelina sativa</i>	y	3(1)	146		
CaCl ₂	PREDICTED: serpin-ZX	43526	<i>Brassica rapa</i>	n	7(2) 1(1)	308 57		
CaCl ₂	PREDICTED: protein trichome birefringence-like 37	43293	<i>Brassica rapa</i>	y	5(1)	173		
CaCl ₂	PREDICTED: fasciclin-like arabinogalactan protein 2	43220	<i>Brassica rapa</i>	y	5(1) 3(1)	149 144		
CaCl ₂	PREDICTED: probable fructose-bisphosphate aldolase 2, chloroplastic	43181	<i>Brassica rapa</i>	n	11(7) 10(5)	745 642		
CaCl ₂	PREDICTED: fasciclin-like arabinogalactan protein 2	43178	<i>Brassica rapa</i>	y	3(1) 5(0)	111 108		
CaCl ₂	PREDICTED: probable fructose-bisphosphate aldolase 2, chloroplastic	43126	<i>Brassica rapa</i>	n	11(6) 10(5)	704 601		
CaCl ₂	hypothetical protein EUTSA_v10000191mg	43121	<i>Eutrema salsugineum</i>	n	9(6)	551		
CaCl ₂	BnaA07g16660D	43064	<i>Brassica napus</i>	n	19(5)	558		
CaCl ₂	PREDICTED: uncharacterized protein LOC103853624	43034	<i>Brassica rapa</i>	y	9(4)	409		
CaCl ₂ u NaCl	unnamed protein product	43004	<i>Thellungiella halophila</i>	n	12(4)	521	8(5) 2(1)	446 94
CaCl ₂	PREDICTED: GDSL esterase/lipase At1g54020-like	42996	<i>Brassica rapa</i>	y	4(2)	204		
CaCl ₂	PREDICTED: GDSL esterase/lipase At3g05180	42798	<i>Brassica rapa</i>	y	2(1)	116		
CaCl ₂ u NaCl	PREDICTED: fasciclin-like arabinogalactan protein 8	42798	<i>Brassica rapa</i>	y	7(4) 7(1)	457 253	5(1) 4(0)	201 90
CaCl ₂	Sedoheptulose-1,7-bisphosphatase	42794	<i>Arabidopsis thaliana</i>	n	17(5)	454		
CaCl ₂	BnaA06g37230D	42783	<i>Brassica napus</i>	n	11(7) 10(5)	724 644		
CaCl ₂	sedoheptulose-1,7-bisphosphatase	42719	<i>Brassica rapa</i> ssp. <i>chinensis</i>	n	22(8) 13(4)	669 468		
CaCl ₂	ubiquitin 10.2	42639	<i>Brassica napus</i>	n	4(0)	52		
CaCl ₂	BnaAnng08670D	42621	<i>Brassica napus</i>	y	10(7)	568		
CaCl ₂	PREDICTED: basic 7S globulin 2-like	42621	<i>Brassica rapa</i>	y	10(7)	568		
CaCl ₂	PREDICTED: protein trichome birefringence-like 40	42532	<i>Brassica rapa</i>	y	4(1)	137		
CaCl ₂	BnaA06g22560D	42523	<i>Brassica napus</i>	y	6(2)	266		
NaCl	AT3g14310/MLN21_9	42216	<i>Arabidopsis thaliana</i>	n			26(8)	565
CaCl ₂	PREDICTED: LRR receptor-like serine/threonine-protein kinase ERECTA	42115	<i>Brassica rapa</i>	y	2(1)	98		

CaCl ₂	PREDICTED: peroxidase 32	41867	<i>Brassica rapa</i>	n	8(4)	466		
CaCl ₂ ∪ NaCl	BnaC09g08690D	41815	<i>Brassica napus</i>	n	10(4) 9(1)	492 313	12(3)	411
CaCl ₂	hypothetical protein CARUB_v10011511mg	41555	<i>Capsella rubella</i>	n	11(4)	377		
CaCl ₂	PREDICTED: uncharacterized protein LOC103865900	41229	<i>Brassica rapa</i>	y	2(1)	89		
CaCl ₂	BnaC09g08190D	41153	<i>Brassica napus</i>	n	19(8) 4(2)	737 172		
CaCl ₂	PREDICTED: ferredoxin--NADP reductase, leaf isozyme 2, chloroplastic	41071	<i>Brassica rapa</i>	n	16(7) 4(2)	615 217		
CaCl ₂	PREDICTED: ferredoxin--NADP reductase, leaf isozyme 1, chloroplastic	41032	<i>Brassica rapa</i>	n	19(7)	744		
CaCl ₂	PREDICTED: alpha-L-fucosidase 3-like	40901	<i>Brassica rapa</i>	y	10(6)	538		
CaCl ₂	PREDICTED: ferredoxin--NADP reductase, leaf isozyme 1, chloroplastic-like	40834	<i>Camelina sativa</i>	n	16(6)	581		
CaCl ₂	PREDICTED: uncharacterized protein LOC103866589	40812	<i>Brassica rapa</i>	y	2(2)	138		
CaCl ₂	hypothetical protein MIMGU_mgv1a008865mg	40812	<i>Erythranthe guttata</i>	n	14(6) 2(1)	491 86		
CaCl ₂ ∪ NaCl	PREDICTED: GDSL esterase/lipase At1g29670	40777	<i>Brassica rapa</i>	y	37(20) 6(4)	132 1 367	12(6)	544
CaCl ₂ ∪ NaCl	beta-1,3-glucanase	40691	<i>Brassica rapa ssp. chinensis</i>	n	3(3)	226	2(1)	100
CaCl ₂	ferredoxin-NADP(+)-oxidoreductase 1	40649	<i>Arabidopsis thaliana</i>	n	17(6)	576		
CaCl ₂	BnaAnng14060D	40627	<i>Brassica napus</i>	y	3(2)	129		
CaCl ₂	ferredoxin-NADP+ reductase	40487	<i>Arabidopsis thaliana</i>	n	3(1)	124		
CaCl ₂	leucine-rich repeat-containing protein	40475	<i>Arabidopsis thaliana</i>	y	15(4)	522		
CaCl ₂	PREDICTED: GDSL esterase/lipase At1g29670	40468	<i>Camelina sativa</i>	y	13(7)	412		
CaCl ₂	PREDICTED: DNA-damage-repair/toleration protein DRT100	40461	<i>Brassica rapa</i>	y	26(10) 10(2)	939 324		
CaCl ₂	GDSL esterase/lipase	40427	<i>Arabidopsis thaliana</i>	y	11(5)	375		
CaCl ₂	BnaA01g36810D	40377	<i>Brassica napus</i>	y	19(6) 6(1)	739 214		
CaCl ₂	BnaC01g32420D	40351	<i>Brassica napus</i>	y	14(5)	627		
CaCl ₂	hypothetical protein CARUB_v10001211mg	40249	<i>Capsella rubella</i>	y	41(11)	543		
CaCl ₂ ∪ NaCl	PREDICTED: peroxidase 12-like	40219	<i>Brassica rapa</i>	y	14(5)	573	11(5)	544
CaCl ₂ ∪ NaCl	hypothetical protein EUTSA_v10013887mg	40216	<i>Eutrema salsugineum</i>	y	61(15)	702	28(11)	588
CaCl ₂ ∪ NaCl	PREDICTED: peroxidase 12	40200	<i>Brassica rapa</i>	y	21(12)	847	12(6)	585
CaCl ₂	UF642 I-Gall-responsive protein 1	40185	<i>Arabidopsis thaliana</i>	y	47(13)	607		
CaCl ₂	PREDICTED: uncharacterized protein LOC104706866	40176	<i>Camelina sativa</i>	y	43(13)	658		
CaCl ₂ ∪ NaCl	BnaC09g45170D	40137	<i>Brassica napus</i>	y	58(13)	626	28(11)	588
CaCl ₂ ∪ NaCl	PREDICTED: uncharacterized protein LOC103850771	40126	<i>Brassica rapa</i>	y	79(18)	873	36(14)	821
CaCl ₂ ∪ NaCl	BnaA02g01000D	40124	<i>Brassica napus</i>	y	78(19)	933	36(14)	827
NaCl	PREDICTED: DNA-damage-repair/toleration protein DRT100-like	40104	<i>Brassica rapa</i>	y			2(1)	103
CaCl ₂ ∪ NaCl	hypothetical protein AALP_AA8G432300	40091	<i>Arabis alpina</i>	y	44(11)	648	15(7)	430
CaCl ₂ ∪ NaCl	uncharacterized protein	40083	<i>Arabidopsis thaliana</i>	y	17(2)	291	9(4)	300
NaCl	PREDICTED: uncharacterized protein LOC103850912	40076	<i>Brassica rapa</i>	y			14(2)	181

CaCl ₂ ∪ NaCl	BnaC01g06040D	40043	<i>Brassica napus</i>	y	8(1)	138	7(2)	184
NaCl	PREDICTED: peroxidase 12-like	40002	<i>Camelina sativa</i>	y			7(3)	329
CaCl ₂	PREDICTED: peroxidase 12-like	39928	<i>Camelina sativa</i>	y	11(3)	405		
CaCl ₂ ∪ NaCl	uncharacterized protein	39905	<i>Arabidopsis thaliana</i>	y	63(15)	715	31(11)	619
CaCl ₂	hypothetical protein EUTSA_v10004442mg	39891	<i>Eutrema salsugineum</i>	y	60(12)	719		
CaCl ₂ ∪ NaCl	PREDICTED: uncharacterized protein LOC103874406	39878	<i>Brassica rapa</i>	y	91(27)	114 6	24(7)	484
CaCl ₂ ∪ NaCl	PREDICTED: aldose 1-epimerase	39739	<i>Brassica rapa</i>	y	4(1)	104	4(1)	153
CaCl ₂ ∪ NaCl	PREDICTED: uncharacterized protein LOC103854751	39727	<i>Brassica rapa</i>	y	67(17)	911	22(5)	392
NaCl	PREDICTED: bark storage protein A-like	39711	<i>Brassica rapa</i>	n			3(1)	132
CaCl ₂	PREDICTED: peroxidase 34-like	39632	<i>Camelina sativa</i>	y	11(8)	448		
CaCl ₂ ∪ NaCl	horseradish peroxidase isoenzyme HRP_1805	39600	<i>Armoracia rusticana</i>	y	6(3)	267	7(3)	291
NaCl	PREDICTED: peroxidase 34-like isoform X1	39544	<i>Camelina sativa</i>	y			10(5)	417
CaCl ₂ ∪ NaCl	PREDICTED: peroxidase 34-like	39541	<i>Brassica rapa</i>	y	15(9)	529	13(5)	466
NaCl	hypothetical protein CARUB_v10017532mg	39510	<i>Capsella rubella</i>	y			6(3)	274
CaCl ₂ ∪ NaCl	PREDICTED: peroxidase 34	39508	<i>Camelina sativa</i>	y	9(5)	453	9(4)	376
CaCl ₂	peroxidase 33	39496	<i>Arabidopsis thaliana</i>	y	9(4)	328		
CaCl ₂ ∪ NaCl	peroxidase 32	39438	<i>Eutrema halophilum</i>	y	6(2)	240	5(2)	198
CaCl ₂ ∪ NaCl	PREDICTED: uncharacterized protein LOC103870618	39384	<i>Brassica rapa</i>	y	35(14)	106 2	14(7)	477
CaCl ₂	Peroxidase C1A	39380	<i>Armoracia rusticana</i>	y	8(4)	355		
CaCl ₂ ∪ NaCl	hypothetical protein CARUB_v10017534mg	39365	<i>Capsella rubella</i>	y	8(6) 3(0)	297 74	6(2)	257
CaCl ₂	peroxidase	39359	<i>Brassica napus</i>	y	5(3)	270		
CaCl ₂ ∪ NaCl	BnaC05g44040D	39356	<i>Brassica napus</i>	y	31(14)	947	10(3)	326
NaCl	hypothetical protein AALP_AA6G200400	39344	<i>Arabis alpina</i>	y			7(3)	239
NaCl	germination-related protein	39331	<i>Arabidopsis thaliana</i>	y			5(2)	214
CaCl ₂ ∪ NaCl	peroxidase 34	39330	<i>Arabidopsis thaliana</i>	y	13(9) 6(0)	565 196	13(5)	442
CaCl ₂	hypothetical protein CARUB_v10014019mg	39326	<i>Capsella rubella</i>	y	1(1)	75		
CaCl ₂	PREDICTED: uncharacterized protein LOC103848900	39312	<i>Brassica rapa</i>	y	14(6) 1(1)	540 75		
CaCl ₂ ∪ NaCl	PREDICTED: peroxidase C2	39252	<i>Brassica rapa</i>	y	33(13) 12(2)	113 4 381	28(10) 5(1)	106 7 231
CaCl ₂ ∪ NaCl	horseradish peroxidase isoenzyme HRP_25148.1(C1C)	39250	<i>Armoracia rusticana</i>	y	6(4) 5(1)	297 180	11(5)	499
CaCl ₂ ∪ NaCl	polygalacturonase inhibitor protein 15	39183	<i>Brassica napus</i>	y	1(1)	101	1(1)	93
CaCl ₂ ∪ NaCl	Peroxidase C1B	39144	<i>Armoracia rusticana</i>	y	6(3) 4(1)	222 133	5(2) 5(0)	188 128
CaCl ₂	hypothetical protein CARUB_v10005183mg	39100	<i>Capsella rubella</i>	n	4(2)	235		
CaCl ₂ ∪ NaCl	ATPCA/ATPRX33/PRX33	39028	<i>Arabidopsis lyrata</i> ssp. <i>lyrata</i>	y	3(2) 2(0)	149 71	3(1) 3(0)	128 102
CaCl ₂	PREDICTED: peroxidase 34	38984	<i>Brassica rapa</i>	y	10(6)	546		
CaCl ₂	BnaA01g13860D	38960	<i>Brassica napus</i>	n	9(4)	361		
CaCl ₂ ∪ NaCl	BnaA01g20660D	38909	<i>Brassica napus</i>	y	13(9)	566	11(5)	415
CaCl ₂	hypothetical protein AALP_AA3G314000	38880	<i>Arabis alpina</i>	y	6(2)	234		
CaCl ₂	PREDICTED: GDSL esterase/lipase	38871	<i>Brassica rapa</i>	y	3(1)	140		

At5g03610-like								
CaCl ₂	BnaC03g02770D	38730	<i>Brassica napus</i>	y	12(5)	574		
CaCl ₂ ∪ NaCl	polygalacturonase-inhibiting protein 1	38690	<i>Brassica rapa</i> ssp. <i>pekinensis</i>	y	20(11)	919	11(7)	573
CaCl ₂ ∪ NaCl	hypothetical protein ARALYDRAFT_489772	38615	<i>Arabidopsis lyrata</i> ssp. <i>lyrata</i>	y	6(3) 2(0)	254 88	7(2)	214
CaCl ₂	PREDICTED: peroxidase 22-like	38454	<i>Brassica rapa</i>	y	5(1)	118		
NaCl	PREDICTED: peroxidase 37	38402	<i>Camelina sativa</i>	y			8(2)	213
CaCl ₂ ∪ NaCl	BnaC01g09550D	38401	<i>Brassica napus</i>	y	2(0)	74	4(1)	111
NaCl	hypothetical protein CARUB_v10001326mg	38401	<i>Capsella rubella</i>	y			4(2)	130
CaCl ₂	PREDICTED: nitrile-specifier protein 2-like	38343	<i>Brassica rapa</i>	n	9(2)	336		
CaCl ₂	PREDICTED: probable lactoylglutathione lyase, chloroplast	38161	<i>Brassica rapa</i>	n	8(4)	307		
CaCl ₂ ∪ NaCl	PREDICTED: polygalacturonase inhibitor 1-like	38048	<i>Brassica rapa</i>	y	8(5)	453	7(2)	249
CaCl ₂	PREDICTED: polygalacturonase inhibitor 1-like	38036	<i>Brassica rapa</i>	y	2(1)	73		
CaCl ₂	BnaC09g17000D	37960	<i>Brassica napus</i>	y	1(1)	53		
CaCl ₂ ∪ NaCl	PREDICTED: polygalacturonase inhibitor 2-like	37930	<i>Brassica rapa</i>	y	6(1)	233	9(2)	356
CaCl ₂ ∪ NaCl	glucanase 1	37915	<i>Brassica rapa</i> ssp. <i>pekinensis</i>	y	7(6)	481	6(3)	356
CaCl ₂	BnaA10g24070D	37834	<i>Brassica napus</i>	y	3(1)	142		
CaCl ₂ ∪ NaCl	PREDICTED: bark storage protein A-like	37768	<i>Brassica rapa</i>	y	4(2)	240	5(3)	362
CaCl ₂ ∪ NaCl	beta-1,3-glucanase 3	37724	<i>Arabidopsis thaliana</i>	y	2(2)	218	4(1)	211
CaCl ₂	BnaA03g55610D	37718	<i>Brassica napus</i>	y	13(4)	522		
CaCl ₂	hypothetical protein AALP_AA8G064000	37702	<i>Arabis alpina</i>	y	2(1)	118		
NaCl	polygalacturonase-inhibiting protein 3	37620	<i>Brassica rapa</i> ssp. <i>pekinensis</i>	y			6(3)	268
CaCl ₂	BnaC09g16910D	37365	<i>Brassica napus</i>	y	5(3)	221		
CaCl ₂ ∪ NaCl	polygalacturonase inhibitor protein 17	37229	<i>Brassica napus</i>	y	18(6)	753	9(7)	486
CaCl ₂	PREDICTED: peroxidase 17-like	37189	<i>Brassica rapa</i>	y	2(1)	112		
CaCl ₂ ∪ NaCl	polygalacturonase inhibitor protein 14	37122	<i>Brassica napus</i>	y	14(5)	659	9(6)	428
CaCl ₂ ∪ NaCl	BnaA05g26870D	37094	<i>Brassica napus</i>	y	8(4)	415	6(1)	178
CaCl ₂	polygalacturonase inhibitor protein 7	36994	<i>Brassica napus</i>	y	10(4)	462		
CaCl ₂ ∪ NaCl	BnaA08g00680D	36966	<i>Brassica napus</i>	n	3(1)	163	5(2)	269
CaCl ₂	hypothetical protein AALP_AA3G131900	36792	<i>Arabis alpina</i>	y	3(1)	131		
CaCl ₂ ∪ NaCl	PREDICTED: putative glucose-6-phosphate 1-epimerase	36699	<i>Brassica rapa</i>	y	18(13)	888	17(7)	718
CaCl ₂	hypothetical protein CARUB_v10014170mg	36644	<i>Capsella rubella</i>	y	3(2)	126		
NaCl	polygalacturonase inhibitory protein	36344	<i>Brassica rapa</i> ssp. <i>oleifera</i>	y			6(2)	270
CaCl ₂	PREDICTED: polygalacturonase inhibitor 1-like	36324	<i>Brassica rapa</i>	y	14(10)	736		
CaCl ₂	PREDICTED: malate dehydrogenase 1, mitochondrial	35900	<i>Brassica rapa</i>	n	3(1)	128		
CaCl ₂	peroxidase 12, partial	35809	<i>Brassica rapa</i>	n	2(1)	125		
NaCl	PREDICTED: oxygen-evolving enhancer protein 1-2, chloroplastic	35622	<i>Brassica rapa</i>	n			3(1)	137
NaCl	hypothetical protein CARUB_v10001493mg	34383	<i>Capsella rubella</i>	n			4(1)	177
NaCl	PREDICTED: polyubiquitin	34137	<i>Brassica rapa</i>	n			1(1)	86
NaCl	PREDICTED: uncharacterized protein LOC103858498	33800	<i>Brassica rapa</i>	y			1(1)	59

NaCl	PREDICTED: uncharacterized protein LOC103855233	32778	<i>Brassica rapa</i>	y			5(1) 2(0)	207 65
CaCl ₂	BnaA07g08530D	32587	<i>Brassica napus</i>	y	4(1)	141		
CaCl ₂ u NaCl	PREDICTED: uncharacterized protein LOC103847210	31989	<i>Brassica rapa</i>	y	4(2)	236	10(3) 2(1)	494 127
CaCl ₂ u NaCl	BnaA10g22530D	31960	<i>Brassica napus</i>	y	4(2)	232	10(2)	478
CaCl ₂ u NaCl	hypothetical protein EUTSA_v10014244mg	31870	<i>Eutrema salsugineum</i>	y	6(1)	237	5(2)	280
NaCl	PREDICTED: xyloglucan endotransglucosylase/hydrolase protein 24- like	31803	<i>Brassica rapa</i>	y			4(1)	152
CaCl ₂ u NaCl	PREDICTED: uncharacterized protein LOC103850724	31733	<i>Brassica rapa</i>	y	8(4)	436	4(1)	211
CaCl ₂	PREDICTED: glycine-rich cell wall structural protein	31446	<i>Brassica rapa</i>	y	4(1)	169		
CaCl ₂	PREDICTED: basic endochitinase CHB4-like	31243	<i>Brassica rapa</i>	y	4(2)	211		
CaCl ₂	endochitinase	30916	<i>Brassica rapa ssp. chinensis</i>	n	7(6)	372		
CaCl ₂	BnaC09g00220D	30762	<i>Brassica napus</i>	n	3(1)	122		
CaCl ₂	PREDICTED: cysteine-rich repeat secretory protein 38-like	30656	<i>Brassica rapa</i>	n	6(1)	210		
CaCl ₂ u NaCl	BnaC02g00880D	30274	<i>Brassica napus</i>	y	2(1)	136	2(1)	104
CaCl ₂ u NaCl	PREDICTED: ribosome-recycling factor, chloroplastic-like	30213	<i>Brassica rapa</i>	n	18(8)	526	4(2)	206
CaCl ₂	PREDICTED: basic endochitinase CHB4-like	29876	<i>Brassica rapa</i>	y	2(2)	177		
CaCl ₂ u NaCl	receptor-like protein kinase-related family protein	29847	<i>Arabidopsis thaliana</i>	y	7(1)	148	3(1)	132
NaCl	chitinase	29691	<i>Brassica rapa</i>	y			1(1)	66
CaCl ₂	PREDICTED: basic endochitinase CHB4	29669	<i>Brassica rapa</i>	y	3(3)	174		
CaCl ₂ u NaCl	PREDICTED: cysteine-rich repeat secretory protein 55	29565	<i>Brassica rapa</i>	y	12(3)	364	5(2)	242
CaCl ₂	BnaA09g55740D	29359	<i>Brassica napus</i>	n	15(6)	530		
CaCl ₂	hypothetical protein EUTSA_v10001590mg	29330	<i>Eutrema salsugineum</i>	y	2(1)	77		
CaCl ₂	hypothetical protein AALP_AA3G105100	29124	<i>Arabis alpina</i>	n	3(1)	108		
CaCl ₂	PREDICTED: oxygen-evolving enhancer protein 2-1, chloroplastic isoform X1	28311	<i>Camelina sativa</i>	n	2(1)	69		
CaCl ₂	PREDICTED: oxygen-evolving enhancer protein 2, chloroplastic-like	28221	<i>Brassica rapa</i>	n	3(1)	159		
CaCl ₂ u NaCl	PREDICTED: histone H1.2	28116	<i>Brassica rapa</i>	n	3(1)	136	4(1)	126
CaCl ₂ u NaCl	PREDICTED: osmotin-like protein	28114	<i>Brassica rapa</i>	y	10(3)	278	3(1)	99
CaCl ₂	triosephosphate isomerase	27439	<i>Brassica rapa ssp. chinensis</i>	n	2(2)	143		
CaCl ₂	chalcone-flavanone isomerase 1 protein	27182	<i>Brassica rapa ssp. oleifera</i>	n	3(1)	111		
NaCl	PREDICTED: histone H1.2-like	26787	<i>Brassica rapa</i>	n			6(2)	209
CaCl ₂	PREDICTED: pathogenesis-related protein R major form-like	26267	<i>Camelina sativa</i>	y	2(1)	67		
CaCl ₂ u NaCl	PREDICTED: pathogenesis-related protein 5- like isoform X1	26117	<i>Brassica rapa</i>	y	2(1)	91	1(1)	74
CaCl ₂	BnaA01g12890D	26100	<i>Brassica napus</i>	n	9(2)	189		
NaCl	PREDICTED: 60S ribosomal protein L6-3-like	25920	<i>Brassica rapa</i>	n			1(1)	61
CaCl ₂	PREDICTED: polyubiquitin 11-like	25768	<i>Brassica rapa</i>	n	3(0)	76		
CaCl ₂ u NaCl	trypsin inhibitor B precursor	24979	<i>Brassica rapa</i>	y	17(13)	417	20(14)	395
CaCl ₂ u NaCl	Kunitz-type cysteine protease inhibitor	24919	<i>Brassica rapa</i>	y	19(13)	568	24(18)	506
CaCl ₂	water-soluble chlorophyll protein	24908	<i>Brassica oleracea var.</i>	y	13(8)	451		

<i>botrytis</i>								
CaCl ₂ u NaCl	PREDICTED: kunitz-type serine protease inhibitor DrTI-like	24867	<i>Brassica rapa</i>	y	8(4)	325	16(9)	302
CaCl ₂	PREDICTED: peroxiredoxin Q, chloroplastic isoform X1	24214	<i>Brassica rapa</i>	n	5(1)	172		
NaCl	PREDICTED: peroxiredoxin Q, chloroplastic isoform X2	24086	<i>Brassica rapa</i>	n			5(1)	142
CaCl ₂ u NaCl	BnaA06g19660D	24080	<i>Brassica napus</i>	n	7(2)	322	10(4)	352
NaCl	PREDICTED: kunitz-type serine protease inhibitor DrTI	24024	<i>Brassica rapa</i>	y			10(2)	305
CaCl ₂	PREDICTED: putative oxygen-evolving enhancer protein 2-2 isoform X2	23903	<i>Camelina sativa</i>	n	6(4) 5(3)	288 241		
CaCl ₂ u NaCl	PREDICTED: putative oxygen-evolving enhancer protein 2-2 isoform X2	23876	<i>Brassica rapa</i>	n	7(4) 6(4)	368 271	2(1)	111
CaCl ₂ u NaCl	PREDICTED: kunitz-type serine protease inhibitor DrTI-like	23763	<i>Brassica rapa</i>	y	6(2)	326	6(1)	243
CaCl ₂	PREDICTED: 21 kDa protein	22727	<i>Brassica rapa</i>	y	3(2) 2(1)	144 133		
CaCl ₂ u NaCl	PREDICTED: 21 kDa protein-like	22621	<i>Brassica rapa</i>	y	3(3) 2(2)	206 188	2(1) 1(1)	114 66
CaCl ₂	PREDICTED: photosystem I reaction center subunit II-1, chloroplastic	22589	<i>Brassica rapa</i>	n	7(2) 5(0)	298 132		
CaCl ₂	PREDICTED: 21 kDa protein-like	22473	<i>Camelina sativa</i>	y	2(1)	133		
CaCl ₂ u NaCl	BnaA08g22890D	22267	<i>Brassica napus</i>	y	3(1)	119	3(1)	138
CaCl ₂ u NaCl	PREDICTED: germin-like protein 1	22190	<i>Brassica rapa</i>	y	2(1)	101	2(1)	99
NaCl	PREDICTED: 21 kDa protein-like	22093	<i>Brassica rapa</i>	y			2(1)	88
NaCl	hypothetical protein EUTSA_v10014670mg	22088	<i>Eutrema salsugineum</i>	y			13(4)	278
CaCl ₂	PREDICTED: germin-like protein 1	22055	<i>Brassica rapa</i>	y	9(3)	316		
CaCl ₂	PREDICTED: dehydrin ERD14	22031	<i>Brassica rapa</i>	n	6(3)	187		
NaCl	PREDICTED: germin-like protein subfamily 3 member 3	22029	<i>Brassica rapa</i>	y			10(3) 1(1)	269 146
CaCl ₂ u NaCl	germin-like protein	22023	<i>Arabidopsis thaliana</i>	y	6(2)	156	9(1)	188
CaCl ₂	BnaA03g56080D	22013	<i>Brassica napus</i>	y	7(2)	213		
CaCl ₂ u NaCl	PREDICTED: germin-like protein 1	22003	<i>Brassica rapa</i>	y	8(3)	271	10(2)	239
CaCl ₂	PREDICTED: 21 kDa protein	21846	<i>Brassica rapa</i>	y	2(2) 2(0)	143 99		
CaCl ₂	hypothetical protein AALP_AA8G370300	21479	<i>Arabis alpina</i>	n	2(1)	104		
CaCl ₂	polyubiquitin 10	21432	<i>Arachis hypogaea</i>	n	5(1) 4(1)	200 97		
CaCl ₂	BnaC09g37120D	21248	<i>Brassica napus</i>	y	3(2)	127		
CaCl ₂ u NaCl	PREDICTED: 60S ribosomal protein L18-2	20997	<i>Brassica rapa</i>	n	1(1)	75	1(1)	59
CaCl ₂	PREDICTED: 60S ribosomal protein L18-2	20811	<i>Brassica rapa</i>	n	4(2) 5(0)	156 174		
CaCl ₂	PREDICTED: calmodulin-7-like	20616	<i>Brassica rapa</i>	n	7(1)	228		
CaCl ₂	temperature-induced lipocalin	20571	<i>Brassica rapa</i>	n	5(1)	143		
CaCl ₂	PREDICTED: early nodulin-like protein 3	20468	<i>Brassica rapa</i>	y	3(1)	74		
CaCl ₂	PREDICTED: uncharacterized protein LOC103828992	20284	<i>Brassica rapa</i>	n	3(1)	130		
CaCl ₂	PREDICTED: mavicyanin-like	20126	<i>Brassica rapa</i>	y	1(1)	59		
NaCl	PREDICTED: 50S ribosomal protein L12-1, chloroplastic	20070	<i>Brassica rapa</i>	n			1(1)	63
CaCl ₂	PREDICTED: ribonuclease UK114	19956	<i>Brassica rapa</i>	n	6(2) 5(1) 4(0)	176 183 139		
CaCl ₂ u NaCl	PREDICTED: putative DNA-binding protein At1g48610	19452	<i>Brassica rapa</i>	n	2(1)	110	2(1)	136

CaCl ₂ ∪ NaCl	copper/zinc superoxide dismutase	19131	<i>Brassica rapa</i>	n	9(4)	179	9(3)	230
CaCl ₂	BnaC05g13970D	18852	<i>Brassica napus</i>	n	2(2)	147		
CaCl ₂ ∪ NaCl	PREDICTED: LOW QUALITY PROTEIN: calmodulin	18186	<i>Brassica rapa</i>	n	8(2)	314	4(1)	219
CaCl ₂	PREDICTED: probable calcium-binding protein CML27	18070	<i>Brassica rapa</i>	n	2(2) 2(1)	147 94		
NaCl	PREDICTED: ubiquitin-40S ribosomal protein S27a-3-like	17962	<i>Brassica rapa</i>	n			2(1)	90
CaCl ₂ ∪ NaCl	PREDICTED: pathogenesis-related protein 1-like	17927	<i>Brassica rapa</i>	y	5(2) 3(1)	147 88	3(1)	112
NaCl	PREDICTED: ubiquitin-40S ribosomal protein S27a-3-like	17925	<i>Brassica rapa</i>	n			1(1)	57
CaCl ₂	unnamed protein product	17876	<i>Arabidopsis thaliana</i>	n	3(2)	129		
CaCl ₂ ∪ NaCl	PREDICTED: cell wall / vacuolar inhibitor of fructosidase 1	17851	<i>Brassica rapa</i>	y	5(1) 6(1)	310 229	5(2) 3(1)	310 124
CaCl ₂ ∪ NaCl	pathogenesis-related protein 1	17815	<i>Brassica rapa</i> ssp. <i>oleifera</i>	y	5(2) 3(1)	147 88	3(1)	112
CaCl ₂	predicted protein	17775	<i>Arabidopsis lyrata</i> ssp. <i>lyrata</i>	y	3(1)	62		
CaCl ₂	hypothetical protein CARUB_v10010544mg, partial	17365	<i>Capsella rubella</i>	n	3(2)	181		
CaCl ₂ ∪ NaCl	DC 1.2 homolog	17144	<i>Arabidopsis thaliana</i>	n	1(1) 1(1)	98 74	1(1)	80
CaCl ₂ ∪ NaCl	PREDICTED: putative phosphatidylglycerol/phosphatidylinositol transfer protein DDB_G0282179	16470	<i>Brassica rapa</i>	y	1(1) 1(1)	103 63	2(2)	87
CaCl ₂	PR4-type protein	16223	<i>Arabidopsis lyrata</i> ssp. <i>lyrata</i>	y	4(1) 4(0)	97 91		
NaCl	PREDICTED: pathogenesis-related protein PR-4-like	16113	<i>Brassica rapa</i>	y			3(1)	172
CaCl ₂ ∪ NaCl	BnaC03g33880D	16059	<i>Brassica napus</i>	y	10(4) 11(4)	325 307	7(2)	253
CaCl ₂ ∪ NaCl	PREDICTED: pathogenesis-related protein PR-4-like	16043	<i>Camelina sativa</i>	y	4(3) 6(2)	188 146	3(1) 3(1)	158 121
CaCl ₂ ∪ NaCl	hypothetical protein AALP_AA3G041800	16002	<i>Arabis alpina</i>	y	7(3) 6(3)	146 145	5(1)	86
CaCl ₂ ∪ NaCl	PREDICTED: pathogenesis-related protein PR-4-like	15957	<i>Brassica rapa</i>	y	5(3) 7(3)	160 146	3(1)	135
CaCl ₂	BnaCnng21510D	15933	<i>Brassica napus</i>	n	1(1)	114		
CaCl ₂	PREDICTED: glycine-rich RNA-binding protein 10 isoform X1	15873	<i>Brassica rapa</i>	n	3(1)	131		
CaCl ₂	hypothetical protein CARUB_v10010551mg	15362	<i>Capsella rubella</i>	n	6(1)	151		
CaCl ₂	BnaA09g54410D	15337	<i>Brassica napus</i>	n	3(1)	96		
NaCl	PREDICTED: photosystem I reaction center subunit IV A, chloroplastic	15035	<i>Brassica rapa</i>	n			1(1)	68
CaCl ₂ ∪ NaCl	PREDICTED: photosystem I reaction center subunit IV A, chloroplastic-like	14958	<i>Brassica rapa</i>	n	1(1)	55	1(1) 2(0)	55 75
CaCl ₂ ∪ NaCl	PREDICTED: ubiquitin-60S ribosomal protein L40-like	14911	<i>Brassica rapa</i>	n	3(0)	75	6(1)	154
CaCl ₂ ∪ NaCl	PREDICTED: EG45-like domain containing protein 2 isoform X1	14867	<i>Brassica rapa</i>	y	17(8) 10(1)	397 191	19(7) 7(1)	453 166
CaCl ₂	BnaC07g15050D	14768	<i>Brassica napus</i>	n	3(1)	184		
CaCl ₂ ∪ NaCl	PREDICTED: 60S ribosomal protein L22-2	14096	<i>Brassica rapa</i>	n	1(1)	63	1(1) 1(1)	64 63
CaCl ₂ ∪ NaCl	PREDICTED: non-specific lipid-transfer protein 3-like	14039	<i>Brassica rapa</i>	y	1(1)	83	1(1) 1(1)	65 64
CaCl ₂ ∪ NaCl	PREDICTED: basic blue protein	13968	<i>Brassica rapa</i>	y	1(1) 2(0)	64 71	2(1) 1(1)	58 62
CaCl ₂ ∪ NaCl	BnaC04g26730D	13881	<i>Brassica napus</i>	y	1(1)	59	1(1)	64
CaCl ₂	PREDICTED: uncharacterized protein LOC103846942	13874	<i>Brassica rapa</i>	y	2(1)	65		

CaCl ₂	thioredoxin H-type	13752	<i>Brassica rapa</i>	n	6(1) 1(0)	194 54		
CaCl ₂ ∪ NaCl	PREDICTED: probable mediator of RNA polymerase II transcription subunit 37e	13524	<i>Brassica rapa</i>	n	1(1)	64	1(1)	68
CaCl ₂	BnaA01g05410D	13056	<i>Brassica napus</i>	n	2(1)	104		
CaCl ₂	PREDICTED: non-specific lipid-transfer protein 5-like	13012	<i>Brassica rapa</i>	y	6(0)	67		
CaCl ₂	PREDICTED: non-specific lipid-transfer protein 1	12573	<i>Brassica rapa</i>	y	2(2)	109		
CaCl ₂ ∪ NaCl	PREDICTED: non-specific lipid-transfer protein 6-like	12557	<i>Brassica rapa</i>	y	4(2) 3(1)	181 172	4(3) 2(1)	209 128
CaCl ₂	PREDICTED: non-specific lipid-transfer protein B isoform X1	12491	<i>Brassica rapa</i>	y	4(2)	142		
CaCl ₂ ∪ NaCl	PREDICTED: non-specific lipid-transfer protein D	12461	<i>Brassica rapa</i>	y	5(3) 2(1)	161 78	7(4) 3(1)	142 73
CaCl ₂ ∪ NaCl	PREDICTED: non-specific lipid-transfer protein A	12298	<i>Brassica rapa</i>	y	8(5) 4(2)	76 87	8(4) 3(2)	85 74
CaCl ₂ ∪ NaCl	PREDICTED: cysteine proteinase inhibitor 4-like	12293	<i>Brassica rapa</i>	y	10(2) 4(1)	276 124	6(2) 5(0)	243 170
CaCl ₂ ∪ NaCl	PREDICTED: non-specific lipid-transfer protein A	12279	<i>Brassica rapa</i>	y	1(1)	74	1(1)	87
CaCl ₂ ∪ NaCl	PREDICTED: non-specific lipid-transfer protein 4-like	12052	<i>Brassica rapa</i>	y	2(2) 2(0)	118 69	2(2)	130
NaCl	BnaAnng33460D, partial	11740	<i>Brassica napus</i>	n			2(1)	129
NaCl	BnaC09g21810D	11478	<i>Brassica napus</i>	n			7(2) 5(1)	164 175
NaCl	BnaC07g48010D	11378	<i>Brassica napus</i>	y			4(1) 2(1)	122 91
CaCl ₂	BnaC04g06750D	10750	<i>Brassica napus</i>	n	1(1)	75		
NaCl	PREDICTED: non-specific lipid-transfer protein 2-like	10468	<i>Brassica rapa</i>	y			2(2)	90

Table 8: All Brassicaceae proteins found in MS data for CaCl₂ as well as NaCl cell wall extractions from *B. rapa* ssp. *pekinensis*. For each protein hit the top number of peptides (P) was shown that match the protein sequence of which the significant ones are shown in brackets. A significance threshold of 0.05 was used. Furthermore the top Mascot score (S) was displayed for each predicted protein. Localisation of the proteins was predicted by searching for a signal peptide with SignalP 4.1. y: yes, n: no.

	Protein	Mass [Da]	Species	P	S	SP	C [%]	Gene	ID%	BS
1	PREDICTED: protein ASPARTIC PROTEASE IN GUARD CELL 2-like	46743	<i>Brassica rapa</i>	3(2)	149	y	7	Bra014819	100	2127
1	aspartyl protease family protein	46258	<i>Arabidopsis thaliana</i>	3(1)	126	y	7	Bra014819	93.8	1662
1	PREDICTED: DNA-damage- repair/toleration protein DRT100	40527	<i>Brassica oleracea</i> <i>var. oleracea</i>	2(1)	106	y	6	Bra035741	99.1	1779
1	PREDICTED: DNA-damage- repair/toleration protein DRT100-like	40507	<i>Camelina sativa</i>	2(1)	102	y	6	Bra035741	92.3	1732
2 3*	polygalacturonase-inhibiting protein	37620	<i>Brassica rapa</i> ssp. <i>pekinensis</i>	1(1)	89	y	4	Bra005919	100	724

Table 9: Complete MS results of all detected Brassicaceae proteins for interaction study of SSC_GH28-6 with *B. rapa* ssp. *pekinensis* cell wall protein extracts. Protein bands (first column) were indicated in Figure 11 with arrows. For each protein hit the top number of peptides (P) was displayed that match the protein sequence of which the significant ones were shown in brackets. A significance threshold of 0.05 was used. Furthermore the Mascot score (S), coverage (C) and BLAST score (BS) and identity with the best hit of the *B. rapa* genome (Gene) in BLAST analysis (ID%) was displayed for each predicted protein. Localisation of the proteins was predicted by searching for a signal peptide (SP) with SignalP 4.1. y: yes, n: no.

	Protein	Mass [Da]	Species	P	S	SP	C [%]	Gene	ID%	BS
13	BnaA04g24070D	41324	<i>Brassica napus</i>	7(5)	458	y	27	Bra016917	97.7	1823
12	PREDICTED: uncharacterized protein LOC103865900	41229	<i>Brassica rapa</i>	2(2)	119	y	7	Bra016917	100	1861
13	hypothetical protein EUTSA_v10016810mg	41179	<i>Eutrema salsugineum</i>	4(2)	169	y	8	Bra016917	91.0	1667
13	PREDICTED: uncharacterized protein LOC103866589	40812	<i>Brassica rapa</i>	9(4) 5(3)	388 310	y	29 15	Bra004651	100	1941
11	PREDICTED: GDSL esterase/lipase At1g29670	40777	<i>Brassica rapa</i>	9(6)	534	y	33	Bra010820	100	1906
13	hypothetical protein ARALYDRAFT_483262	40755	<i>Arabidopsis lyrata ssp. lyrata</i>	6(1)	203	y	19	Bra004651	88.3	1678
13	PREDICTED: uncharacterized protein LOC104793095	40719	<i>Camelina sativa</i>	7(2) 3(1)	280 140	y	25 10	Bra004651	91.9	1581
13	PREDICTED: uncharacterized protein LOC104785200	40640	<i>Camelina sativa</i>	7(2) 3(2)	320 160	y	25 10	Bra004651	92.4	1618
12	uncharacterized protein	40585	<i>Arabidopsis thaliana</i>	2(1)	101	y	5	Bra004651	90.6	1721
13	leucine-rich repeat-containing protein	40475	<i>Arabidopsis thaliana</i>	7(3) 10(4) 7(3)	347 415 354	y	18 21 18	Bra035741	93.8	1747
13	PREDICTED: DNA-damage-repair/toleration protein DRT100	40461	<i>Brassica rapa</i>	13(6) 19(8) 17(7)	639 791 722	y	37 40 37	Bra035741	100	1808
13	BnaA01g36810D	40377	<i>Brassica napus</i>	8(3) 11(4) 8(3)	381 449 390	y	20 23 20	Bra035741	92.0	1728
13	hypothetical protein CARUB_v10001211mg	40249	<i>Capsella rubella</i>	12(7) 8(3)	449 415	y	27 18	Bra009841	89.5	1720
13	hypothetical protein EUTSA_v10013887mg	40216	<i>Eutrema salsugineum</i>	14(9) 15(6)	581 583	y	28 28	Bra023324	95.3	1697
12	PREDICTED: peroxidase 12	40200	<i>Brassica rapa</i>	5(1)	160	y	14	Bra016127	100	1842
11	hypothetical protein EUTSA_v10008016mg	40199	<i>Eutrema salsugineum</i>	5(2)	161	y	17	Bra030156	92.6	1679
13	UF642 I-Gall-responsive protein 1	40185	<i>Arabidopsis thaliana</i>	12(6) 13(6) 7(3)	415 527 384	y	36 35 16	Bra009841	91.6	1739
13	PREDICTED: uncharacterized protein LOC104706866	40176	<i>Camelina sativa</i>	12(8) 14(7)	499 571	y	25 32	Bra009841	93.6	1712
13	BnaC09g45170D	40137	<i>Brassica napus</i>	15(9)	566	y	32	Bra008963	96.4	1833
12	PREDICTED: uncharacterized protein LOC106316810	40135	<i>Brassica oleracea var. oleracea</i>	15(6)	589	y	31	Bra008963	96.4	1834
13	PREDICTED: uncharacterized protein LOC103850771	40126	<i>Brassica rapa</i>	18(11) 16(6)	666 590	y	38 33	Bra023324	100	1762
13	BnaA02g01000D	40124	<i>Brassica napus</i>	18(11)	672	y	38	Bra008963	91.5	1755
13	hypothetical protein AALP_AA8G432300	40091	<i>Arabis alpina</i>	13(7) 14(7) 9(2)	520 627 383	y	27 32 16	Bra009841	94.8	1746
12	uncharacterized protein	40083	<i>Arabidopsis thaliana</i>	5(2)	173	y	11	Bra011349	92.6	1797
12	PREDICTED: uncharacterized protein LOC103850912	40076	<i>Brassica rapa</i>	6(1)	145	y	11	Bra011349	100.0	1917
13	uncharacterized protein	39905	<i>Arabidopsis thaliana</i>	15(9) 15(6) 12(3)	618 622 478	y	30 30 23	Bra023324	94.7	1707
12	PREDICTED: uncharacterized protein LOC103874406	39878	<i>Brassica rapa</i>	25(10) 16(6)	953 575	y	59 31	Bra009841	100	1835
12	PREDICTED: peroxidase 34-like	39541	<i>Brassica rapa</i>	5(1) 7(2)	158 280	y	15 19	Bra018006	100	1773
12	PREDICTED: uncharacterized protein LOC103870618	39384	<i>Brassica rapa</i>	22(14) 14(5)	971 562	y	60 44	Bra029693	100	1786
12	hypothetical protein CARUB_v10017534mg	39365	<i>Capsella rubella</i>	3(1)	100	y	10	Bra039816	89.5	856

12	hypothetical protein EUTSA_v10020990mg	39363	<i>Eutrema salsugineum</i>	5(3)	184	y	12	Bra040046	92.6	1775
12	BnaC05g44040D	39356	<i>Brassica napus</i>	19(12)	834	y	56	Bra029693	99.4	1779
12	hypothetical protein CARUB_v10014019mg	39326	<i>Capsella rubella</i>	10(6)	444	y	34	Bra029693	93.8	1687
11	hypothetical protein CARUB_v10017550mg	39304	<i>Capsella rubella</i>	3(1)	121	y	7	Bra018006	85.4	1535
12	polygalacturonase inhibitor protein 15	39183	<i>Brassica napus</i>	1(1)	83	y	5	Bra005916	97.1	879
11	Peroxidase C1B	39144	<i>Armoracia rusticana</i>	3(2)	174	y	9	Bra029933	88.2	1596
11	ATPCA/ATPRX33/PRX33	39028	<i>Arabidopsis lyrata</i> ssp. <i>lyrata</i>	2(1)	99	y	6	Bra029933	91.5	1560
12	PREDICTED: polygalacturonase inhibitor 2-like	38737	<i>Brassica oleracea</i> var. <i>oleracea</i>	6(3)	354 280	y	21 19	Bra005917	95.5	896
11	BnaC03g02770D	38730	<i>Brassica napus</i>	6(3)	265	y	19	Bra005917	95.5	899
12	polygalacturonase inhibitor protein	38729	<i>Brassica napus</i>	6(3)	346	y	19	Bra005917	95.5	899
12	polygalacturonase-inhibiting protein 1	38690	<i>Brassica rapa</i> ssp. <i>pekinensis</i>	6(2) 6(3)	282 284	y	24 20	Bra005917	99.4	929
11	PREDICTED: polygalacturonase inhibitor 1-like	38048	<i>Brassica rapa</i>	8(3)	366	y	27	Bra034774	100	1705
10	PREDICTED: glucan endo-1,3-beta-glucosidase, acidic isoform-like	37959	<i>Brassica rapa</i>	1(1)	62	y	3	BG3	100	1534
11	PREDICTED: polygalacturonase inhibitor 2-like	37930	<i>Brassica rapa</i>	4(1)	154	y	10	Bra009238	100	1587
11	PREDICTED: polygalacturonase inhibitor 2	37795	<i>Camelina sativa</i>	3(1)	98	y	5	Bra009235 Bra005917	71.0 70.1	600 597
11	PREDICTED: bark storage protein A-like	37768	<i>Brassica rapa</i>	2(1)	130	y	7	Bra013793	100	1681
11	polygalacturonase-inhibiting protein 3	37620	<i>Brassica rapa</i> ssp. <i>pekinensis</i>	7(3) 5(1)	332 259	y	25 21	Bra005919	100	724
11	BnaC09g16910D	37365	<i>Brassica napus</i>	2(1) 3(2)	103 73	y	6 8	Bra027987	91.3	611
10	hypothetical protein EUTSA_v10013887mg	37317	<i>Eutrema salsugineum</i>	14(2)	332	n	20	Bra023324	95.3	1697
11	polygalacturonase inhibitor protein 14	37122	<i>Brassica napus</i>	5(3)	280	y	18	Bra005918	93.2	795
11	BnaA05g26870D	37094	<i>Brassica napus</i>	8(3)	360	y	25	Bra034774	98.2	1675
11	polygalacturonase inhibiting protein 2	37091	<i>Arabidopsis thaliana</i>	2(1)	86	y	5	Bra009238 Bra005917	74.1 72.5	1088 644
11	PREDICTED: putative glucose-6-phosphate 1-epimerase	36699	<i>Brassica rapa</i>	4(1)	156	y	19	Bra013931	100.0	1612
11	hypothetical protein CARUB_v10014170mg	36644	<i>Capsella rubella</i>	3(1)	113	y	9	Bra038700	90.3	1427
11	polygalacturonase inhibitory protein	36344	<i>Brassica rapa</i> ssp. <i>oleifera</i>	17(10)	641	y	49	Bra038700	99.4	1626
9	BnaC01g17620D	36030	<i>Brassica napus</i>	1(1)	86	n	4	ATQC	96.5	1336
11	PREDICTED: probable xyloglucan endotransglucosylase/hydrolase protein 7	36023	<i>Brassica oleracea</i> var. <i>oleracea</i>	2(1)	84	n	6	XTH7	99.3	1595
11	peroxidase 12, partial	35809	<i>Brassica rapa</i>	2(1)	108	n	8	Bra016127	99.7	1654
11	hypothetical protein CARUB_v10001493mg	34383	<i>Capsella rubella</i>	3(1) 4(1)	114 164	n	8 10	Bra028635	90.0	291
11	PREDICTED: probable xyloglucan endotransglucosylase/hydrolase protein 5	34318	<i>Brassica rapa</i>	3(1) 4(2) 3(1)	143 203 92	y	10 10 10	Bra008796	100	1549
11	PREDICTED: xyloglucan endotransglucosylase/hydrolase	34273	<i>Brassica rapa</i>	5(2) 13(5) 9(2)	288 625 286	y	18 37 30	EXGT-A1	100	1615
10	PREDICTED: uncharacterized protein LOC103858498	33800	<i>Brassica rapa</i>	7(7) 7(5)	447 412	y	23 27	EXO	100	1427
10	xyloglucan endotransglycosylase	33727	<i>Brassica rapa</i> ssp. <i>pekinensis</i>	6(4) 6(4)	340 329	y	23 25	XTH7	99.3	1595

10	BnaA03g23810D	33523	<i>Brassica napus</i>	4(3)	220	y	19	EXO	98.3	1186
10	hypothetical protein ARALYDRAFT_919741	33156	<i>Arabidopsis lyrata</i> ssp. <i>lyrata</i>	6(2)	236	y	11	Bra024280	93.2	1122
10	PREDICTED: protein EXORDIUM- like 2	33012	<i>Camelina sativa</i>	6(1)	199	y	11	Bra024280	93.1	901
10	PREDICTED: uncharacterized protein LOC103873843	32859	<i>Brassica rapa</i>	7(2) 5(1)	255 195	y	16 14	Bra024280	100	1464
10	PREDICTED: uncharacterized protein LOC103855233	32778	<i>Brassica rapa</i>	8(3) 5(2)	380 247	y	34 17	Bra031927	100	1604
9	PREDICTED: uncharacterized protein LOC103850725	32606	<i>Brassica rapa</i>	3(1)	186	y	9	Bra028634	100	1518
9	daikon cysteine protease RD21	32103	<i>Raphanus sativus</i>	1(1)	77	n	5	Bra033657	98.1	1058
10	PREDICTED: xyloglucan endotransglucosylase/hydrolase protein 24	32050	<i>Brassica rapa</i>	2(1)	110	y	9	Bra011179	100	1419
10	PREDICTED: uncharacterized protein LOC103847210	31989	<i>Brassica rapa</i>	15(4) 8(4)	461 450	y	28 22	Bra009384	100	1559
10	BnaC09g47090D	31970	<i>Brassica napus</i>	13(3)	372	y	35	Bra009384	97.3	1528
10	BnaA10g22530D	31960	<i>Brassica napus</i>	13(3)	403	y	28	Bra009384	98.7	1548
10	hypothetical protein 9 EUTSA_v10014244mg	31870	<i>Eutrema</i> <i>salsugineum</i>	7(1) 5(2)	248 251	y	20 13	Bra028635	93.3	299
10	PREDICTED: chitinase 10	31869	<i>Brassica rapa</i>	2(1)	107	y	8	Bra036316	100	1417
10	PREDICTED: xyloglucan endotransglucosylase/hydrolase protein 24-like	31803	<i>Brassica rapa</i>	3(1) 5(3)	131 335	y	12 21	Bra024089	100	1367
10	PREDICTED: uncharacterized protein LOC103850724	31733	<i>Brassica rapa</i>	8(1) 9(4)	245 402	y	18 28	Bra028635	100	1477
9	PREDICTED: cysteine-rich repeat secretory protein 38-like	30656	<i>Brassica rapa</i>	6(2)	328	n	23	Bra031321	100	1246
9	BnaC02g00880D	30274	<i>Brassica napus</i>	3(1)	205	y	11	Bra028634	91.2	1058
9	xyloglucosyl transferase 2, partial	30162	<i>Brassica juncea</i>	4(3)	292	n	19	Bra011179	97	1405
9	PREDICTED: protein EXORDIUM- like 4	29958	<i>Camelina sativa</i>	4(1)	164	y	12	Bra009384	95.2	336
9	receptor-like protein kinase-related family protein	29847	<i>Arabidopsis thaliana</i>	15(4)	230	y	19	Bra037480	90.9	375
9	BnaCnng73250D, partial	29814	<i>Brassica napus</i>	7(3)	244	n	30	Bra007070	98.9	1417
9	protein exordium like 4	29803	<i>Arabidopsis thaliana</i>	5(1)	169	y	12	Bra009384	87.8	747
7	PREDICTED: kunitz-type serine protease inhibitor DrTI	24024	<i>Brassica rapa</i>	2(2)	79	y	4	Bra016073	100	1070
7	PREDICTED: germin-like protein subfamily 3 member 3	22029	<i>Brassica rapa</i>	3(1)	123	y	17	Bra006567	100	1065
7	germin-like protein	22023	<i>Arabidopsis thaliana</i>	3(1)	102	y	17	Bra006567 Bra020113	95.3 95.3	879 877
7	PREDICTED: germin-like protein 1	21767	<i>Brassica rapa</i>	4(2)	89	y	21	Bra003874	100	985
7	PREDICTED: STS14 protein	20388	<i>Brassica rapa</i>	2(1)	108	y	13	Bra037162	100	745

Table 10: Complete MS results of all detected Brassicaceae proteins for interaction study of PCO_GH28-1 with *B. rapa* ssp. *pekinensis* cell wall protein extracts. Protein bands (first column) were indicated in Figure 12 with arrows. For each protein hit the top number of peptides (P) was displayed that match the protein sequence of which the significant ones were shown in brackets. A significance threshold of 0.05 was used. Furthermore the Mascot score (S), coverage (C) and BLAST score (BS) and identity with the best hit of the *B. rapa* genome (Gene) in BLAST analysis (ID%) was displayed for each predicted protein. Localisation of the proteins was predicted by searching for a signal peptide (SP) with SignalP 4.1. y: yes, n: no.

	Protein	Mass [Da]	Species	P	S	SP	C [%]	Gene	ID%	BS
12	leucine-rich repeat-containing protein	40475	<i>Arabidopsis thaliana</i>	6(1)	270	y	15	Bra035741	93.8	1747
12	PREDICTED: DNA-damage-repair/toleration protein DRT100	40461	<i>Brassica rapa</i>	13(5)	597	y	33	Bra035741	100	1808
12	BnaA01g36810D	40377	<i>Brassica napus</i>	7(1)	298	y	17	Bra035741	92	1728
12	hypothetical protein AALP_AA8G432300	40091	<i>Arabis alpina</i>	7(1)	269	y	16	Bra009841	94.8	1746
12	PREDICTED: uncharacterized protein LOC103874406	39878	<i>Brassica rapa</i>	11(2)	393	y	28	Bra009841	100	1835
12	PREDICTED: uncharacterized protein LOC103870618	39384	<i>Brassica rapa</i>	5(2)	218	y	16	Bra029693	100	1786
12 11	PREDICTED: polygalacturonase inhibitor 1-like	38048	<i>Brassica rapa</i>	19(9) 18(9)	726 735	y	43 48	Bra034774	100	1705
12 11	PREDICTED: polygalacturonase inhibitor 1-like	38046	<i>Brassica oleracea</i> <i>var. oleracea</i>	16(8) 15(9)	647 666	y	34 37	Bra034774	98.8	1690
11	BnaC09g16910D	37365	<i>Brassica napus</i>	1(1)	61	y	4	Bra027987	91.3	611
11	BnaA05g26870D	37094	<i>Brassica napus</i>	18(8)	681	y	47	Bra034774	98.2	1675
11	hypothetical protein CARUB_v10014170mg	36644	<i>Capsella rubella</i>	10(4)	185	y	13	Bra038700	90.3	1427
11	polygalacturonase inhibitory protein	36344	<i>Brassica rapa</i> ssp. <i>oleifera</i>	40(19)	897	y	59	Bra038700	99.4	1626
11	PREDICTED: polygalacturonase inhibitor 1-like	36118	<i>Brassica oleracea</i> <i>var. oleracea</i>	31(15)	663	y	50	Bra038700	97.2	1583

Table 11: Complete MS results of all detected Brassicaceae proteins for interaction study of PCO_GH28-3 with *B. rapa* ssp. *pekinensis* cell wall protein extracts. Protein bands (first column) were indicated in Figure 12 with arrows. For each protein hit the top number of peptides (P) was displayed that match the protein sequence of which the significant ones were shown in brackets. A significance threshold of 0.05 was used. Furthermore the Mascot score (S), coverage (C) and BLAST score (BS) and identity with the best hit of the *B. rapa* genome (Gene) in BLAST analysis (ID%) was displayed for each predicted protein. Localisation of the proteins was predicted by searching for a signal peptide (SP) with SignalP 4.1. y: yes, n: no.

14 Acknowledgement

First, I would like to thank Dr. David G. Heckel for the opportunity to perform my Master's thesis in his Department of Entomology at the Max Planck Institute for Chemical Ecology. Furthermore, I thank him for discussion and the help in organisational matters.

I would like to express special gratitude to my great supervisors, Dr. Roy Kirsch and Dr. Yannick Pauchet, for providing the topic of my Master's thesis, their constant guidance, advice, patience and many helpful discussions. Additionally, I would like to thank Dr. Roy Kirsch for proof-reading this thesis and the support.

Moreover, I would like to thank Dr. Natalie Wielsch, Jan Krüger and Dr. Anne-Christin Warskulat for the gel preparation, MS measurements and data processing. Thank must also go to Jören Carstens for informatical help with the MS data evaluation.

Also, I would like to thank Prof. Dr. Wilhelm Boland for the help in organizational matters.

Warm thanks are due to Dr. Peter Rahfeld for the many helpful discussions about protein expression and purification.

I would like to thank Domenica Schnabelrauch for sequencing and the green-house team for rearing the plants.

Furthermore, I thank Bianca Wurlitzer and all the other co-workers of the Max Planck Institute for Chemical Ecology for the nice working atmosphere and helpfulness in all aspects during my Master's thesis.

And in the end, I would like to express my gratitude for all their loving support and care to my mum and dad, who made this possible for me.

15 Declaration of originality

I hereby declare that this thesis and the work reported herein was my own work. Information derived from the published and unpublished work of others was acknowledged in the text and references of the bibliography. This thesis has not been submitted in any form for study or examination achievements or another degree at any university.

Place, Date

Signature